

AD/A-002 633

RECOMMENDED REVISIONS TO SELECTED
PORTIONS OF MIL-F-8785(B) AND BACK-
GROUND DATA

Irving L. Ashkenas, et al

Systems Technology, Incorporated

Prepared for:

Air Force Flight Dynamics Laboratory

August 1973



DISTRIBUTED BY:

NTIS

National Technical Information Service
U. S. DEPARTMENT OF COMMERCE

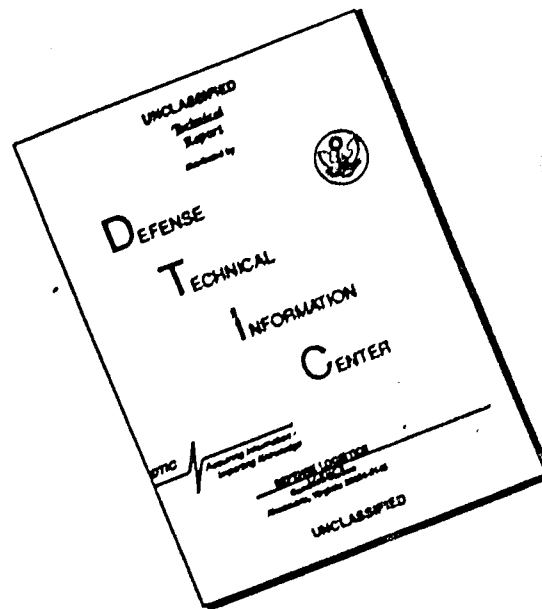
NOTICE

When Government drawings, specifications, or other data are used for any purpose other than in connection with a definitely related Government procurement operation, the United States Government thereby incurs no responsibility nor any obligation whatsoever; and the fact that the government may have formulated, furnished, or in any way supplied the said drawings, specifications, or other data, is not to be regarded by implication or otherwise as in any manner licensing the holder or any other person or corporation, or conveying any rights or permission to manufacture, use, or sell any patented invention that may in any way be related thereto.



Copies of this report should not be returned unless return is required by security considerations, contractual obligations, or notice on a specific document.

DISCLAIMER NOTICE



THIS DOCUMENT IS BEST QUALITY AVAILABLE. THE COPY FURNISHED TO DTIC CONTAINED A SIGNIFICANT NUMBER OF PAGES WHICH DO NOT REPRODUCE LEGIBLY.

Unclassified

SECURITY CLASSIFICATION OF THIS PAGE (When Data Entered)

AD/A002633

REPORT DOCUMENTATION PAGE		READ INSTRUCTIONS BEFORE COMPLETING FORM
1. REPORT NUMBER AFFDL TR-73-76	2. GOVT ACCESSION NO.	3. RECIPIENT'S CATALOG NUMBER
4. TITLE (and Subtitle) RECOMMENDED REVISIONS TO SELECTED PORTIONS OF MIL-F-8785(B) AND BACKGROUND DATA		5. TYPE OF REPORT & PERIOD COVERED Final: Nov 71 - Oct 73
		6. PERFORMING ORG. REPORT NUMBER STI-TR-1017-1
7. AUTHOR(s) I. L. Ashkenas R. H. Hoh S. J. Craig		8. CONTRACT OR GRANT NUMBER(s) F33615-72-C-1456
9. PERFORMING ORGANIZATION NAME AND ADDRESS Systems Technology, Inc. 13766 S. Hawthorne Blvd. Hawthorne, Ca. 90250		10. PROGRAM ELEMENT, PROJECT, TASK AREA & WORK UNIT NUMBERS 62201F/8219-04-06
11. CONTROLLING OFFICE NAME AND ADDRESS AFFDL/FGC W-PAFB, Oh. 45433		12. REPORT DATE August 1973
		13. NUMBER OF PAGES 176 175
14. MONITORING AGENCY NAME & ADDRESS (if different from Controlling Office) Same as 11.		15. SECURITY CLASS. (of this report) Unclassified
		15a. DECLASSIFICATION/DOWNGRADING SCHEDULE N/A
16. DISTRIBUTION STATEMENT (of this Report) Approved For Public Release; Distribution Unlimited		
17. DISTRIBUTION STATEMENT (of the abstract entered in Block 20, if different from Report) Same as 16.		
18. SUPPLEMENTARY NOTES None		
19. KEY WORDS (Continue on reverse side if necessary and identify by block number) Flying Qualities Handling Qualities Flight Control Military Specifications Reproduced by NATIONAL TECHNICAL INFORMATION SERVICE US Department of Commerce Springfield, VA. 22151		
20. ABSTRACT (Continue on reverse side if necessary and identify by block number) This document covers the results obtained in one phase of a continuing series of programs to update, expand and reorganize the requirements of MIL-F-8785(B), <u>Flying Qualities of Piloted Airplanes</u> . The present studies concentrated on, and suggest revisions in, the requirements for heading control, airplane normal and failure states, and Category C short-period requirements.		

DD FORM 1 JAN 73 1473

EDITION OF 1 NOV 65 IS OBSOLETE

Unclassified

SECURITY CLASSIFICATION OF THIS PAGE (When Data Entered)

FOREWORD

This document is the Final Report of a study by Systems Technology, Inc., Hawthorne, California, for the United States Air Force under Contract F33615-72-C-1456, "Analysis and Preparation of Flying Qualities Requirements for Piloted Airplanes." The contract was under the direction of Mr. F. L. George of the Flight Dynamics Laboratory, Control Criteria Branch, Wright-Patterson Air Force Base, Ohio.

The technical work on this contract at Systems Technology, Inc., was under the direction of Mr. I. L. Ashkenas, the Principal Investigator, who also served as Project Engineer. The authors gratefully acknowledge contributions to the technical effort made by Messrs. G. L. Teper and R. K. Heffley.

This report was submitted by the authors August 1973.

This report has been reviewed and is approved.



G. B. WESTBROOK
Chief, Control Criteria Branch
Air Force Flight Dynamics Laboratory

TABLE OF CONTENTS

	<u>Page</u>
I. INTRODUCTION	1
II. FLYING QUALITIES CRITERIA FOR HEADING CONTROL	3
Recommended Specification Revisions	3
Background for the Recommended Revisions	7
III. REQUIREMENTS FOR AIRPLANE NORMAL AND FAILURE STATES	31
Suggested Revisions	31
Discussion	32
IV. CATEGORY C SHORT-PERIOD REQUIREMENTS	50
Recommended Specification Revisions	50
Background for the Recommended Revisions	54
REFERENCES	73
APPENDIX A. CALCULATION OF μ	79
APPENDIX B. SUMMARY OF DATA USED IN HEADING CONTROL CORRELATIONS	84
APPENDIX C. MULTIPLE/SINGLE-AXIS RATING DATA	90
APPENDIX D. SUMMARY OF DATA ANALYZED FOR ATTITUDE RESPONSE REQUIREMENTS	103
APPENDIX E. MULTILoop PILOTING ASPECTS OF LONGITUDINAL APPROACH PATH CONTROL	122

Preceding page blank

LIST OF FIGURES

	<u>Page</u>
1. Aileron-Rudder Coordination Limits	4
2. Pilot Rating Data for Category A Flight (Ref. 14)	6
3. Asymptotes of Aileron-Rudder Crossfeed	12
4. Typical Rudder Time Histories for Zero Sideslip	16
5. Required Crossfeed for $N_{\delta_{ac}}' = 0$	18
6. Effect of $ \phi/\beta _d$ and $N_{\delta_{ac}}'/L_{\delta_{ac}}'$ on Pilot Ratings in Turbulence (Ref. 12 Data)	21
7. Pilot Rating Boundaries for Acceptable Roll Control in Turbulence with $N_{\delta_{ac}}'/L_{\delta_{ac}}' < 0.03$ (From Ref. 11)	23
8. Pilot Rating Correlation with Crossfeed Parameters	25
9. Pilot Rating Correlations when $ N_{\delta_{ac}}'/L_{\delta_{ac}}' < 0.03$	26
10. Correlation Data on $\Delta\phi_{max}/k$ vs. ψ_β Plot	28
11. Comparison of Pilot Opinions Obtained From Flying Separate Modes of Airframe Motion With Pilot Opinion Obtained From Flying Complete Six-Degree-of-Freedom System (Ref. 15)	32
12. A Comparison of Rating Transformations (Ref. 23)	34
13. Secondary Task Score Variation With Ratings for Best-Gain Configurations (Ref. 21)	35
14. $R(\lambda_n)$ Fit to Ref. 21 Data (Fig. 13)	37
15. Final Correlations Obtained With Product Method (Eq. 25)	45
(Figure 3 of Specification). Longitudinal Attitude Control — Category C Requirements	51
16. Application of Criterion — Typical Cases	53
16a. Typical Case Indicating Deficiency in Definition of $\Delta\phi$ for Neal's Criterion	61
16b. Longitudinal Maneuver Response Requirements	62
17. Comparison With Other Semi-Empirical Boundaries	68

	<u>Page</u>
18. Correlation of Criterion With Available Data	69
19. Typical Crossplots in the Region of Rate Response System . .	70
20. Pilot Ratings of ILS Approach Task; Basic and Rate Command Control (Ref. 40)	71
21. Effects of Pilot Equalization on Attitude Closure With a Rate Command System	72
22. Required Rudder Time Response to Coordinate a Unit Step Aileron Input	80
23. Frequency Response for Aileron-Rudder Crossfeed (Ref. 5, Configuration LH70+20+37)	81
24. Comparison of Eq. A-1 and Eq. A-2	83
25. Comparison of Pilot Rating of Controllability for One and Two Axes: Optimum Ratio	90
26. Comparison of Pilot Rating of Controllability for One and Two Axes: Optimum Ratio	91
27. Effect of Turbulence on Rating Trends	114
28. Crossplot for Constant Phase Gradient	115
29. Crossplot for Constant Phase Gradient	116
30. Crossplot for Constant Phase Gradient	117
31. Crossplot for Constant Phase Gradient	118
32. Block Diagram of Pitch Rate Command/Attitude Hold Control System (Ref. 43)	119
33. Block Diagram of Pitch Rate Command System (Ref. 40)	120
34. Block Diagram of Pitch Attitude Command System (Ref. 40) . .	121
35. Two Representative Piloting Techniques	125
36. Effect of Various Control and Configuration Characteristics on Manual STOL Mode Path Control (Ref. 15)	150
37. Attitude Loop System Survey	158
38. Speed Control With Relatively Loose Attitude Control; $u, \theta \rightarrow \delta_e$	161
39. System Survey of Closed-Loop Airspeed Control With Attitude .	163

	<u>Page</u>
40. Effect of Control Techniques on Pilot Rating with Strong "Dynamic" Coupling ($\zeta_\theta = 0.6$, $\omega_\theta = 0.5$; $1/T_{h1} = +0.21$)	164

LIST OF TABLES

	<u>Page</u>
1. Parameters Defining the Aileron-Rudder Crossfeed	11
2. Physical Interpretation of μ	17
3. Ground Rules for Application of Rating Data to Heading Control Criteria	20
4. Summary of Correlated Data	24
5. Review of Ref. 16 Data Linearity with Rating (Levels 1 to 2)	49
6. Data Considered During Current Study	56
7. Criteria Forms Considered	59
8. Definitions and Rules of Application (Ref. 28 Criterion) . . .	62
9. Semi-Empirical Level 1 Boundaries Derived from Various Sources	66
10. Semi-Empirical Level 3 Boundaries Derived from Various Sources	67
11. Raw Data for All Data Runs	93
12. Averaged Values of Single Axis Runs for Two Axis Experiment	98
13. Averaged Values for Two Axis Runs	98
14. Averaged Values of Single Axis Runs for Three Axis Experiment	98
15. Averaged Values of Three Axis Runs	99
16. Reference 18 Data Used in Figure 15 Correlations	100
17. Pilot Ratings for Individual Axes and Overall System for Combinations of Flight Director and SAS Configuration . . .	102
18. Reference 31 Data	104
19. Reference 40 Data	105
20. Reference 34 Data	105
21. Reference 33 Data	106

	<u>Page</u>
22. Estimated Stability Derivatives of the Evaluation Configurations	108
23. Data Summary for Evaluation Configurations	109
24. Reference 43 Data	110
25. Reference 39 Data	111
26. Reference 36 Data	112
27. Reference 37 Data	113
28. Transfer Function Forms and Literal Approximate Factors . . .	131
29. Test Configurations and Range of Variables	149
30. Computed Closed-Loop Parameters and Properties	154

SECTION I

INTRODUCTION

The recent revision to MIL-F-8785B(ASG), Flying Qualities of Piloted Airplanes, was an extensive program of updating, expansion, and reorganization. The present program, a continuation of these and other efforts, had limited objectives aimed primarily at discrete targets of opportunity as governed by the availability of experimental data and by the potential significance of the specification on aircraft/flight control system designs of the near future. These target areas are:

1. Heading control (turn coordination) problems in landing approach.
2. Multiple degradation effects on associated flying qualities Level requirements.
3. The lower limits on "short-period" dynamic requirements for landing approach.
4. Path and speed control problems in landing approach.

In-depth studies, which included applicable pilot/vehicle closed-loop analyses and detailed data correlations, were conducted in each of the above areas. The conclusions stemming from these efforts are given in each section as a proposed revision, presented separately, followed by a general summary of the key considerations, the pertinent substantiation data and analyses, and finally by recommendations for additional research or experimental programs. Each section is thus largely self-contained, allowing the casual reader ready access to the proposed revisions and key considerations without the necessity of wading through voluminous backup material. To further reduce clutter, the references for all sections are given in a single listing and the data tables and usage pertinent to, and referenced in, each section are appended, in proper succession, at the back of the report.

Because there are no recommended spec revisions stemming from the work done on path and speed control problems, Item 4 above, this area is covered largely by reference, in Section IV, to a recent paper on the subject (Ref. 27),

also included herein as Appendix E. This work (supported in part by the present Air Force contract, in part by FAA-funded studies, but largely by contractor and authors' contributions) exposes and illustrates, with applicable data and analyses, a large variety of possible path/speed control problems; and indicates that simple correlations (e.g., with dy/du as in 8785) cannot, in general, be universally applied. In the present absence of definitive data and correlations, it is recommended that Appendix E be used as the basis for a design guide supplement to the spec in the area of approach path/speed control.

SECTION II

FLYING QUALITIES CRITERIA FOR HEADING CONTROL

RECOMMENDED SPECIFICATION REVISIONS

3.3.2.4 Heading Control

The magnitude and shaping of the rudder required to coordinate aileron inputs, i.e., keep sideslip zero, shall be within the following limits.

1. For $|N'_{\delta_{ac}}/L'_{\delta_{ac}}|$ greater than 0.03:

The aileron-rudder shaping parameter, μ , and the control crosscoupling parameter, $N'_{\delta_{ac}}/L'_{\delta_{ac}}$, shall be within the limits specified in Fig. 1.

2. For $|N'_{\delta_{ac}}/L'_{\delta_{ac}}|$ less than or equal to 0.03:

The parameter, $(N'_{\delta_{rc}}/L'_{\delta_{ac}})\delta_{rc}(3)$, shall fall within the following limits.

$$-0.39 \leq \frac{N'_{\delta_{rc}}}{L'_{\delta_{ac}}} \delta_{rc}(3) \leq 0.12 \quad \text{Level 1}$$

$$-1.15 \leq \frac{N'_{\delta_{rc}}}{L'_{\delta_{ac}}} \delta_{rc}(3) \leq 0.78 \quad \text{Level 2}$$

The aileron and rudder parameters, $N'_{\delta_{ac}}$, $L'_{\delta_{ac}}$, and $N'_{\delta_{rc}}$ shall be determined in the stability axis system (x-axis along the aircraft velocity vector).

3.3.2.4.1 Lateral Ride Qualities

The lateral accelerations at the cockpit resulting from abrupt full travel aileron inputs shall not be unacceptable to the crew. While no numerical requirements are specified, this paragraph is intended to prevent extreme lateral accelerations on the crew in aircraft with the cockpit location well forward of the center of gravity.

3.3.2.6 Coordination of Steady Turns

(Title change only)

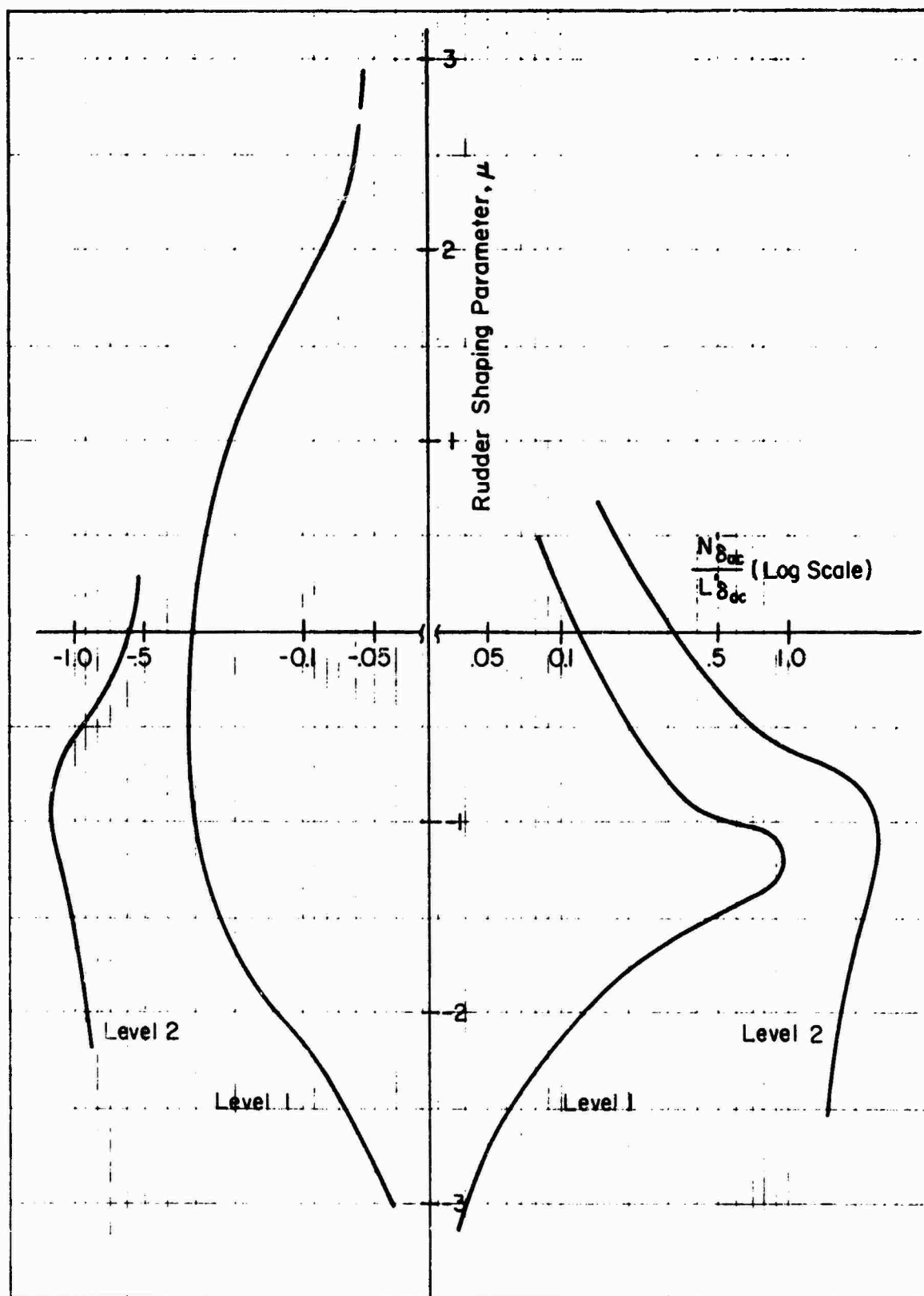


Figure 1. Aileron-Rudder Coordination Limits

Discussion

This revision to MIL-F-8785B is intended to replace the current aileron-only specification, in Paragraphs 3.3.2.4 and 3.3.2.4.1, with a criterion which accounts for the pilot's normal use of rudder for precise control of aircraft heading. Because of the lack of available data for up and away flight, it was not possible to define limits for Categories A and B at this time. A review of the data (Ref. 14) currently available for Category A flight (see Fig. 2) indicates that the allowable crosscoupling is considerably reduced for precision tracking in the up and away configuration.* This result is felt to reflect the highly magnified lateral acceleration cues felt by the pilot in response to misuse of the rudders in high speed flight.

Due to the extreme forward and high location of the cockpit relative to the flight x-axis in some aircraft (SST, space shuttle, etc.), "coordinated flight" can result in large lateral accelerations at the pilot's station. These results obtained in Ref. 4 indicated that while these ride quality problems do not affect the pilot's rating of heading control, they are undesirable from a pilot comfort standpoint. It was felt that this effect is important enough to add a requirement for satisfactory ride qualities. Preliminary correlation of ride quality comments in the Ref. 4 experiments with peak lateral accelerations indicates that about 0.3 g's was found to be objectionable. These accelerations were associated with lateral control inputs during normal maneuvering to line up on the localizer.

When applying the specification for heading control it is important to consider that heading is an outer loop in the pilot/vehicle control structure. It follows that application of the heading criteria to aircraft with unacceptable inner-loop characteristics will result in erroneous conclusions. Since the basic philosophy of application of the MIL-F-8785B specification is that an aircraft must meet all applicable parts, it did not seem necessary to make a separate requirement for good roll control (inner loop). However, a good guideline to follow when applying the

*Note that the $N'_{\delta ac}/L'_{\delta ac}$ scale is considerably expanded in Fig. 2.

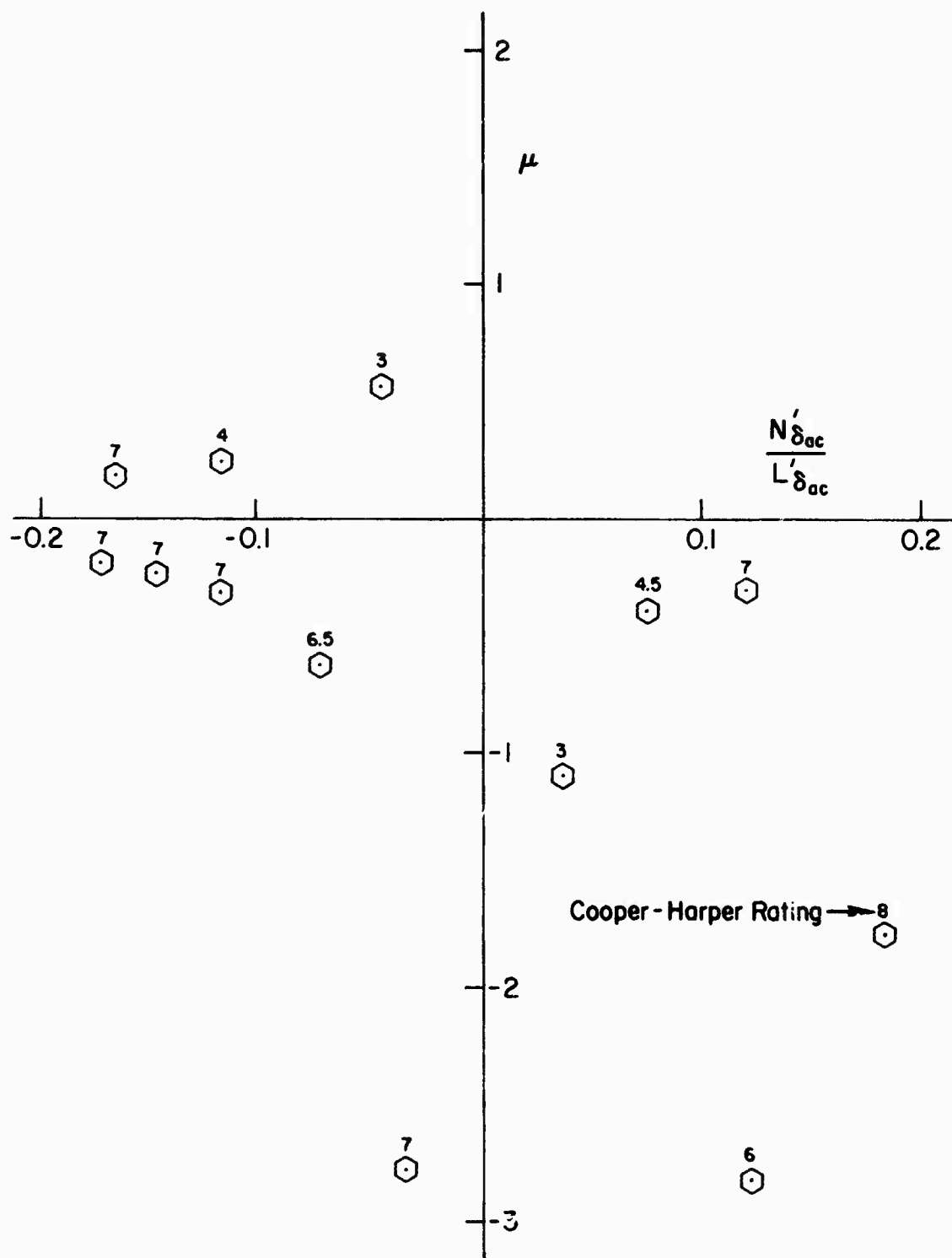


Figure 2. Pilot Rating Data for Category A Flight (Ref. 14)

heading control specification is to first insure that the aircraft meets the requirements of Paragraphs 3.3.1.1, 3.3.1.2, 3.3.1.4, 3.3.2.1, and 3.3.2.2. The requirement stated in 3.3.2.1 regarding the lateral-directional response to atmospheric turbulence is qualitative in nature and therefore difficult to comply with. While the research accomplished during formulation of the heading control specification did not completely unravel the interactions between $|\phi/\beta|_d$ and aircraft lateral turbulence response, the following results were obtained.

- For aircraft with $|N'_{\delta_{ac}}/L'_{\delta_{ac}}| > 0.03$, roll control problems in turbulent air become significant when $|\phi/\beta|_d > 1.5$.
- When control crosscoupling is negligible ($|N'_{\delta_{ac}}/L'_{\delta_{ac}}| \leq 0.03$), larger values of $|\phi/\beta|_d$ are acceptable. The boundaries defined in Fig. 7 tentatively define the acceptable limits of roll-sideslip coupling in terms of L'_p for Class I, II, and IV aircraft with high L'_p and negligible control crosscoupling.

While these results were felt to be too indefinite to form a basis for quantification of Paragraph 3.3.2.1, they do form a reasonably good guideline for application of the heading control specification. It should be noted that restricting $|\phi/\beta|_d$ to less than 1.5 for aircraft with $|N'_{\delta_{ac}}/L'_{\delta_{ac}}| > 0.03$ may be overly conservative. A few data points were found for $|\phi/\beta|_d > 1.5$ with acceptable pilot ratings. These points suggest that a separate (more restrictive) boundary may be plotted on Fig. 1 for $|\phi/\beta|_d$ between 1.5 and 3.0 as more data become available.

Finally, it is felt that Paragraph 3.3.2.6 should be relabeled "coordination of steady turns" in order to eliminate confusion that may arise from the heading control paragraph which involves coordination while rolling into and out of turns.

BACKGROUND FOR THE RECOMMENDED REVISIONS

Introduction

The ability to make precise changes in aircraft heading is a key factor in pilot evaluation of lateral-directional handling qualities. Deficiencies in heading control are directly traceable to excitation of the dutch roll

mode due to roll-yaw crosscoupling effects. It is commonly accepted piloting technique to reduce these excursions by appropriate use of the aileron and rudder, usually referred to as "coordinating the turn." The problem is that existing criteria (see, for instance, Refs. 1-3) for heading control consider aileron-only turns, ignoring or attempting to treat indirectly the effect of rudder control. The fact that these criteria are not satisfactory is shown in Ref. 4, where several configurations which violated boundaries set by aileron-only considerations were given good to excellent pilot ratings. The approach taken here is that the aileron-rudder shaping necessary to coordinate the turn is the dominant factor in pilot evaluation of heading control.

Approach

A comprehensive review of the pilot commentary made during the heading control experiments reported in Refs. 4 and 5 indicated that the rudder characteristics necessary to coordinate turns played a dominant role in the evaluations. While the use of "coordinated" aileron and rudder is accepted as common piloting technique, a quantitative measure of what exactly is acceptable or desirable is not known. The purpose of this study was to provide a quantitative measure of the aileron-rudder sequencing required to achieve coordinated turns and to correlate this with pilot opinion ratings from available data. To achieve this end we shall consider the aileron-to-rudder crossfeed necessary to obtain perfectly coordinated turns. This idealized crossfeed provides a measure of pilot acceptability of heading control because it is indicative of:

- The complexity of the rudder activity necessary to achieve perfectly coordinated turns.
- The heading excursions that occur when the pilot does not use rudder.

In general, coordinated flight implies minimum roll-yaw coupling which can be quantified in many ways, some of which are:

1. Zero sideslip angle ($\beta = 0$).
2. Zero lateral acceleration at the c.g.

3. Turn rate consistent with bank angle and speed
($r = g\phi/U_0$).
4. Zero lateral acceleration at the cockpit (ball
in the middle).

Conditions 1-3 are equivalent when the side forces due to aileron, Y_{δ_a} , and due to turn rate, Y_r , are very small, which is usually the case. The fourth turn coordination criterion is complicated by pilot location effects which, however, appear to be mainly associated with ride qualities and not with heading control itself (Ref. 4). Based on these considerations it appears that sideslip angle is an appropriate indicator of turn coordination. Accordingly, the following formulation undertakes to identify the parameters that govern the aileron-rudder shaping required to maintain coordinated flight as defined by zero sideslip angle ($\beta = 0$).

With an aileron-rudder crossfeed, Y_{CF} , the rudder, by definition, is given by:

$$\delta_{rc} = Y_{CF}\delta_{ac} \quad (1)$$

where δ_{rc} and δ_{ac} represent deflections of the cockpit controls which have their primary effect on rudder and aileron, respectively.* For the assumed ideal zero sideslip) coordination:

$$\beta = \frac{N_{\delta_{ac}}^{\beta}}{\Delta} + Y_{CF} \frac{N_{\delta_{rc}}^{\beta}}{\Delta} \delta_{ac} \equiv 0 \quad (2)$$

whereby the ideal crossfeed is:

$$Y_{CF} = \frac{\delta_{rc}}{\delta_{ac}} = - \frac{N_{\delta_{ac}}^{\beta}}{N_{\delta_{rc}}^{\beta}} \quad (3)$$

For most configurations $N_{\delta_{ac}}^{\beta}$ and $N_{\delta_{rc}}^{\beta}$ look like first-order polynomials (see Ref. 6) in the frequency range of interest, therefore:

$$Y_{CF} = - \frac{N_{\delta_{ac}}^{\beta}[s + (1/T_{\beta_a})]}{N_{\delta_{rc}}^{\beta}[s + (1/T_{\beta_r})]} \quad (4)$$

*Use of δ_{rc} and δ_{ac} accounts for control gearing and SAS effects. Use of δ_r and δ_a could be misleading in that these symbols are well established in the literature as the control surface deflections.

It is usually more convenient to express the control crosscoupling term, N'_{δ_w} , in Eq. 4 as the ratio of yawing to rolling acceleration, $N'_{\delta_w}/L'_{\delta_w}$. Since the rudder sensitivity can be separately optimized and does not usually represent a basic airframe limitation, it is appropriate to remove it from the rudder crossfeed equation. The resulting modified crossfeed, Y'_{CF} , is given as follows:

$$Y'_{CF} = Y_{CF} \frac{N'_{\delta_{rc}}}{L'_{\delta_{ac}}} = \frac{N'_{\delta_{rc}} \delta_{rc}}{L'_{\delta_{ac}} \delta_{ac}} = - \frac{N'_{\delta_{ac}} [s + (1/T_{\beta_a})]}{L'_{\delta_{ac}} [s + (1/T_{\beta_r})]} \quad (5)$$

Equation 5 indicates that the aileron-to-rudder shaping required to maintain coordinated flight ($\beta = 0$) is directly related to the separation between the aileron and rudder sideslip zeros. Using the approximations for $1/T_{\beta_a}$ and $1/T_{\beta_r}$ given in Ref. 6, the separation between these zeros is shown to be a function of the control crosscoupling and roll rate coupling as follows:

$$\frac{1}{T_{\beta_a}} - \frac{1}{T_{\beta_r}} = \underbrace{\left(\frac{L'_{\delta_{ac}}}{N'_{\delta_{ac}}} - \frac{L'_{\delta_{rc}}}{N'_{\delta_{rc}}} \right)}_{\substack{\text{Control} \\ \text{Cross} \\ \text{Coupling} \\ \text{Terms}}} \underbrace{\left(N'_p - \frac{g}{U_0} \right)^*}_{\substack{\text{Roll} \\ \text{Coupling} \\ \text{Term}}} \quad (6)$$

Equation 6 merely serves to confirm the notion that the pilot's rudder coordination requirements are directly related to the crosscoupling derivatives.

In order to provide a basis for correlation of pilot opinion with the required aileron-rudder shaping, the zero separation is normalized by $1/T_{\beta_r}$ and a "rudder shaping parameter," μ , is defined as follows:

$$\mu \equiv \frac{T_{\beta_r}}{T_{\beta_a}} - 1 \quad (7)$$

*As noted earlier, all derivatives are in the stability axis system.

It is useful to note that for many aircraft $T_{\beta r}$ is well approximated by the roll mode time constant, T_R , so that:

$$\mu \doteq \frac{T_R}{T_{\beta a}} - 1 \quad (8)$$

The frequency response characteristics of Y'_{CF} (Eq. 5) as a function of the sign of μ are shown in Fig. 3 in terms of literal expressions for the Bode asymptotes. These asymptotes indicate that the magnitude of the rudder required to coordinate is a function of $N'_{\delta ac}/L'_{\delta ac}$ at all frequencies and that the shaping of the rudder response is determined by μ . These parameters are summarized in terms of their analytical and pilot-centered functions in Table 1.

TABLE 1
PARAMETERS DEFINING THE
AILERON-RUDDER CROSSFEED

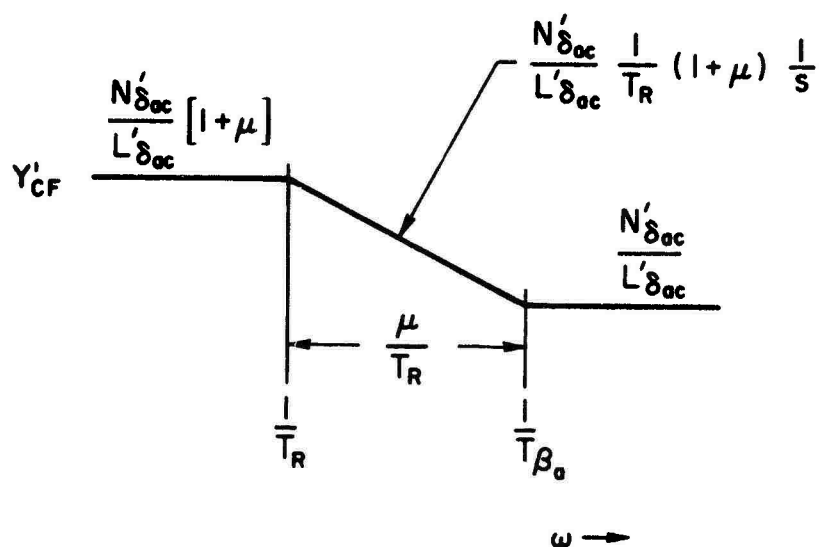
PARAMETER	ANALYTICAL FUNCTION	PILOT-CENTERED FUNCTION
μ	Defines shape of Y_{CF}	Determines complexity of rudder activity necessary for ideally-coordinated turns. Also defines phasing of heading response when rudder is not used.
$\frac{N'_{\delta ac}}{L'_{\delta ac}}$	Defines magnitude of Y_{CF}	Determines magnitude of rudder required and/or high frequency yawing induced by aileron inputs.

Practical Considerations

The parameters $N'_{\delta ac}/L'_{\delta ac}$ and μ are a natural choice for correlation of pilot rating data for heading control since they completely define the aileron-to-rudder crossfeed necessary for turn coordination. Computation of μ is straightforward as long as the β numerators in Eq. 3 are well behaved, i.e., are well represented by the approximation of Eq. 5. Cases where the

For $\mu > 0$

Lag Lead Compensation



For $\mu < 0$

Lead Lag Compensation

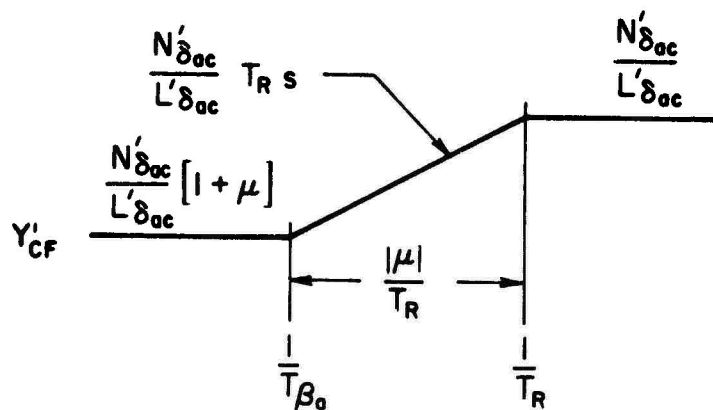


Figure 3. Asymptotes of Aileron-Rudder Crossfeed

β numerators are not well represented by Eq. 5 can be handled by computing an equivalent crossfeed. This involves matching the Bode amplitude and phase of the higher-order system with the first-order model (Eq. 5) in the frequency range of interest. (Reference 7 contains an application of this technique to equivalent short-period characteristics.) From a practical point of view, the frequency range of interest is defined by yawing excursions that are neither too rapid for the pilot to correct (with rudder) nor so slow as to be considered steady-state trim. The high-frequency zeros which occur at approximately N'_0/Y'_0 in the sideslip numerators are a typical example of the former. These roots give rise to rapid initial rudder reversals which are not indicative of representative pilot activity and do not enter into the coordination problem. (An example of this effect is shown in Appendix B.) Other typical examples are high frequency SAS and control actuator modes.

An approximate upper bound on the frequency range of interest can be obtained from the experiments and tracking models of Refs. 8 and 9, respectively. The Ref. 8 experiments, which involved a rudder-only tracking task, show that the pilot's effective neuromuscular lag (τ_e) is approximately 0.2 seconds. From the "crossover" pilot model of Ref. 9, it is possible to compute a maximum crossover frequency (neglecting possible dutch roll "interference") indicative of tight tracking (maximum pilot effort). The crossover model is given as:

$$Y_p Y_c = \frac{\omega_c e^{-\tau_e j\omega}}{j\omega} \quad (9)$$

where ω_c is the gain-crossover frequency (frequency corresponding to unity open-loop pilot-vehicle gain). For stable closures the phase margin, given by:

$$\phi_M = \frac{\pi}{2} - \tau_e \omega_c = \frac{\pi}{2} - 0.2 \omega_c \quad (10)$$

must be positive. Reasonable minimum phase margins of the order of 20 deg yield a corresponding maximum crossover frequency of 6.1 rad/sec. While this number is approximate and may not apply directly to aileron-rudder

coordination, it is indicative of the maximum frequency for piloted use of rudder control.

A lower bound on the frequency range of interest is set by the minimum acceptable outer heading loop crossover frequency (the inner bank angle loop is also properly closed) on the basis that lateral-directional attitude changes below this frequency are basically steady-state maneuvers. Results of a simulation experiment involving SST configurations indicated that a minimum heading crossover of about $1/3$ rad/sec was necessary for desirable handling qualities (see Ref. 10). More maneuverable type aircraft will undoubtedly require increased heading bandwidth; therefore $1/3$ rad/sec represents a conservative lower limit for all aircraft categories. It should be noted that rudder coordination in steady turns is treated separately in Paragraph 3.3.2.6 of MIL-F-8785B.

Even with the frequency range of interest defined as above (i.e., $1/3$ to 6 rad/sec), there will be practical difficulties relative to matching and interpreting the frequency domain definition of μ for those situations where the ideal crossfeed departs significantly from the first-order form of Eq. 5. In such cases, it is simpler and more direct to determine μ on the basis of the rudder time response characteristics. For instance, assuming the Eq. 5 form and in view of the definition of μ (Eq. 7), the rudder required to coordinate a step wheel or stick input is given by:

$$\delta_{rc}(t) = \delta_{rc0} \left[1 + \mu \left(1 - e^{-t/T_{\beta r}} \right) \right] \quad (11)$$

where:

$\delta_{rc0} = -N'_{\delta ac} \delta_{ac} / N'_{\delta rc}$ neglects the high-frequency $N'_{\delta ac} / Y'_{\delta ac}$ dynamics in accordance with the 6 rad/sec cutoff frequency

Note that δ_{rc} refers to the rudder pedal motion (thereby eliminating effects of rudder gearing and accounting for the SAS). Solving Eq. 11 for the rudder shaping parameter, μ :

$$\mu = \left[\left(\frac{\delta_{rc}(t)}{\delta_{rc0}} - 1 \right) \frac{1}{1 - e^{-t/T_{\beta r}}} \right] \quad (12)$$

The value of μ computed from the time-history (Eq. 12) is independent of the final time chosen and is equivalent to that obtained from the Bode asymptotes of the first-order model in Fig. 3. However, for cases where the β numerators are not well approximated by the first-order model, the value of μ depends on the value of t (used in Eq. 12) which is properly set by the lower limit on the frequency range of interest; $\omega_{\min} = 1/3$, or $t = 3.0$ seconds.

Based on the above considerations, the "standard" procedure utilized to compute the values of μ was to eliminate all roots of the β numerators above values of about 6 rad/sec but to take into account their effect on the high-frequency gain; and to set all roots much below 0.33 rad/sec to zero. If the resulting Y_{CF}' was of first-order form (Eq. 5) the value of μ was determined through direct use of the Eq. 7 definition. If not, the rudder time history to a step δ_{ac} input was computed and used, as in Eq. 12, to calculate the value of $\mu \doteq [\delta_{rc}(3)/\delta_{rc0} - 1][1/(1 - e^{-3/T_{Br}})]$.^{*} An example calculation of μ is given in Appendix A.

Figure 4 presents typical coordinating ($\beta = 0$) rudder time histories for step aileron inputs on a grid of μ vs. $N_{\delta_{ac}}'/L_{\delta_{ac}}'$. Moving vertically on this grid changes the shape (μ) of the crossfeed, Y_{CF}' , keeping the initial value (high-frequency gain) constant. Moving horizontally produces a change in the crossfeed gain ($N_{\delta_{ac}}'/L_{\delta_{ac}}'$) at all frequencies without changing the shape. Note that this is consistent with Table 1 and Fig. 3, where it is shown that μ dictates the required aileron-to-rudder shaping and $N_{\delta_{ac}}'$ defines the magnitude of the gain for all times (and frequencies). A physical interpretation relating the crosscoupling derivatives $N_{\delta_{ac}}'$ and N_p' with the rudder shaping parameter, μ , is given in Table 2.

Making use of the fact that required aileron-to-rudder coordination is completely defined by $N_{\delta_{ac}}'/L_{\delta_{ac}}'$ and μ , it is now possible to test our original hypothesis, i.e., pilot rating of heading control is dominated by these coordination requirements. This is accomplished by plotting applicable pilot rating data on a grid of μ vs. $N_{\delta_{ac}}'/L_{\delta_{ac}}'$. Note that every point on this plane defines a unique aileron-rudder time history as discussed above.

^{*} $\delta_{rc}(3)$ is the required rudder pedal position for "perfect" ($\beta = 0$) coordination 3 seconds after a step aileron control input.

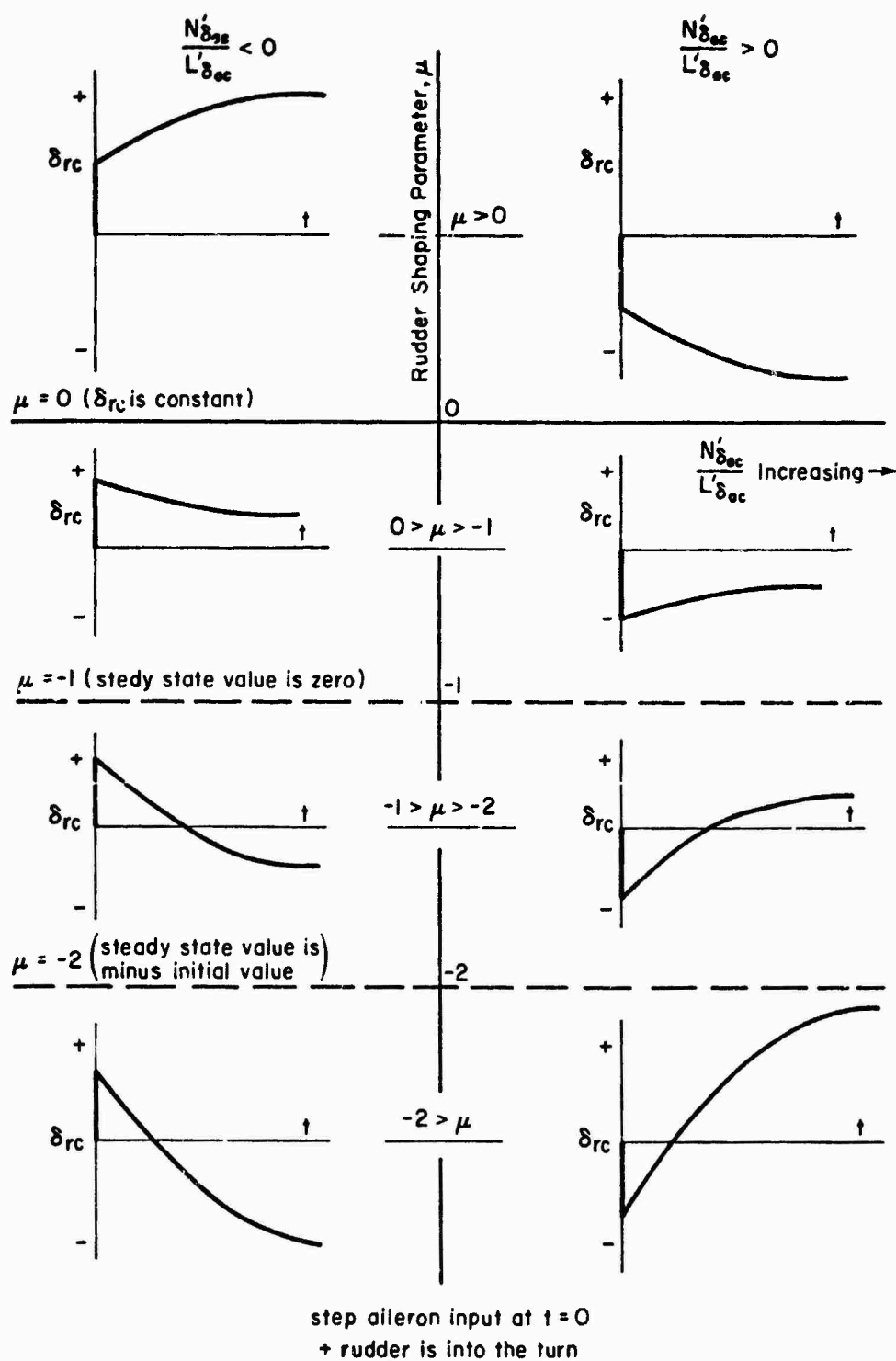


Figure 4. Typical Rudder Time Histories for Zero Sideslip

TABLE 2
PHYSICAL INTERPRETATION OF μ

VALUE OF RUDDER SHAPING PARAMETER	ROLL YAW CROSSCOUPLING CHARACTERISTICS
$\mu > 0$	$N'_{\delta_{ac}}$ and N'_p are additive, indicating that the crosscoupling effects increase with time after an aileron input.
$\mu = 0$	$N'_p = g/U_0$, indicating that all roll-yaw crosscoupling is due to $N'_{\delta_{ac}}$. The aileron-rudder cross-feed is therefore a pure gain.
$-1 < \mu < 0$	$N'_{\delta_{ac}}$ and N'_p are opposing. Initial crosscoupling induced by $N'_{\delta_{ac}}$ is reduced by N'_p as the roll rate builds up. Exact cancellation takes place when $\mu = -1$, resulting in a zero rudder requirement for steady rolling.
$\mu \ll -1$	Low frequency and high frequency crosscoupling effects are of opposite sign, indicating a need for complex rudder reversals for coordination. If rudder is not used, the nose will appear to oscillate during turn entry and exit.

$N'_{\delta_{ac}}/L'_{\delta_{ac}}$ Near Zero

Analysis of available pilot rating data and pilot commentary, Refs. 4, 10, and 11, indicates that control crosscoupling effects are not a factor when $|N'_{\delta_{ac}}/L'_{\delta_{ac}}| < 0.03$. This is also consistent with the fact that the rudder shaping parameter, μ , is largely meaningless as $\delta_{rc0} \rightarrow 0$ (see Eq. 12). For $N'_{\delta_{ac}}/L'_{\delta_{ac}}$ identically zero, the required aileron-rudder crossfeed takes the Bode asymptote form shown in Fig. 5. The rudder magnitude required to coordinate mid-frequency and high-frequency aileron (wheel) inputs is seen to be dependent on the roll crosscoupling, $g/U_0 - N'_p$, whereas low-frequency rudder requirements are dependent on N'_r . The required rudder shaping has the characteristics of a rate system (ramp δ_{rc} to step δ_{ac} input) at low and high frequency. Note that rudder reversals are still possible since $1/T_{\beta_a}$ is negative for negative $g/U_0 - N'_p$ (proverse roll yaw coupling). However, unlike the cases with high aileron yaw, these reversals are of little practical significance. For example, if the high-frequency rudder response is large (large $|g/U_0 - N'_p|$), then the reversal occurs at very low frequency (small $1/T_{\beta_a}$) — out of the range of interest. If the high-frequency rudder response is small, all effects, including the reversal effect, are negligible. Accordingly, aileron-rudder shaping per se is not

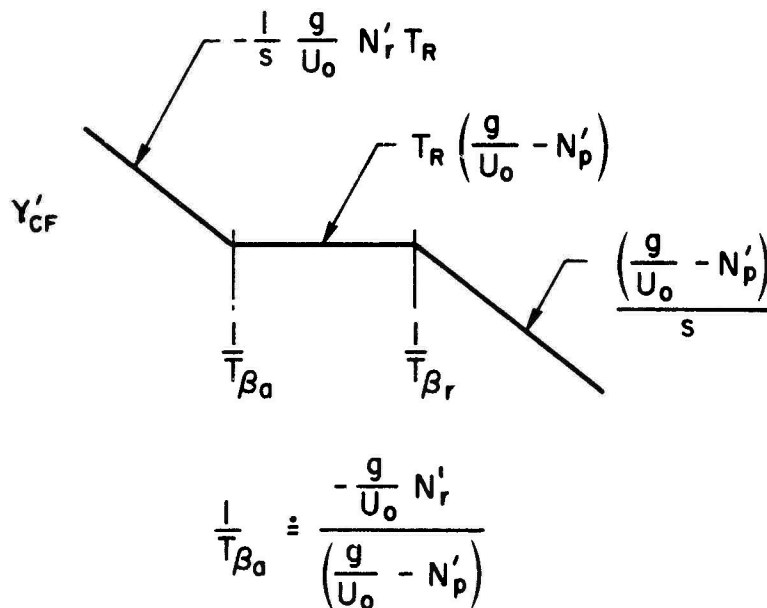


Figure 5. Required Crossfeed for $N'_{\delta_{ac}} = 0$

the essence of the problem, which reduces, instead, to concern with the general magnitude of the required rudder crossfeed.

From Fig. 5 it is seen that $g/U_0 - N_p'$ provides a good measure of such magnitude; and, in fact, correlation of pilot rating data (for $|N_{\delta_{ac}}'/L_{\delta_{ac}}'| < 0.03$ with $g/U_0 - N_p'$ is quite good. However, difficulties associated with estimating an effective $g/U_0 - N_p'$ for augmented airframes presents practical problems which make this parameter somewhat unattractive. Also, for configurations with $1/T_{\beta_a}$ close to $1/T_{\beta_r}$, the effects due to N_r' (see Fig. 5) can be important. A more general approach is to compute a time history based on a unit step aileron input into Y_{CF}' . Physically, this represents the required rudder control power for coordination of a unit step aileron control input, that is (from Eq. 5):

$$Y_{CF}'\delta_{ac} = \frac{N_{\delta_{rc}}'}{L_{\delta_{ac}}'} \delta_{rc} \quad (13)$$

Utilizing the same response time considerations as in the computation of μ , $Y_{CF}'\delta_{ac}$ at $t = 3$ seconds, or $(N_{\delta_{rc}}'/L_{\delta_{ac}}')\delta_{rc}(3)$, is suggested as the correlating parameter for $|N_{\delta_{ac}}'/L_{\delta_{ac}}'| < 0.03$.

Experimental Data Correlations

On the basis of the foregoing, pilot ratings should correlate: for $|N_{\delta_{ac}}'/L_{\delta_{ac}}'| > 0.03$, with μ and $N_{\delta_{ac}}'/L_{\delta_{ac}}'$; and for $|N_{\delta_{ac}}'/L_{\delta_{ac}}'| < 0.03$, with $(N_{\delta_{rc}}'/L_{\delta_{ac}}')\delta_{rc}(3)$. However, before proceeding with such correlations, it is necessary to establish ground rules to isolate pilot ratings which are primarily oriented towards heading control. In this regard it is important to note that heading is basically an outer loop (see Ref. 10) and cannot be satisfactory if the inner loop (bank angle) is not satisfactory. The ground rules listed in Table 3 reflect basic requirements for good inner-loop and other (except heading control) handling characteristics. The requirements on ζ_d , ω_d , and T_R are based on the current MIL-F-8785B limits for Level 1 flying qualities. The Level 2 boundary on ϕ_{osc}/ϕ_{ave} is used because the Level 1 boundary appeared too restrictive, i.e., many data points with good pilot ratings were found to plot outside the Level 1 ϕ_{osc}/ϕ_{ave} boundary. This result is also found in Ref. 12 and a less conservative boundary is proposed there. The restriction on $|\phi/\beta|_d$ for $|N_{\delta_{ac}}'/L_{\delta_{ac}}'|$ greater than 0.03 is based on

TABLE 3

GROUND RULES FOR APPLICATION OF RATING DATA
TO HEADING CONTROL CRITERIA

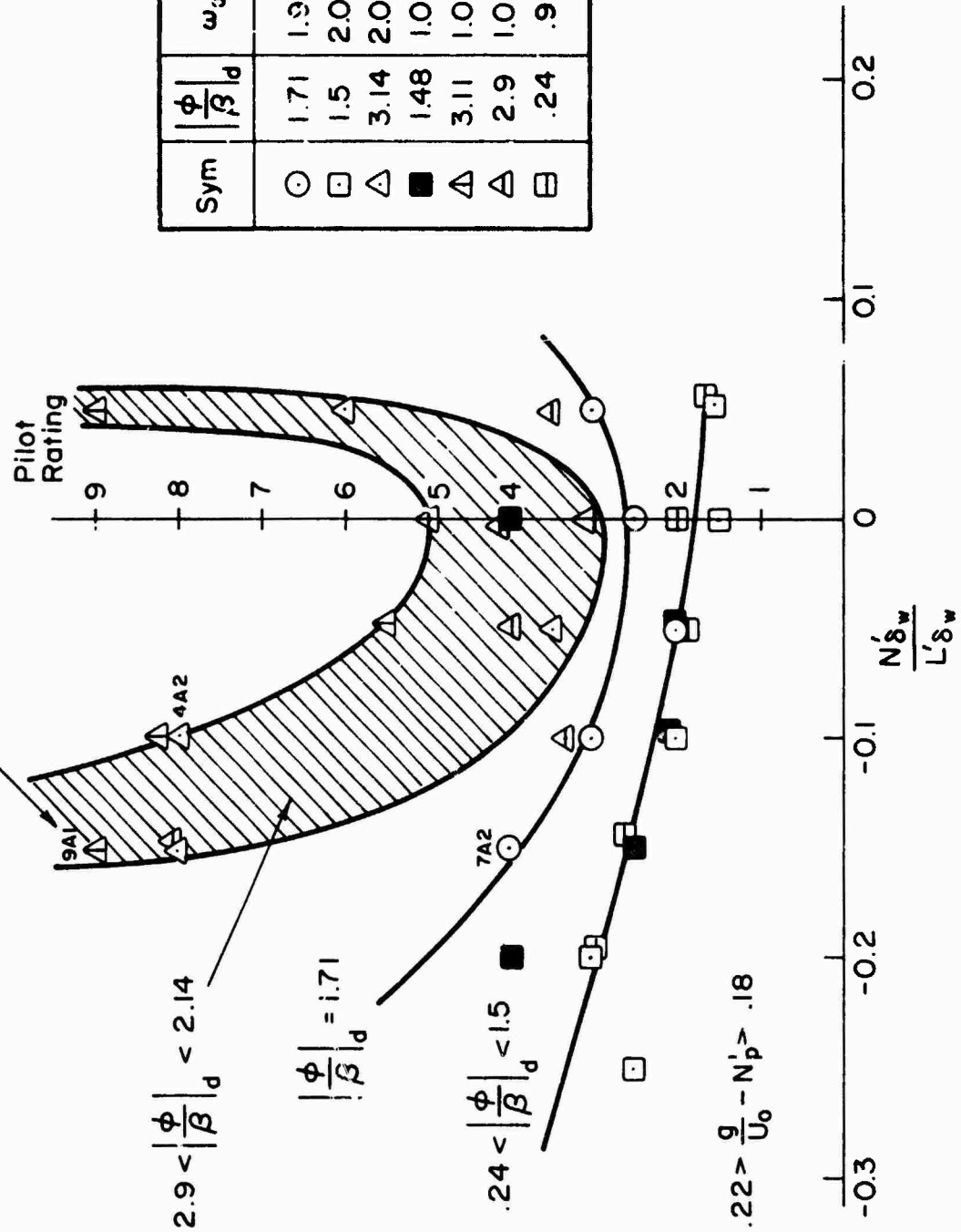
1. $T_R < 1.25$
2. $\omega_d > 0.4$
3. $\xi_d > 0.08$ and $\xi_d \omega_d > 0.15$
4. $|\phi/\beta|_d < 1.5$ when turbulence is a factor and $|N'_{\delta_{ac}}/L'_{\delta_{ac}}| > 0.03$
5. Meets Fig. 7 boundaries when $|N'_{\delta_{ac}}/L'_{\delta_{ac}}| \leq 0.03$
6. Meets Level 2 ϕ_{osc}/ϕ_{ave} in Ref. 2
7. Pilot comments do not indicate:
 - a. significant roll control problems
 - b. control power or sensitivity problems
 - c. nonlinear control system problems such as friction, breakout, etc.
 - d. excessive gust response

results obtained from the in-flight simulation data of Refs. 12 and 13. The Ref. 12 data plotted in Fig. 6 show that pilot ratings are very sensitive to increasing values of $|N'_{\delta_{ac}}/L'_{\delta_{ac}}|$ when $|\phi/\beta|_d > 1.5$. The pilot commentary corresponding to selected points in Fig. 6 are given below to help explain the data.

- Configuration 7A2. "Difficulty in coordination in terms of maintaining heading under turbulent conditions."
- Configuration 9A1. "Problems in non-turbulent conditions magnified in turbulence. Pilot must cope with rudders and some aileron to keep aircraft in control."
- Configuration 4A2. "Rapid deterioration of handling qualities in turbulence."

This commentary is consistent with the results obtained in Ref. 11 where it is shown that increasing dihedral (large $|\phi/\beta|_d$) is primarily a problem

Configuration number to identify
pilot commentary in text



Sym	$\left \frac{\phi}{\beta} \right _d$	ω_d	ζ_d	Group
○	1.71	1.98	.1	2
□	1.5	2.01	.24	3
△	3.14	2.02	.1	4
■	1.48	1.01	.29	7
△	3.11	1.09	.12	9
△	2.9	1.03	.25	10
□	.24	.98	.34	12

Figure 6. Effect of $\left| \frac{\phi}{\beta} \right|_d$ and $N'\delta_w/L'\delta_w$ on Pilot Ratings in Turbulence (Ref. 12 Data)

when turbulence is a factor. Such effects can be interpreted in terms of basic piloting technique as follows. The problem of flying a constant heading in turbulence primarily consists of keeping the average bank angle at zero. Because of the inherent neutral stability of an aircraft in roll ($L_{\phi} = 0$), the pilot is required to continually use aileron to pick up a low wing to keep the aircraft from turning. If the aircraft has large aileron-yaw crosscoupling (large $N'_{\delta_{ac}}/L'_{\delta_{ac}}$), each aileron input will induce a large sideslip which further magnifies the effect of turbulence. This sort of rolling and sideslipping is extremely disconcerting and may, in some cases, border on loss of control. Rather than accept this, the pilot must use coordinated rudder with aileron when regulating against rolling gusts. The increased workload imposed by this requirement gives rise to the rapid deterioration in rating with increasing aileron-yaw crosscoupling. On the other hand, aircraft with low $|\phi/\beta|_d$ exhibit a snaking tendency in turbulence, requiring very little aileron input to keep wings level. Because of the inherent directional stability (r_p), the lateral oscillations tend to average out with little effect on the lateral flight path angle. The data presented in Fig. 6 quantitatively define the value of $|\phi/\beta|_d$ where heading control is contaminated by roll control problems (in turbulence) as about 1.5. This is the basis for Ground Rule No. 4 (Table 3).

It is clear from the above discussion and Fig. 6 that when aileron cross-coupling is small, the effect of dihedral is less critical. This is accounted for by using the variable stability Navion data from Ref. 11 where the dihedral (L'_p) was varied over a wide range with low or zero $|N'_{\delta_{ac}}/L'_{\delta_{ac}}|$. The 3-1/2 pilot rating boundaries from these experiments are given in Fig. 7 and form the basis for Ground Rule No. 5.* Comparison of these boundaries with other low $|N'_{\delta_{ac}}/L'_{\delta_{ac}}|$ data (Refs. 12 and 13) is favorable. They were used to allow inclusion of certain of the $|\phi/\beta|_d > 1.5$ data for $|N'_{\delta_{ac}}/L'_{\delta_{ac}}| < 0.03$ and thereby to permit an expanded base for the pertinent correlations. It should be noted that attempts to isolate these $|\phi/\beta|_d$ characteristics using ϕ_{osc}/ϕ_{ave} were not successful. It is felt that the reason for this is that ϕ_{osc}/ϕ_{ave} is an aileron-only parameter, whereas the roll control problems under discussion are related to rudder coordination requirements.

*The boundary for $\zeta_d = 0.4$ is based on only a few data points and was faired by the author.

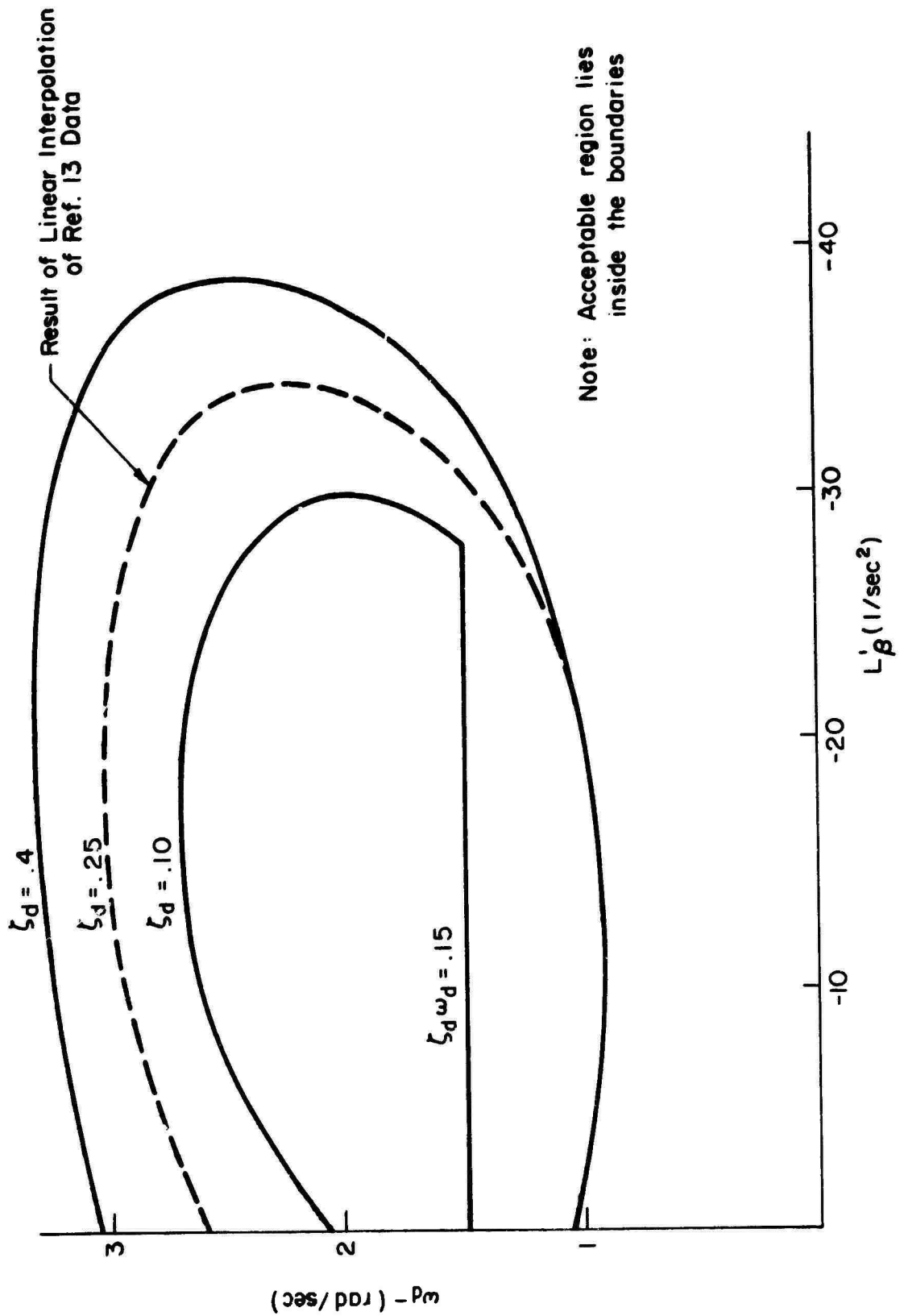


Figure 7. Pilot Rating Boundaries for Acceptable Roll Control in Turbulence with $N'_{\delta ac}/L'^{\zeta}_{\delta ac} < 0.03$ (From Ref. 11)

A summary of the data considered is given in Table 4. Each of the data points found to be applicable to heading control (met the ground rules) is plotted and faired on a logarithmic grid of $N'_{\delta_{ac}}/L'_{\delta_{ac}}$ vs. μ in Fig. 8. When $N'_{\delta_{ac}}/L'_{\delta_{ac}}$ is near zero (≤ 0.03) the pilot rating data are plotted versus $(N'_{\delta_{ac}}/L'_{\delta_{ac}})\delta_{rc}(3)$ in Fig. 9. Due to a lack of data for large adverse N_p it was necessary to extrapolate the data fairing in Fig. 9 to obtain a Level 2 requirement for $(N'_{\delta_{ac}}/L'_{\delta_{ac}})\delta_{rc}(3)$. This boundary should be adjusted as more data become available. Only in-flight and moving-base simulator data were considered. With the exception of one or two points the data from all the sources in Table 4 coalesce quite nicely. The criterion in Fig. 8 is conservative in that the few points that "do not fit" are rated better than the other data in the same region.

TABLE 4
SUMMARY OF CORRELATED DATA

TYPE OF AIRCRAFT SIMULATED	DESCRIPTION OF SIMULATOR	REF.	TOTAL NUMBER OF DATA POINTS	NUMBER OF POINTS MEETING GROUND RULES
Executive Jet and Military Class II	Variable Stability T33	12	84	16
STOL	Variable Stability Helicopter	5	109	30
General Aviation (Light Aircraft)	Variable Stability Navion	13	26	6
Jet Fighter- Carrier Approach	Variable Stability Navion	11	36	22
Space Shuttle Vehicle	6 DOF Moving Base with Redifon Dis- play (NASA Ames FSAA)	4	52	52
STOL	3 DOF Moving Base (NASA Ames S-16)	1	8	7

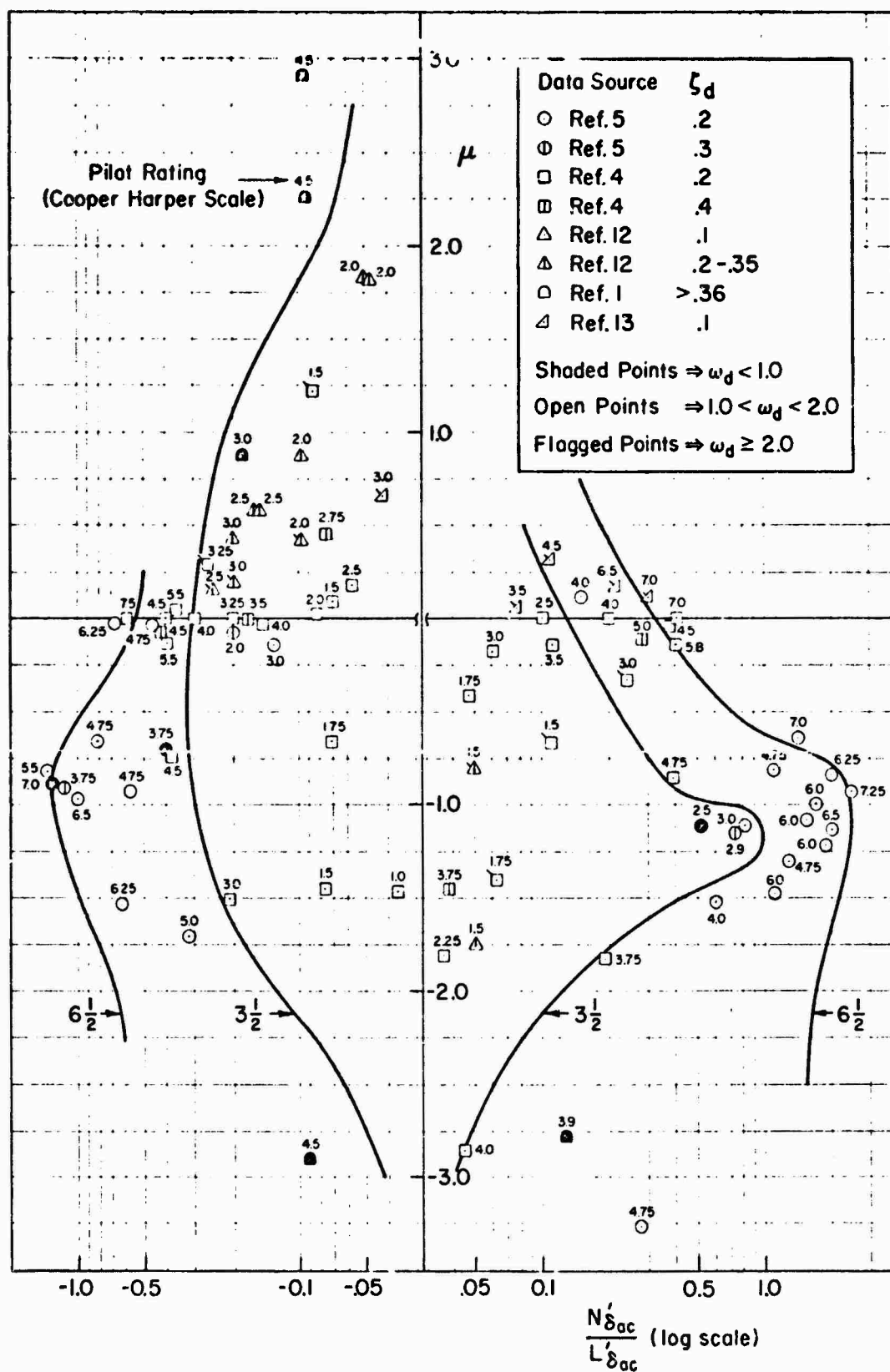


Figure 9. Pilot Rating Correlation with Crossfeed Parameters

Sym	Data Source	ζ_d
○	Ref. 5	.2
□	Ref. 4	.2
▢	Ref. 4	.4
△	Ref. 13	.1
◁	Ref. 11	.1-.2
▷	Ref. 11	.4
◻	Ref. 1	.24-.37
△	Ref. 12	.1-.2
△	Ref. 12	.34

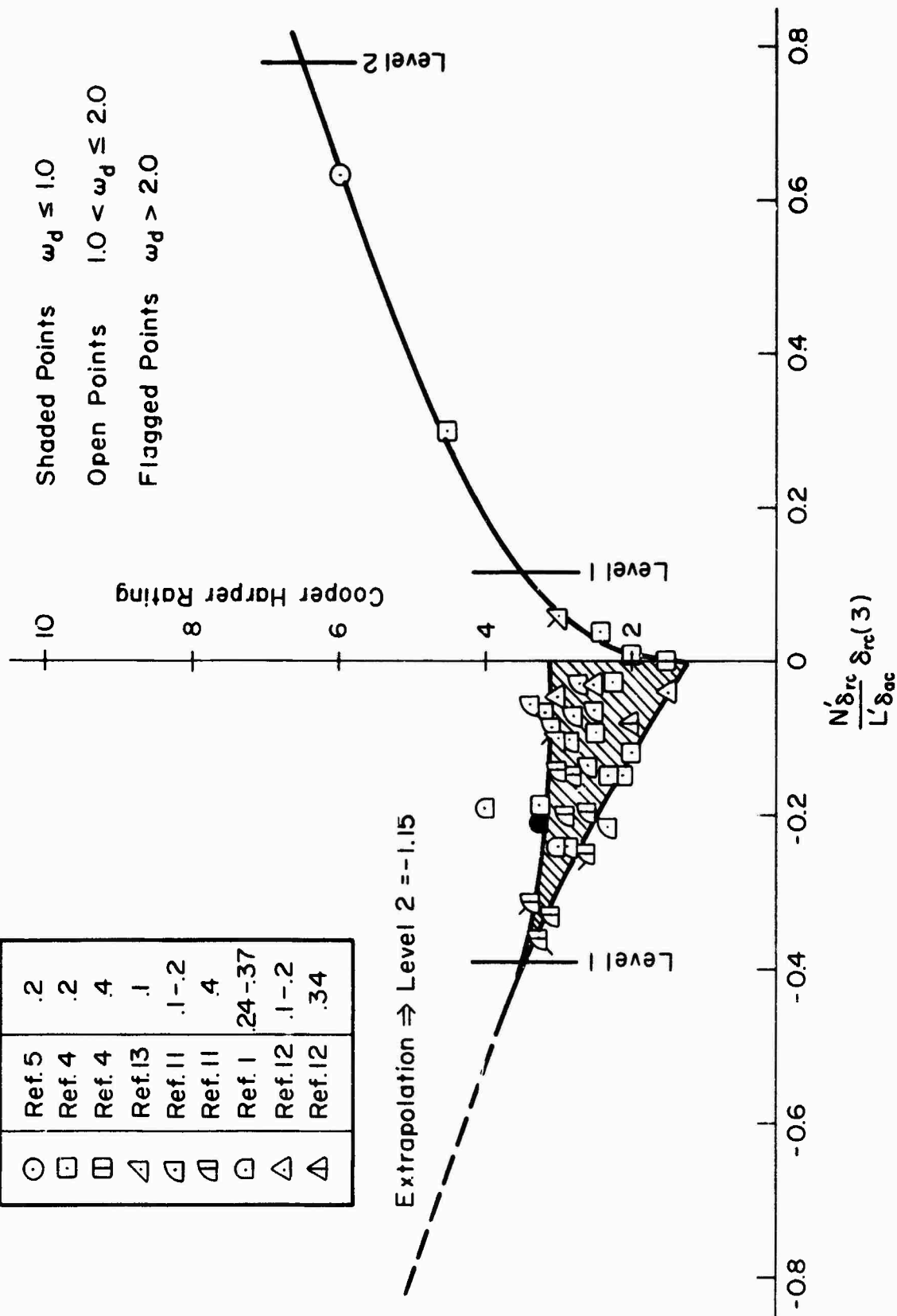


Figure 9 Pilot Rating Correlations when $|N' \delta_{ac} / L' \delta_{ac}| < 0.03$

The data plotted in Figs. 8 and 9 are replotted on the current MIL-F-8785B sideslip criterion in Fig. 10 to compare the rudder coordination boundaries with boundaries set by aileron-only considerations. Many very good pilot ratings are seen to fall outside even the 6-1/2 boundary in Fig. 10. The pilot commentary from three of the Ref. 4 configurations which fall outside the 6-1/2 (Level 2) boundary in Fig. 10 but have ratings of 4.5 and better are given below.

4B

- "Required considerable rudder for directional control."
- "Can do better with rudders."
- "Has a tendency to snap around with aileron."

5A

- "Has to be coordinated." "Is simple to coordinate."
- "Bad without rudder." "Rudder makes it flyable. Give it a 7 without rudder and a 4.5 with rudder."

5B

- "Good heading control configuration; easy to lead aileron with rudder."
- "Give it a pilot rating of 5.5 without rudder and a 3.5 with the rudder."

These comments reflect the pilots' ability to use rudder to improve the aircraft heading characteristics. The poor correlation between pilot ratings and the current specification (Fig. 10) is therefore felt to be directly attributable to the fact that rudder control is not accounted for.

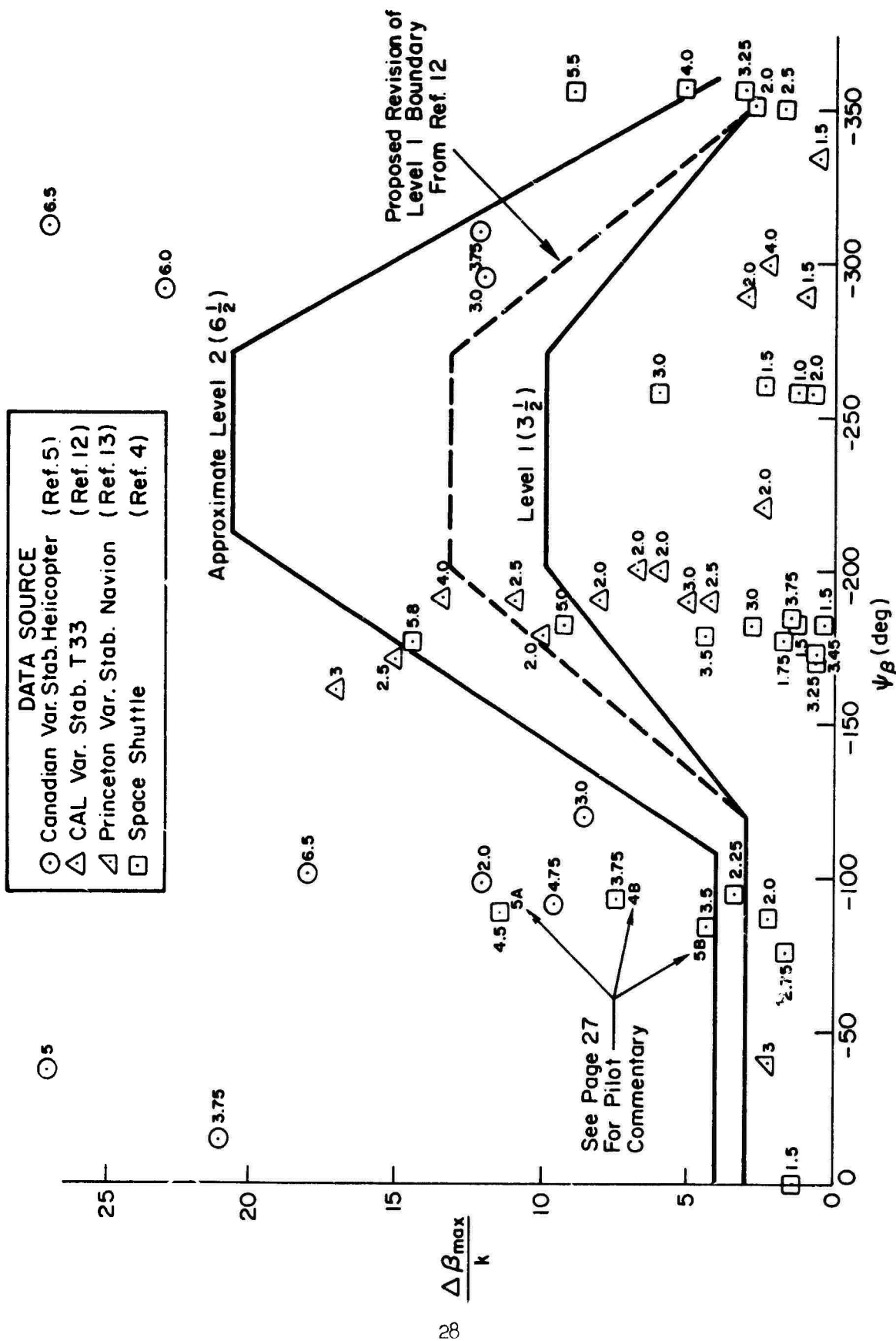


Figure 10. Correlation Data on $\Delta \beta_{\max}$ k vs. ψ_{β} Plot

Physical Interpretation

The iso-opinion lines in Fig. 8 indicate that some values of the rudder shaping parameter, μ , are more desirable than others in that they are less sensitive to an increase in aileron yaw. The following observations help to explain this trend in terms of pilot-centered considerations.

- Moderately high proverse (positive) $N'_{\delta_{ac}}$ is acceptable in the region where $\mu = -1$. Physically, this corresponds to a sudden initial heading response in the direction of turn followed by decreasing rudder requirements. (Required steady state rudder is zero when $\mu = -1$, see Fig. 4.) It is felt that the pilots are accepting the initial proverse yaw as a heading lead and are not attempting to use cross control rudder.
- The allowable values of proverse $N'_{\delta_{ac}}$ decrease rapidly as μ becomes greater than -1 . Physically this corresponds to an increase in the requirement for low frequency cross control rudder activity (see Fig. 4) which is highly objectionable.
- The pilot ratings are less sensitive to the required rudder shaping when $N'_{\delta_{ac}}$ is negative (adverse yaw). Note that adverse yaw is consistent with conventional piloting technique.
- The rapid decrease in ratings that occurs as μ becomes much less than -1 is due to the rudder reversal required in this region (see Fig. 4). If the rudders are not used, the nose of the aircraft will appear to wander back and forth as the pilot rolls into and out of turns.

It is significant that the pilot rating correlations are not dependent on the type of aircraft and in fact are shown to be valid for vehicles ranging from light aircraft to fighter, STOL, and space shuttle configurations. This result indicates that good heading control characteristics are dependent on a fundamental aspect of piloting technique (aileron-rudder coordination) and that such factors as aircraft size, weight, approach speed, etc., can be neglected for all practical purposes. It is felt that

the invariance of ratings with aircraft "class" is related to the pilot's ability to adapt to different situations and to rate accordingly. Finally, the excellent correlation of pilot ratings with the aileron-rudder crossfeed characteristics indicates that the required rudder coordination is indeed the dominant factor in pilot evaluation of heading control.

The rudder shaping parameter is attractive as a heading control criterion because the handling quality boundaries are easily interpreted in terms of pilot-centered considerations.

Conclusions

The main conclusions are summarized as follows:

- Pilot evaluation of heading control is highly correlatable with the aileron-rudder sequencing required to coordinate turns.
- Very good correlation has been obtained with data from widely varying classes of aircraft.

The results to date have been very encouraging. The crossfeed parameter seems to have great potential as a heading control criterion. Additional experimental data to investigate certain regions of the criterion planes in Figs. 8 and 9 are highly desirable.

SECTION III

REQUIREMENTS FOR AIRPLANE NORMAL AND FAILURE STATES

SUGGESTED REVISIONS

6.7.2 Level Definitions. To determine the degradation in flying qualities parameters for a given Airplane Failure State the following definitions are provided:

a. Level 1 is better than or equal to the Level 1 boundary, or number, given in Section 3. When both longitudinal and lateral directional parameters lie on or very near the Level 1 boundary, the flight situation involved may be marginal relative to its Level 1 status; further study and disposition is then required.

b. Level 2 comprises conditions where, for a given flight situation:

(1) Longitudinal (or lateral-directional) parameters are better than, or equal to, Level 1; and lateral-directional (or longitudinal) parameters are worse than Level 1, but no worse than the Level 2 boundary or number; or

(2) Both longitudinal and lateral directional parameters are worse than Level 1 but no worse than the boundaries or numbers halfway between the Level 1 and Level 2 boundaries or numbers.

Note: The halfway rule is intended to reflect ratings halfway between Levels 1 and 2. It does so for most of the specification criteria; however, there are some (e.g., 3.2.1.2, 3.3.1.2, 3.3.2.4, 3.3.4) where the halfway points between Levels 1 and 2 criteria are not halfway points in ratings. In such cases the "halfway" boundary should be selected according to the Ref. 16 (or other applicable) data to reflect a rating halfway between Levels 1 and 2.

c. Level 3 is worse than Level 2, but no worse than the Level 3 boundary, or number.

When a given boundary, or number, is identified as Level 1 and Level 2, this means that flying qualities outside the boundary conditions shown, or worse than the number given, are at best Level 3 flying qualities. Also, since Level 1 and Level 2 requirements are the same, flying qualities must be within this common boundary, or number, in both the Operational and Service Flight Envelopes for Airplane Normal States (3.1.10.1). Airplane Failure States that do not degrade flying qualities beyond this common boundary are not considered in meeting the requirements of 3.1.10.2. Airplane Failure States that represent degradations to Level 3 must, however, be included in the computation of the probability of encountering Level 3

degradations in both the Operational and Service Flight Envelopes. Again degradation beyond the Level 3 boundary is not permitted regardless of component failures.

3.1.10.1 Requirements for Airplane Normal States. — No change

3.1.10.2 Requirements for Airplane Failure States. — No change

1.5 Levels of Flying Qualities. — No change

DISCUSSION

General

The suggested revision reflects available experimental evidence for a cumulative deterioration in overall flying qualities when more than one control axis is degraded. Among the earliest such recorded evidence is that given in Fig. 11 (from Ref. 15), reproduced below for illustrative purposes.

Here it is clear that to retain overall (i.e., complete six degree of freedom) Level 2 flying qualities as defined in Ref. 16 (Cooper rating < 5.5), the individual longitudinal and lateral-directional flying qualities must each be considerably better than the Level 2 (Cooper rating = 5.5) boundary.

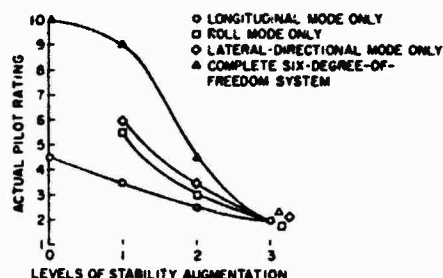


Figure 23.- Comparison of pilot opinions obtained from flying separate modes of airframe motion with pilot opinion obtained from flying complete six-degree-of-freedom system. (Ref. 15)

Figure 11

In order to determine, as generally as possible, how individual ratings in each of two or three axes combine to give an overall rating, the available data contained in Refs. 17-20 were examined in light of certain theoretical considerations, discussed below. The data of Ref. 15, shown above, were not seriously considered because they relate to ratings for a complete re-entry trajectory and appear to be noncorresponding sets; i.e., the particular flight conditions leading to the individual axis ratings are not necessarily those which combine to give the overall rating.

Theoretical Considerations

It is possible, of course, to simply "massage" the given data to obtain best-fit laws which correlate the individual with the combined-axis ratings. Such a course of action would undoubtedly yield overall results similar to those obtained (e.g., see Ref. 18). However, it would provide little insight into questions relating to "illegitimate" mathematical operations on noninterval ratings; and to the workload effects of combined axes. The correlation procedure actually used took both these considerations into account.

Relative to the nature of flying qualities rating scales, McDonnell (Ref. 21) and Madill (Ref. 22) have each derived transformations which convert ordinal ratings to an interval scale as shown in Fig. 12 (taken from Ref. 23). The ψ' transformation (Ref. 21) is based on the use of collected "scores," for word and phrase descriptors of flying qualities, to establish successive intervals. The R'' transformation (Ref. 22) results from the observation that histograms of the variations in pilot ratings presented in Ref. 24 can be fitted by a Binomial Distribution for nine trials. A similar conclusion was reached by Gedeon (Ref. 25), based on in-flight ratings of five sailplane types by from 38 to 70 pilots each. The data bases used by Madill and Gedeon suggest that the R'' transformation may be more generally applicable to flying qualities data than the ψ' transformation. However, the R'' transformation still suffers in that it has little apparent physical connection with the attentional, workload demands on the pilot, which are crucial to the issue of combined axes effects.

While not specifically denoted a transformation in the sense discussed above, the Ref. 21 rating correlations with λ_s , the secondary task score, can serve both to identify an interval transformation and to relate ratings to attentional demands on the pilot. Figure 13, which displays the Ref. 21 correlations, shows that the best-gain ratings are linear with λ_s . The ratings are those for control of only the (primary) single axis configurations shown in Fig. 13; the values of λ_s were the maximum λ 's achievable when controlling both the primary axis and a secondary (roll) axis with unstable dynamics given by $\lambda/(s - \lambda)$, where the value of λ was varied as a function

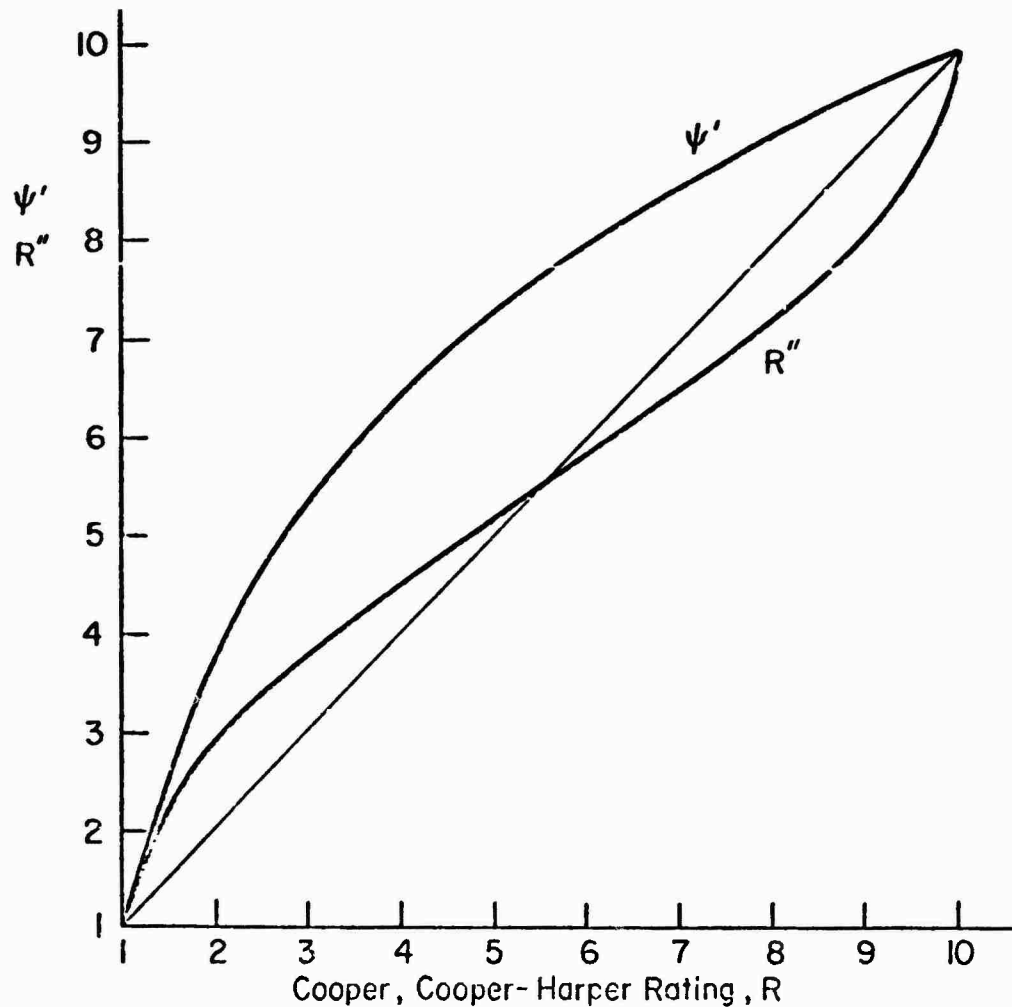


Figure 12. A Comparison of Rating Transformations (Ref. 23)

of the primary task performance. The result of the so-paced combined primary and secondary tasks was that the pilot was completely saturated relative to any additional visual-motor activities. Thus the values of λ_s/λ_c achieved represent the excess capacity available when performing only the primary task. That is, $\lambda_s/\lambda_c \equiv \lambda_n = 1.0$ represents a condition where 100 per cent of the pilot's control capacity is available for tasks other than control of the (single) primary axis (e.g., for full attention to the secondary task); hence the rating is low (good), around 1.0 (see Fig. 14). A rating of 3-1/2 corresponds to a $\lambda_n \doteq 0.66$ or to an available excess

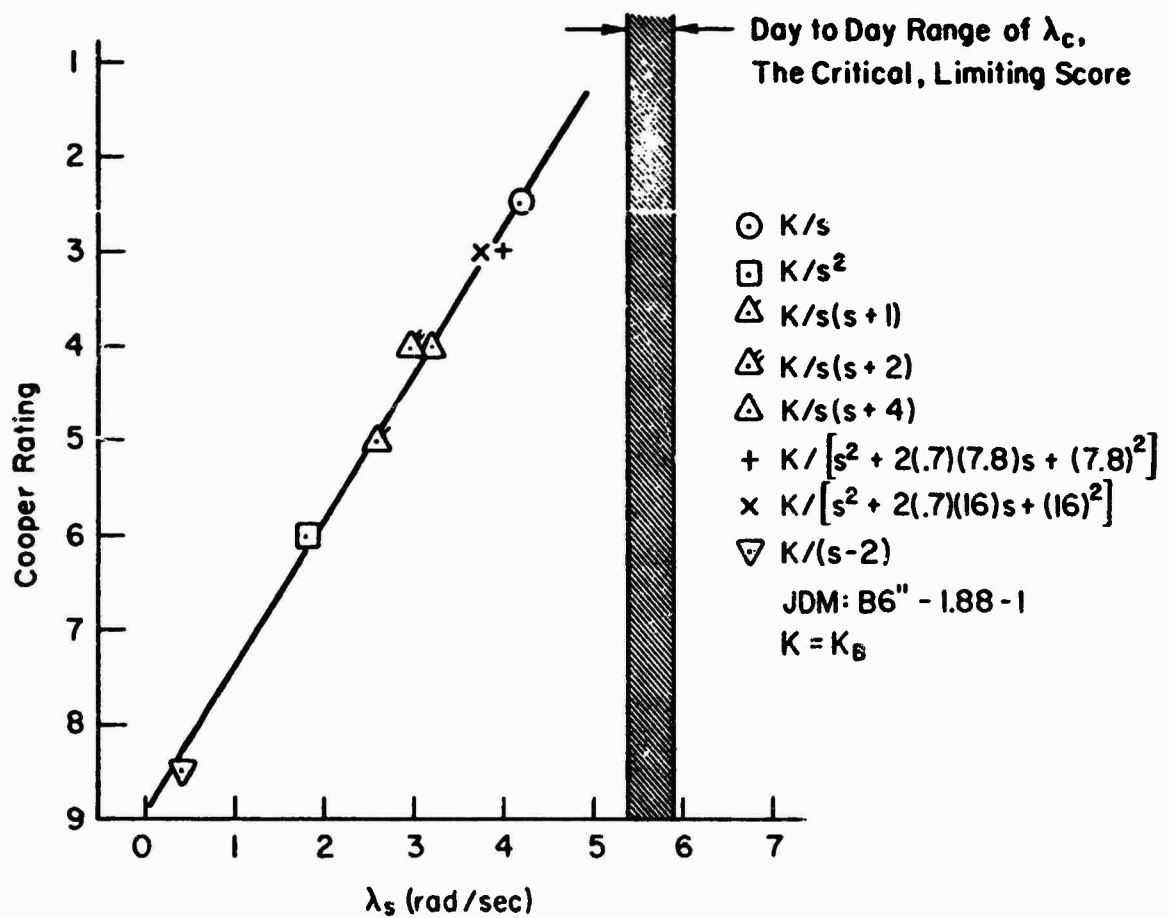


Figure 13. Secondary Task Score Variation with Ratings
for Best-Gain Configurations (Ref. 21)

control capacity of 66 per cent to perform tasks other than the primary; the primary task, itself, requires only 34 per cent of the pilot's capacity. Accordingly, $\lambda_n(R)$ represents the fraction of the pilot's excess control capacity available for other tasks; and $1-\lambda_n(R)$ represents the fraction of the pilot's capacity required to perform the primary task itself. Thus the "transformation" $R(\lambda_n)$ provides an interval scaling of R rendered in terms of an objective quantity, λ_n .

Two basic ways of operating on the single-axis capacity, or attention, demanded of the pilot to yield the combined axes demands were considered. The first assumed that the fractional capacities required for each individual axis, $1-\lambda_n(R)$, could be weighted and summed to yield the combined capacity. The second assumed that fractional excess capacities for the individual axes, $\lambda_n(R)$, could be multiplied to give the combined axes values of λ_n .

For the summation method the weightings assigned to each principal axis of control were the same, consistent with the notion that both longitudinal and lateral-directional control are, in general, equally important. Then, assuming a linear $R(\lambda_n)$ relationship (e.g., Fig. 14), the combined rating, R_m , for m axes of control, can be written in terms of the individual axis ratings, R_i , as follows:

$$\begin{aligned} R_i &= A + B\lambda_{n_i} \\ R_m &= A + B\lambda_{n_m}, \quad \text{where } 1 - \lambda_{n_m} = \sum_{i=1}^m w(1 - \lambda_{n_i}) \end{aligned} \quad (14)$$

$$\lambda_{n_i} = \frac{R_i - A}{B}$$

$$\begin{aligned} R_m &= A + B \left[1 - \sum_{i=1}^m w(1 - \lambda_{n_i}) \right] \\ &= A + B \left[1 - w \sum_{i=1}^m \left(1 - \frac{R_i - A}{B} \right) \right] \\ &= A + B - w \sum_{i=1}^m (B + A - R_i) \end{aligned} \quad (15)$$

and, defining R_0 as the value of R_i for $\lambda_{n_i} = 1.0$; i.e., $R_0 \equiv A + B$

$$R_m = R_0 + w \sum_{i=1}^m (R_i - R_0) = R_0(1 - mw) + w \sum_{i=1}^m R_i \quad (16)$$

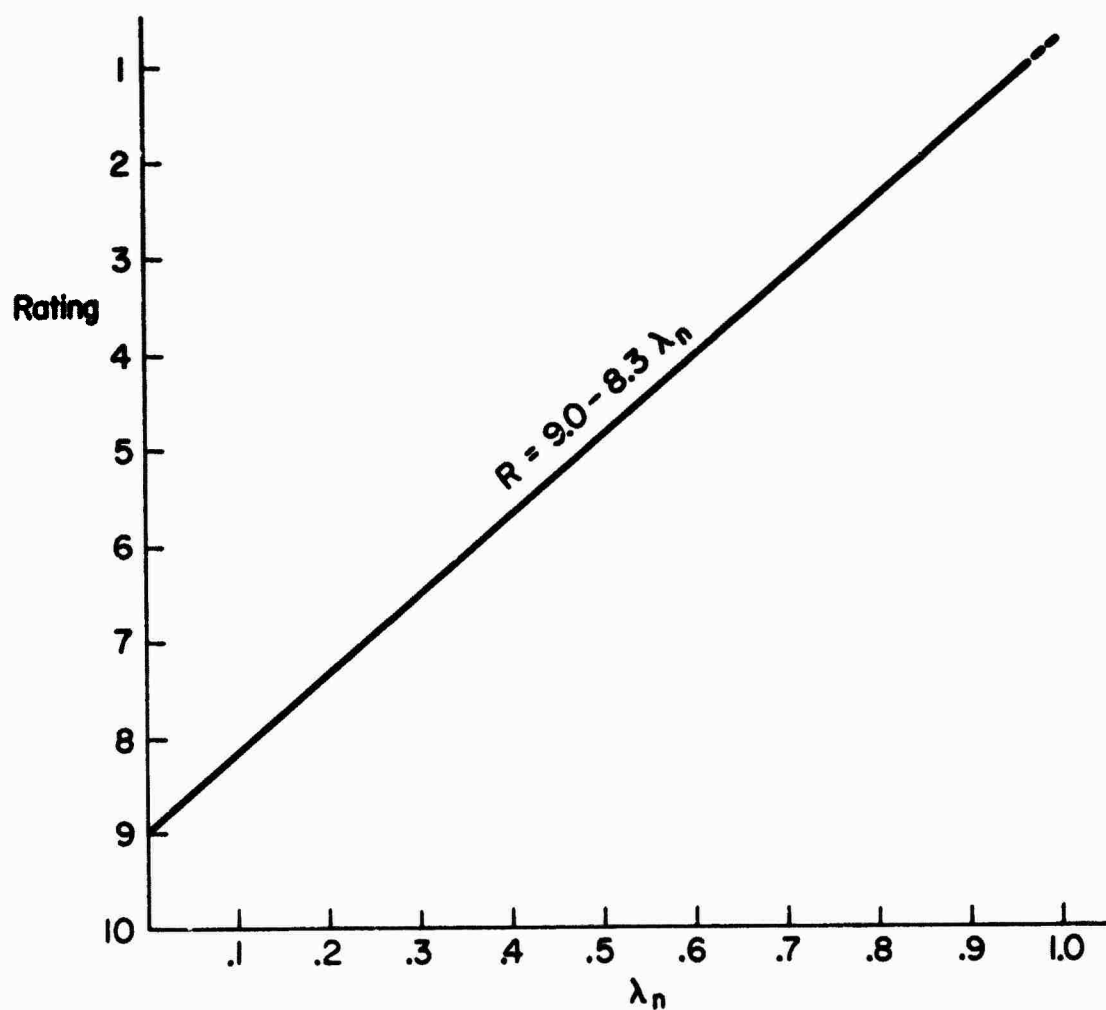


Figure 14. $R(\lambda_n)$ Fit to Ref. 21 Data (Fig. 13)

Preliminary checks using this combining form on the data of Refs. 17 and 18 showed that for an $R_0 = 0.7$, as given by the Fig. 14 plot, the matching value of the weighting, w , was also about 0.7 (a coincidence). The 0.7 weighting is physically satisfying in that it suggests that when two axes are combined the required control actions (and rating), indicative of the attentional or capacity demands on the pilot, tend to sum vectorially; e.g., he moves his controls diagonally rather than in two separate right angle steps. However, there are a number of practical and philosophical problems accruing to this method and form.

For one, the value of λ_{nm} can become negative, and the corresponding R_m can then be greater than 10.0. Both results are questionable philosophically if not practically. That is, values of $R > 10$ have no meaning on a 10 point rating scale; and negative λ_n 's are unrealizable physically although perhaps indicative of an extremely overloaded pilot.

Second, combined ratings can be less than that for an individual axis, an untenable result since the pilot's workload is necessarily higher for the combined situation. This only occurs when there is a relatively wide disparity in the single axis ratings, but such cases are of practical concern. For example, for two "axes" of control representing longitudinal and lateral-directional tasks with ratings R_1 and R_2 , the conditions for R_m less than R_2 , say, can be shown from Eq. 16 to be:

$$\begin{aligned} R_m &= R_2 - \Delta = R_0(1 - 2w) + w(R_1 + R_2) \\ R_2(1 - w) &= R_0(1 - 2w) + wR_1 + \Delta \quad (17) \\ R_2 &= \frac{R_0(1 - 2w) + wR_1 + \Delta}{(1 - w)} \end{aligned}$$

That is, $R_2 > [R_0(1 - 2w) + wR_1]/(1 - w)$ will yield a combined rating less than R_2 . For instance, for the values of R_0 and w cited above, and $R_1 = 2.5$, $R_2 = 5.5$, reflecting the above inequality ($R_2 > 4.9$), gives a value of R_m (Eq. 16) equal to 5.32.

Another facet of the above "problem" is the fact that for three axes of control, taken two at a time, the computed combined rating will depend on the order in which the axes are paired. For example, pairing the yaw and roll axes to produce a composite lateral-directional rating, and combining that rating with the longitudinal rating, produces a different overall rating than simply combining all three axes. This may be shown by the following development, based on the Eq. 16 relationship:

Pairing ϕ and ψ axes

$$R_{\phi\psi} = R_O(1 - 2w) + w(R_\phi + R_\psi)$$

adding θ axis

$$\begin{aligned} R_{\theta+\phi\psi} &= R_O(1 - 2w) + w(R_\theta + R_{\phi\psi}) \\ &= R_O(1 - 2w) + w[R_\theta + R_O(1 - 2w) + w(R_\phi + R_\psi)] \\ &= R_O(1 - 2w)(1 + w) + wR_\theta + w^2(R_\phi + R_\psi) \end{aligned}$$

and, by analogy (18)

$$R_{\psi+\theta\phi} = R_O(1 - 2w)(1 + w) + wR_\psi + w^2(R_\theta + R_\phi)$$

Combining θ , ϕ , ψ axes directly,

$$R_{\theta\phi\psi} = R_O(1 - 3w) + w(R_\theta + R_\phi + R_\psi) \quad (19)$$

Equations 18 and 19 can only be equal if, equating coefficients:

$$\begin{aligned} (1 - 2w)(1 + w) &= 1 - 3w \\ w &= w \\ w^2 &= w ; w = 1 \end{aligned}$$

The direct result given by the last, also satisfies the first equation. Therefore we conclude that the summation method is noncommutative unless the weightings used to sum the individual axis capacities are taken as unity.

If such weightings are used, Eq. 16 becomes

$$R_m = R_o + \sum_{i=1}^m (R_i - R_o) \quad (20)$$

similar to "Method No. 2" of Ref. 20, which used the equation,

$$R_m = R_{best} + \sum_{i=1}^m \Delta R_i \quad (21)$$

where R_{best} = Rating for "best" (tested) multiple axis configuration

ΔR_i = Incremental rating between the best i^{th} single axis configuration and the i^{th} single axis configuration making up the multiple axis configuration

Although "Method No. 2" is shown (Ref. 18) to provide reasonable correlation with the Ref. 18 data, the values of R_o are not consistent with the empirical $R(\lambda_n)$ relationships and in fact are quite artistically determined (based on a complete range of available ratings and characteristics). Furthermore the basic form of Eqs. 20 and 21 still suffers from the other problems noted, i.e., R_m can be greater than 10 and combined ratings can be less than for an individual axis. Finally the value of $w = 1$ is not as satisfying on physical grounds as a value around 0.7 as previously discussed.

The product method first suggested and tentatively used in Ref. 26 overcomes some of the philosophical and practical difficulties discussed above. As noted earlier it is based on the assumption that the multiple axis excess capacity, λ_{nm} , is given by the product of the excess capacities for the individual axes. That is

$$\lambda_{nm} = \prod_{i=1}^m \lambda_{ni}$$

and for $R = A + B\lambda_n$ as in Fig. 14

$$R_m = A + B\lambda_{nm} = A + B \prod_{i=1}^m \lambda_{ni} = A + B \prod_{i=1}^m \left(\frac{R_i - A}{B} \right)$$

$$R_m = A + \frac{1}{B^{m-1}} \prod_{i=1}^m (R_i - A) \quad (22)$$

The commutative nature of Eq. 22 can easily be demonstrated, e.g., paralleling Eqs. 18 and 19:

$$R_{\Phi\Psi} = A + (1/B)(R_{\Phi} - A)(R_{\Psi} - A)$$

$$R_{\Theta+\Phi\Psi} = A + (1/B)(R_{\Theta} - A)(R_{\Phi\Psi} - A)$$

$$R_{\Theta+\Phi\Psi} = A + (1/B^2)(R_{\Theta} - A)(R_{\Phi} - A)(R_{\Psi} - A) = R_{\Theta\Psi}$$

Also, combined ratings are always greater than (or equal to) individual ratings, since combined λ_n 's are always less than any individual λ_n . Finally the maximum value of R_m never exceeds A, i.e., for large $R_i < A$, $\prod_{i=1}^m (R_i - A) \rightarrow 0$ (Eq. 22).

This last observation suggests that a logical value for A is 10.0 rather than 9.0 as indicated by the Fig. 14 $R(\lambda_n)$ linear relationship. In fact, application of the product method to the available data using $A = 10.0$ and $B = -8.3$, the slope of the Fig. 14 plot, resulted in a good overall fit to all the available data, as later demonstrated.* In effect such a shift means that for combined axes the single-axis values of λ_n are not quite appropriate to combination using the product rule; that is, relating the combined rating, R_m (Eq. 22), to the single axis $R(\lambda_n)$ denoted by the different value of $A \equiv A_i$ (i.e., $R_i = A_i - B\lambda_n$):

$$R_m = A + \frac{1}{B^{m-1}} \prod_{i=1}^m (R_i - A)$$

$$\left[R_m - (A - A_i) \right] = A_i + \frac{1}{B^{m-1}} \prod_{i=1}^m \left\{ \left[R_i - (A - A_i) \right] - A_i \right\} \quad (23)$$

For the values of $A - A_i$, actually used, $10.0 - 9.0 = 1.0$, this amounts to subtracting an increment of 1.0 from the single-axis ratings to compute the "effective" multiple axis λ_n 's (pertinent to the product rule) from the single-axis $R(\lambda_n)$. The multiple axis rating minus the same increment is

*Many variants of $R(\lambda_n)$, some nonlinear, which fit the Ref. 17 "workhorse" data better, were tried but rejected on the basis of: poorer overall data fits; philosophical difficulties, e.g., $\lambda_n(R)$ too divergent from observations (Fig. 13); or undesirable limiting of R_m to values less than 10.0.

then given by applying the value of the λ_{nm} so computed to the basic (single-axis) $R(\lambda_n)$. In short, a decrement of 1.0 is applied to all ratings, single and multiple axis, when the product rule is applied to the single-axis, empirical $R(\lambda_n)$ relationship.

Recognizing this effect and remembering that the summation method did not involve the use of such a rating decrement, the two methods can be compared relative to their values of $1 - \lambda_{nm}$, the effective fractional capacity required for the multiple axis task. First considering two control axes, the product method gives:

For the basic $R(\lambda_n)$ relationship (Figs. 13, 14)

$$\lambda_{12} = \frac{R_{12} - A_i}{B}$$

where (Eq. 22),

$$R_{12} = A + \frac{(R_1 - A)(R_2 - A)}{B}$$

Therefore

$$1 - \lambda_{12} = 1 - \frac{(A - A_i)}{B} - \frac{(R_1 - A)(R_2 - A)}{B^2}$$

The summation method gives:

$$\begin{aligned} 1 - \lambda_{12} &= w(1 - \lambda_1 + 1 - \lambda_2) \\ &= w\left(2 - \frac{R_1 - A_i}{B} - \frac{R_2 - A_i}{B}\right) \end{aligned}$$

Accordingly the effective weighting, w , corresponding to the product method (i.e., for equal values of $1 - \lambda_{12}$) is,

$$w_{\text{eff}} = \frac{1 + \frac{A_i}{B} - \frac{A}{B} - \frac{(R_1 - A)(R_2 - A)}{B^2}}{2 - \frac{R_1 - A_i}{B} - \frac{R_2 - A_i}{B}} \quad (24)$$

For $A_1 = 9.0$, $A = 10.0$, $B = -8.3$ as actually used,

$$w = \frac{1 + \frac{1}{8.3} - \frac{(R_1 - 10)(R_2 - 10)}{69}}{2 + \frac{R_1 - 9}{8.3} + \frac{R_2 - 9}{8.3}}$$

$$= \frac{-0.330 + 0.145(R_1 + R_2) - 0.0145R_1R_2}{-0.169 + 0.1205(R_1 + R_2)}$$

and for all possible combinations of R_1 and R_2 for values of each lying between 3 and 7, the most interesting region, the value of w is given by 0.73 ± 0.05 . Furthermore, since multiple axis ratings computed with the product method are commutative, the same weighting applies to the addition of a third axis to the combined first two axes (i.e., substitute R_{12} for R_1 and R_3 for R_2 in Eq. 24).

Thus, the product method as implemented is roughly equivalent to the summation rule with an assigned weighting of about 0.7. In effect, the product method results in the physically satisfying vector addition of fractional single- and combined-axis capacities, the desirable positive feature of the summation methods; and it avoids the negative aspects of the summation method.

Data Correlations

The data considered and used (Refs. 17-20) and the reasons for rejecting certain points or series are given in Appendix C. It is pertinent to remark here that all of the data were obtained in ground simulators, both fixed and moving. Also, the rating systems utilized were not all the same, but did employ a 10 point scale, except for the single point gleaned from Ref. 19 which used a 9 point scale. The fact that applicable in-flight data were not found, while disappointing, does not detract, in principle, from the applicability of the results to flight situations. That is, the determination of how single axis ratings combine for multiple axis tasks is not expected to be critically dependent on the specific situations involved. Rather, as indicated by the theoretical considerations above, such combination effects depend on the vector summation of the fractional attention or

capacity demands of the individual axes,* regardless of the exact reasons for such demands. Nevertheless, certain of the data employed do correlate well with flight test results (Ref. 17).

The final correlations obtained for the product method are given in Fig. 15. Here the ordinate is the multiple-axis rating computed, from the observed single-axis ratings, R_i , using Eq. 22 and the values of A and B previously cited ($A = 10$, $B = -8.3$); i.e.,

$$R_m = 10 + \frac{1}{(-8.3)^{m-1}} \prod_{i=1}^m (R_i - 10) \quad (25)$$

The abscissa, of course, is the actual multiple-axis rating for the same set of individual axis ratings. The spread in the individual points is due to the uncertainties in either or both the single-axis and multi-axis rating data (e.g., rating = 4-1/2 to 5). The Ref. 18 data are most pronounced in this respect, the spread here reflecting the differences in single-axis ratings delivered before and after the 3-axis runs, and also differences between the first and second series of 3-axis runs, themselves; the center point is based on the overall averaging of the single and 3-axis data given in Ref. 18 (see Appendix C).

The correlation shown is on the whole quite good for the region of most interest, i.e., ratings between 2 and 7. In fact for this region, and neglecting the spreads shown for the Ref. 18 data, the computed rating agrees with the observed rating within about half a point.

Implications for MIL-F-8785B(ASG) Revision

The impact of the foregoing on the single-axis requirements to achieve various levels of multiple-axis (i.e., whole task) flying qualities is potentially quite drastic. That is, for Level 1 whole task flying qualities corresponding to a multiple-axis rating of 3.5 or better (Ref. 16), the required longitudinal and lateral-directional flying qualities must be better, according to Eq. 25, than about $2.65 + \Delta$ for one and $2.65 - \Delta$ for

*However in-flight ratings of an individual axis may reflect the presence of other axes — see next article.

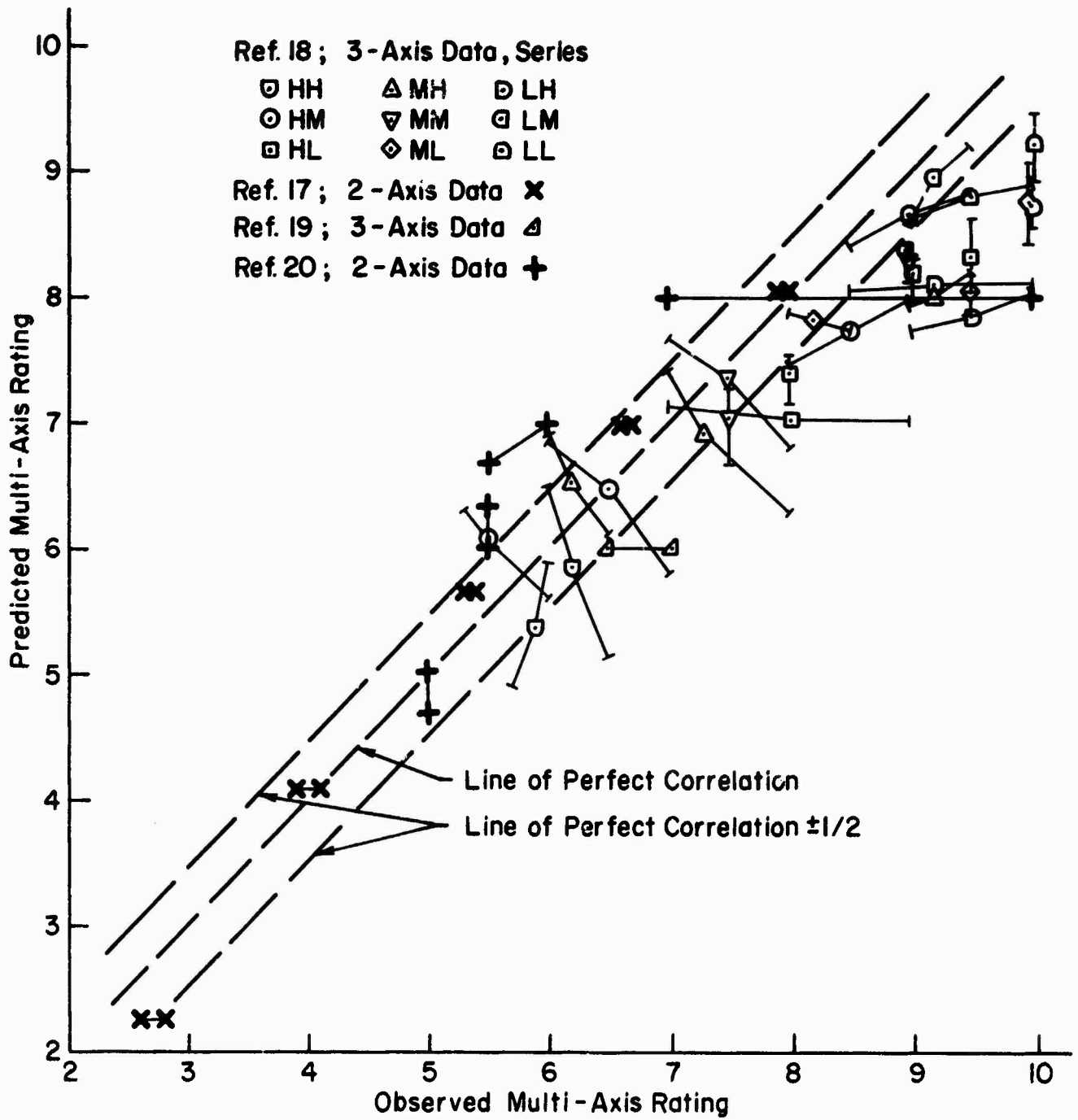


Figure 15. Final Correlations Obtained with Product Method (Eq. 25)

the other (where $2.65 + \Delta < 3.5$). Taking the most beneficial view of the 1/2 rating point "inaccuracy" (Fig. 15) of Eq. 22 increases these values to $2.95 + \Delta$ and $2.95 - \Delta$ (where $2.95 + \Delta < 4$). Such an explicit requirement for longitudinal and lateral-directional flying qualities, which are each a little better than the Level 1 (3.5) boundary is somewhat in keeping with vague undocumented "stories" of aircraft which were not satisfactory because too many of their parameters, while each individually satisfactory, were very near the boundary value (a possibility mentioned also in Ref. 16, Item 1.5).

On the other hand, it must be recognized that the data used (Ref. 16) to establish the various level boundaries were, wherever possible, based on the results of flight-test investigations where tasks other than those being rated were necessarily present. Since such other tasks (or parameters) were supposedly in the "good" (Level 1) region, it seems pertinent to consider that for a configuration rated 3-4 the pilot may have been flying longitudinal and lateral axes each rated about 3. Past experience with preceding versions of the MIL Spec tend to further support the above observation; that is, airplanes near but within the satisfactory boundary values in both longitudinal and lateral-directional handling are generally satisfactory overall.

Because of the above considerations and the lack of definitive in-flight data on multiple-axis effects, it seems inadvisable to alter the Level 1 definition. However it is still appropriate considering the evidence herein, to issue a warning requiring further explicit study of those situations where both longitudinal and lateral-directional flying qualities approach very near the Level 1 boundaries.

The Level 2 boundaries are also based on the practice of "good" (i.e., Level 1) remaining parameters. This means that if one axis of the airplane is worse than Level 1 but better than, or equal to, the Level 2 boundary the other axis must be better than or equal to the Level 1 boundary. This interpretation of the actual data used to establish the Level 2 boundaries is hinted at in Ref. 16, where it is noted that some of the Level 2 boundaries were somewhat arbitrarily "stiffened" so that two axes in the Level 2 region

might still represent Level 2 conditions. The actual "stiffening" required to produce this state of affairs is quite extreme, based on the present findings, and it seems doubtful that such extreme stiffening was actually or uniformly applied to the data.

For example, conceding that longitudinal and lateral-directional axes both rated 3 1/2 (Level 1) yield an overall rating of approximately 3 1/2; and setting these conditions into Eq. 22:

$$3.5 = A + \frac{(3.5 - A)^2}{B}$$

whereby

$$B = 3.5 - A$$

Then for an overall Level 2 boundary rating of 6.5 (Ref. 16),

$$6.5 = A + \frac{(R_1 - A)(R_2 - A)}{B}$$

and

$$(6.5 - A)(3.5 - A) = (R_1 - A)(R_2 - A) \quad (26)$$

The obvious solution by inspection, $R_1 = 3.5$, $R_2 = 6.5$, is consistent with the previously noted requirement that one axis near the Level 2 boundary (6.5) requires the other to be near or better than the Level 1 (3.5) boundary for an overall Level 2 airplane. If both axes are worse than Level 1, the Eq. 26 values of R_1 and R_2 are slightly dependent on the value of A . However for reasonable values of $A = 10 \pm 1$, say, the value of $R_1 = R_2 = 5.24 \pm .05$. That is, two axes each worse than Level 1 should be no worse than a boundary corresponding to a rating of approximately 5. For a linear rating spread between the Level 1 (3.5) and Level 2 (6.5) boundaries, such a boundary would be halfway between the present Level 1 and the unstiffened Level 2 boundaries. It is doubtful that the "stiffening" alluded to and practiced in Ref. 16 is of this magnitude.

The halfway rule also applies to the data obtained using the original Cooper scale which gave a Level 2 boundary rating of 5 1/2 (Level 1 is still 3 1/2). In this case the equivalent to Eq. 26 is,

$$(R_1 - A)(R_2 - A) = (3.5 - A)(5.5 - A) \quad (27)$$

which for $A = 10 \pm 1$ yields $R_1 = R_2 = 4.59 \pm 0.02$, reasonably close to halfway between $3 \frac{1}{2}$ and $5 \frac{1}{2}$.

The foregoing suggests that, neglecting whatever "stiffening" was applied to "some" requirements (Ref. 16), a proper Level 2 definition reflects conditions where:

- a. either the longitudinal or lateral-directional axis is better than, or equal to, Level 1; and the other axis is worse than Level 1 but no worse than the Level 2 boundary, or
- b. both the longitudinal and lateral-directional axes are worse than Level 1 but no worse than a boundary halfway between the Level 1 and Level 2 boundaries.

The halfway rule is at best an approximation to an intermediate Level (CAL or Cooper-Harper Rating ≈ 5) boundary. Its face validity suffers, of course, with specific departures from the approximate linear rating spread assumed. However, as indicated in the Table 5 review, such approximate linearity in the range of ratings between Levels 1 and 2 appears to exist in the majority of the Ref. 16 requirement-generating backup data plots directly relating rating to specific flying qualities parameters. Nevertheless, in view of the (Table 5) noted departures from approximate linearity, it is appropriate to note that the rule is intended to reflect ratings halfway between those for Levels 1 and 2, and that this does not always mean specification parameters halfway between those Levels.

TABLE 5
REVIEW OF REF. 16 DATA LINEARITY WITH RATING
(LEVELS 1 TO 2)

SPEC ITEM	PARAMETER(S)	SPECIFIC SOURCE(S) AND HALFWAY RULE ASSESSMENT, i.e.	OK	NG	
				CONSERVATIVE	UNCONSERVATIVE
3.2.1.2	$\zeta_p (1/T_{h1} = 0)$	Figs. 7, 8, 11 <u>nonlinear</u> ; 1/2 rule <u>conservative</u> ; however Levels 1 and 2 set with little ref. to actual, limited data (p 70)		✓	
3.2.1.3	$1/T_{h1} (\zeta_p > 0)$	Figs. 1, 2, 3 <u>slightly</u> <u>non-linear</u> ; 1/2 rule <u>conservative</u> ; however actual spec values approx. <u>linear</u>	✓		
3.2.2.1.1	ω_{sp} vs n/a	No directly applicable (rating vs parameter) data plots or fairings	—	—	—
3.2.2.1.2	ζ_{sp}	Fig. 1 <u>linear</u> — spec value higher than data but also <u>linear</u>	✓		
3.2.2.2.1	F_s/n	No directly applicable data plots or fairings	—	—	—
3.3.1.1	$\zeta_d, \zeta_d \omega_d$	Figs. 17, 18, 21 (only ones with rating as co- ordinate) show <u>linear</u> fits	✓		
	ω_d	No usable rating data; based on existing aircraft (p 186)	—	—	—
3.3.1.2	τ_R	Fig. 1 very <u>nonlinear</u> (linear with $\log \tau_R$) 1/2 rule <u>unconservative</u>			✓
3.3.1.3	$T_2(\text{spiral})$	Fig. 2 data band is <u>linear</u> ; spec values approx. <u>linear</u>	✓		
3.3.2.2.1	P_{osc}/P_{av}	No directly applicable data plots; however related ratings vs ω_n/ω_d	✓		
3.3.2.3	P_{osc}/P_{av}	(Figs. 21-24) approx. linear (for $3-1/2 < R < 6-1/2$) as also shown in Ref. F.9 (of Ref. 16), Fig. 13 com- posite plot (not included in Ref. 16)			
3.3.2.4 3.3.2.4.1	$\beta_{\text{excursion}}$	Fig. 1 generally <u>nonlinear</u> ; 1/2 rule <u>conservative</u> ; also true for suggested replace- ment Heading Control require- ment, Fig. 8 this report		✓	
3.3.4	ϕ_t	No directly applicable data, but Table 9 spec is <u>non-</u> <u>linear</u> with rating between Levels 1 and 3; 1/2 rule <u>slightly unconservative</u>		✓	
3.3.4.2	F/δ_a	Figs. 9-13, 20 show approx. <u>linearity</u> ; 1/2 rule <u>slightly</u> <u>conservative</u>	✓		

SECTION IV

CATEGORY C SHORT-PERIOD REQUIREMENTS

RECOMMENDED SPECIFICATION REVISIONS

3.2.2 Longitudinal maneuvering characteristics.

3.2.2.1 Short-period response. — No change.

3.2.2.1.1 Short-period frequency and acceleration sensitivity. The short-period undamped natural frequency, ω_{nsp} , shall be within the limits shown in Figs. 1 and 2. [Comment: This deletes all reference to present Fig. 3 which is to be replaced — see below.]

3.2.2.1.2 Short-period damping. Delete all reference to Category C from Table IV.

3.2.2.1.3 Category C requirements [New]. The frequency response characteristics of pitch attitude to stick displacement or force inputs, whichever are critical, shall be such that the parameters $\Delta\phi/\Delta\omega$ and ϕ are within the boundaries of Fig. 3.

3.2.2.1.4 Residual oscillations. — No change except for new number.

6.2.5 Longitudinal parameters.

- ϕ The phase angle (in degrees), at $\omega = 1$ rad/sec, of the pitch attitude to stick force or displacement transfer function (frequency response) assuming a 0.3 sec time delay, i.e., the phase of

$$\frac{\theta(j\omega)}{\delta_s(j\omega)} e^{-0.3j\omega} \quad \text{or} \quad \frac{\theta(j\omega)}{F_s(j\omega)} e^{-0.3j\omega}$$

$$\frac{\Delta\phi}{\Delta\omega}$$

The average phase gradient with frequency, in degrees per rad/sec, of the above-defined frequency response (transfer function) characteristics.

To be measured as the difference in phase angle over a one octave spread (i.e., between $0.707 \omega_\phi$ and $1.414 \omega_\phi$) about a frequency, ω_ϕ , defined in general by $\phi = -135^\circ$; i.e., $\omega_\phi = \omega$ for $\phi = -135^\circ$.

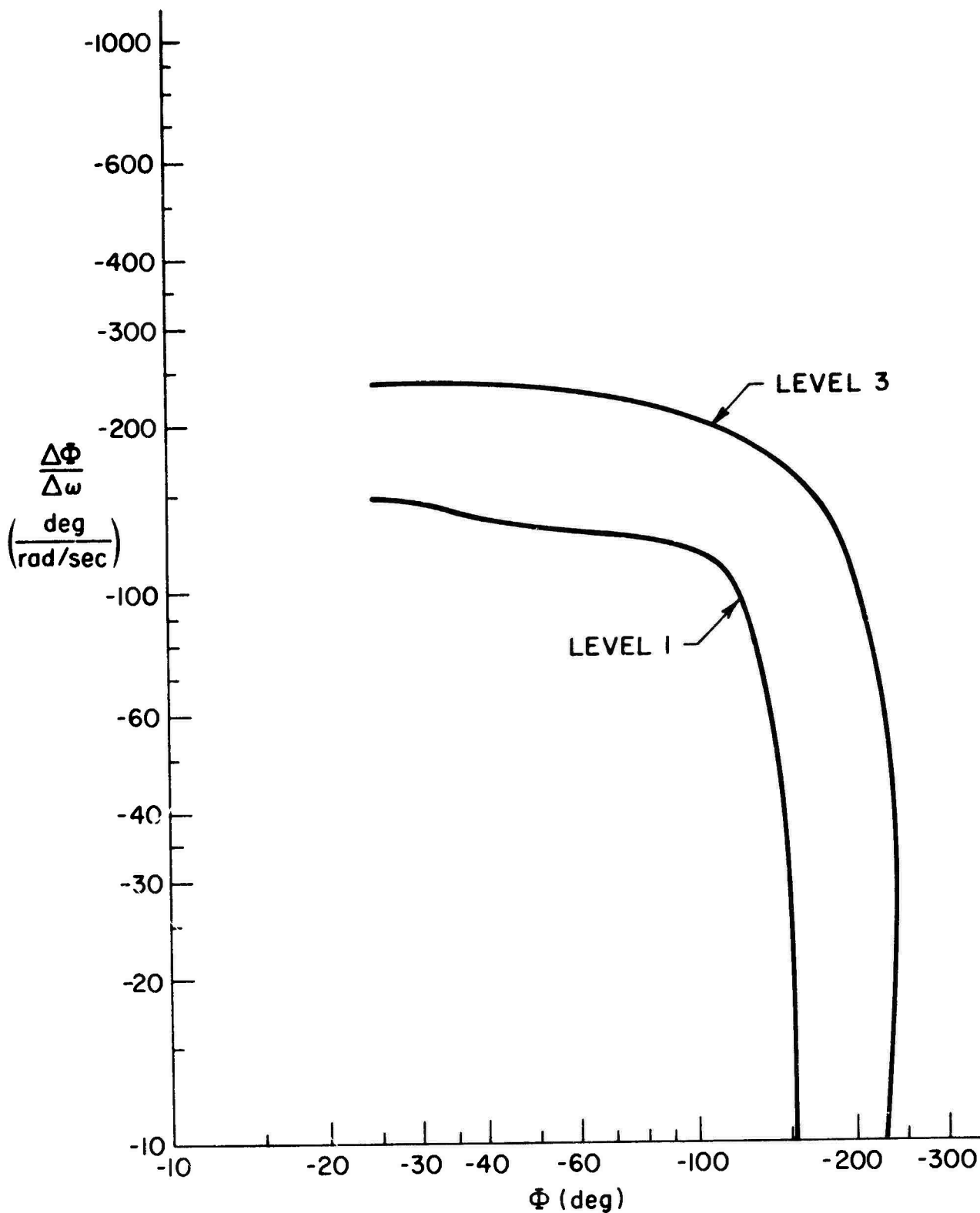


Figure 3 (of Specification). Longitudinal Attitude Control —
Category C Requirements

However, for non-minimum phase systems (i.e., unstable roots) which show increasing phase angle for frequencies greater than 1 rad/sec, the gradient is measured over one octave about a frequency defined by the peak value of Φ . If the peak occurs at 1 rad/sec or less, then the gradient is measured about 1 rad/sec.

Finally, if $\Delta\Phi/\Delta\omega$ is greater than $-10 \text{ deg}/(\text{rad}/\text{sec})$, then the Fig. 3 requirements for $\Delta\Phi/\Delta\omega = -10 \text{ deg}$ will apply.

Discussion

The current specification, MIL-F-8785B(ASG) covering longitudinal maneuvering characteristics for the short-period attitude response, provides separate requirements for the frequency and damping properties. Such provision presupposes that these response properties can be identified regardless of the proximity of the phugoid mode or interactive effects of the flight control and/or augmentation system. This represents an unsatisfactory piecemeal approach to the problem of attitude control requirements. The requirements proposed herewith address the total picture and take advantage of previous experience with partial correlations (e.g., Refs. 28, 31, and 38).

From a practical standpoint, the single measurement of phase properties as opposed to phase and amplitude (in Ref. 28) is relatively easier. The measurement of the phase angle gradient, Φ , is direct and unambiguous. The phase gradient measurement can be troublesome for non-minimum phase systems. Figure 16 illustrates correct usage consistent with the proposed specification "rules." The minimum phase measurement deserves no comment. The two non-minimum cases are illustrated for conditions where the peak phase angle is less than -135 degrees. The first situation shown is one where the peak phase angle occurs at a frequency equal to or less than 1 rad/sec; the gradient is therefore taken at 1 rad/sec. In the second situation, peak Φ occurs at $\omega > 1 \text{ rad}/\text{sec}$ and $\Delta\Phi/\Delta\omega$ is measured about the frequency for peak Φ . In all cases, the phase angle is measured at the 1 rad/sec reference frequency.

Non - Minimum Phase, $\frac{\theta}{F_s}$ or $\frac{\theta}{\delta_s}$

Conventional A/F
Minimum Phase, $\frac{\theta}{F_s}$ or $\frac{\theta}{\delta_s}$

Unstable Phugoid

Unstable Second Order

$\Phi < -135^\circ$; $\omega\Phi_{MAX} < 1 \text{ rad/sec}$

$\Phi < -135^\circ$; $\omega\Phi_{MAX} > 1 \text{ rad/sec}$

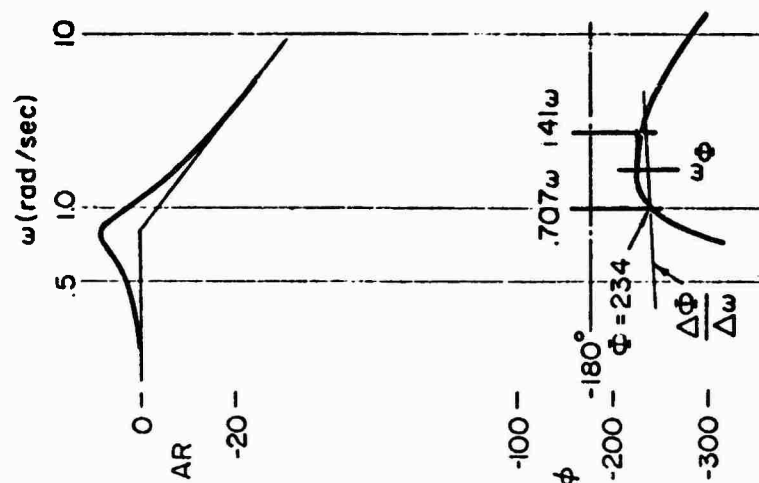
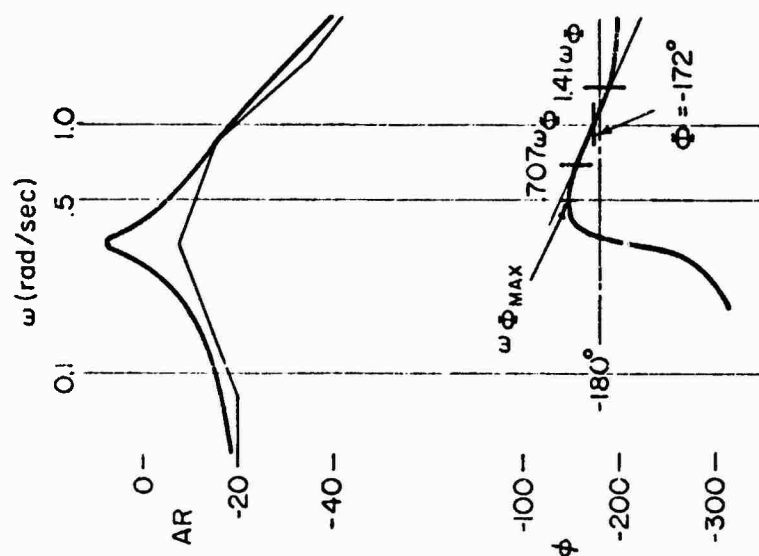
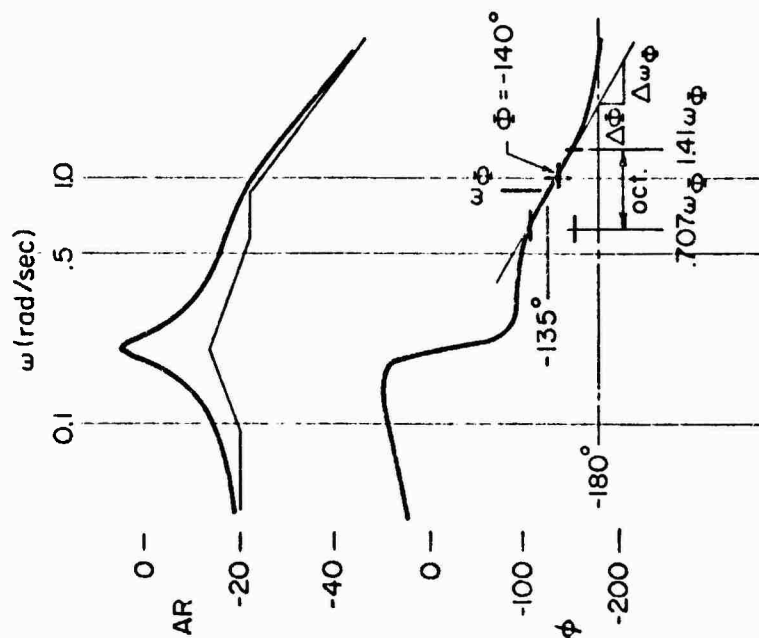


Figure 16. Application of Criterion — Typical Cases

BACKGROUND FOR THE RECOMMENDED REVISIONS

In establishing the background for the foregoing recommended revisions we will emphasize three basic areas: overall objectives, technical approach, and justification of the recommended criteria.

Overall Objectives

These overall objectives centered on providing a specification based on both closed- and open-loop considerations, but preferably expressed in simple open-loop terms, which would apply to:

1. The complete airplane attitude response including both the phugoid and short-period modes.
2. The airplane plus flight control system characteristics (e.g., including lags and delays).
3. The various control element forms resulting from current flight control augmentation concepts.
4. The basic inner attitude response features which are necessary regardless of outer-loop control problems or auxiliary (e.g., direct lift) control.

Satisfaction of the first three conditions is obviously pertinent if the specification is to be applicable to modern flight control system designs which involve command augmentation and higher-order response concepts. The fourth condition recognizes the interplay that exists between path and attitude control, an aspect discussed in considerable detail in Appendix E and briefly reviewed in a later discussion of essential attitude control needs. It is sufficient to note here that marginal path mode properties can be the governing pilot rating factor almost regardless of attitude control characteristics. However, and more to the point, the converse is also true; i.e., attitude control must have a basic integrity of itself to serve as a proper inner loop for the multiple loop path control structure.

As a final comment, the subject of disturbance inputs and their effects is not addressed directly in this study; although it was evident from the data that the disturbance level can significantly alter the pilot ratings (e.g., see Fig. D-1 of Appendix D).

Technical Approach

The exposition of our technical approach involves three elements:

- Data sources
- Essential attitude control aspects
- Criteria forms considered and problems therewith

To enhance the conciseness of the text many of the detailed analyses and data correlation supporting the conclusions given here have been placed in Appendices D and E.

Data Sources. As a first step toward fulfillment of the foregoing objectives, a representative experimental data base covering both "classical" and command augmented airplanes was compiled. This compilation resulted in data which were either considered compatible or anomalous. The "compatible" data were consistent among themselves and with a variety of currently available correlations. The "anomalous" data did not fit in with this set and included both better and worse ratings than expected, i.e., good ratings which occurred in bad regions and vice versa. The reasons and causes for such anomalies were determined by a series of detailed closed-loop analyses and by thoroughly scrutinizing the pilot commentary, and are presented in Appendix E.

The data sources reviewed and utilized herewith are summarized in Table 6. The sources include those previously considered in the earlier short-period attitude control studies of Ref. 31 and more recent flight test and simulator results from various handling quality programs. Note that the flight test program of Ref. 40 and the simulator tests of Ref. 43 provided augmented airframe data for control systems involving rate-command/attitude-hold and rate-command concepts. This supplemented the conventional static stability (M_α type variations) studies typified by the data from Refs. 33 and 37.

The stability and control characteristics and the calculated attitude transfer functions for each data point used are provided in Appendix D. Example frequency response characteristics (i.e., Bode diagrams) for representative cases are also included for reference purposes and to illustrate some of the conclusions reached in the text.

TABLE 1. DATA SOURCES FOR THE CORRELATION STUDY

DATA SOURCE	CONTROL FREQUENCY TYPES	PARAMETER VARIATIONS	SIMULATION PROGRAM	REMARKS
API Report 182-1 (Ref. 31)	Conventional aircraft and helicopter, 2/8	Short-period ξ and ω from M_0 , K_0 , and M_0 variation at fixed level of $1/T_{10}$ or q_0	Flight test, fixed-based and motion 6 DOF simulators	Representative cases were selected which covered recommended levels 1 and 3 boundaries
Princeton University Reports FU-811 (Ref. 37) FU-822 (Ref. 30) FU-888 (Ref. 34)	Conventional aircraft in landing approach, 2/8	Short-period ξ and ω from M_0 , K_0 , and M_0 variation for selected values of $1/T_{10}$	NAVION; flight simulator	FU-888 included backside variations and effects of K_0 on attitude control
Flight Research Center, NASA PA-30 (Ref. 40)	Attitude augmentation	K_0 and ω_0	PA-30 aircraft flight simulator	Landing approach study comparing rate and attitude command augmentation schemes
GPAS (Ref. 39)	Conventional aircraft	M_0 , K_0 variation fixed $1/T_{10}$	GPAS, flight simulator	
Calspan Rept. TB-7011F-2 (Ref. 33)	STOL aircraft dynamics	M_0 , K_0 , ω_0 and $1/T_{10}$ variation, ω_0 and $1/T_{10}$	3-22 variable stability flight simulator	
Ames Research Center, NASA Franklin and Innis (Ref. 47)	STOL aircraft, AUGURA, with attitude augmentation	K_0 and ω_0 variation for selected coefficients and gain and filtering	FSMA, 6 DOF simulator	Rate-command/attitude-hold concept was evaluated for augmented wing STOL aircraft
Ames Research Center, NASA Grief, et al. (Ref. 29)	VTOL aircraft simulation lateral attitude systems	K_0 and ω_0 variation with acceleration command	6 DOF VTOL simulator	Inertial body used to represent airframe; $\omega_0 = M_0/s^2$ where disturbances were simulated by random moment inputs
North American Aviation, NAS-4-791 Lockenour and Shooter (Ref. 42)	Carrier approach simulation, conventional aircraft	M_0 , K_0 , ω_0 variation simulating backside and frontside condition	4 DOF simulator	Effective automatic throttle control augmentation

Essential Attitude Control Aspects. An outcome of the comprehensive review presented in Appendix E was a set of fundamentals covering attitude and path control. Of these, the "pilot-centered" control aspects listed below

- Adequate bandwidth and response
- Inner-outer loop equalization
- Low static gain — trimmability, etc.
- Sensitivity to gain/equalization (e.g., performance reversals and conditional instabilities)

are considered essential for attitude control. Therefore, a viable attitude control criterion should explicitly or implicitly address all of these aspects which are reviewed and discussed briefly in the following.

- Adequate bandwidth and response: Good attitude control starts first and foremost with adequate bandwidth, which essentially means a response which is rapid enough to satisfy the pilot's control needs when either making a maneuver or regulating against a disturbance. Adequate response (to a control input) also refers to its predictability and, in particular, whether the attitude tends to overshoot its steady-state value or droop (i.e., fall off after a few seconds). Neither of these properties is desirable and each is symptomatic of poor closed-loop control. Neal's criterion (Ref. 28) specifically addresses this problem of bandwidth and droop and explicitly covers the two response features.
- Inner-outer loop equalization: In the Category C flight regime, the test of whether the equalization the pilot must introduce to compensate for attitude deficiencies is suitable depends on the path control needs. To insure adequate bandwidth and response in the path modes (e.g., flight path), the pilot in most circumstances is restricted to the introduction of lead equalization. This restriction, as noted in Ref. 44, evolves because inner-loop lags propagate into the outer path loop which is usually already very sluggish.
- Low static gain: Low static gain characteristics in the attitude control element are indicative of cases where low-frequency trimmability or speed stability characteristics are missing or deficient. Such cases will normally restrict the pilot's ability to control flight path or speed with attitude. Furthermore, as explained in Appendix E, if the static gain is sufficiently low, the pilot can be restricted in his ability to adequately damp the phugoid modes and to

separate the path modes, i.e., speed and flight path responses. In addition, low-frequency regulation against gust disturbances and correction of off-nominal approach conditions (e.g., low and slow or high and fast) may be severely degraded. In such off-nominal conditions, very low static gain characteristics prevent the pilot from using attitude in a precise manner to effect a proper energy interchange between speed and rate of descent (see Appendix E).

- Sensitivity to gain and equalization: The pilot's gain and compensation required to provide good closed-loop response characteristics should not be very critical. That is, small or nominal variations in gain or equalization should not have a significant effect on performance. Especially critical are those situations where increases in either gain and/or equalization do not result in commensurate net increases in closed-loop dynamic performance. In many cases, such situations are on the border of, or in a region of "performance reversal" where increasing pilot effort results in degraded performance. Also, where the vehicle is conditionally stable, the range over which the pilot equalization must be introduced for best performance is usually very narrowly restrained.

Criteria Forms Considered and Problems Therewith. A criterion form which met the preceding attitude control considerations and was also simple and easily applied did not evolve from first principles. Rather, the process was essentially a trial-and-error effort in which a number of forms were considered and examined. These included so-called "open-loop" response parameters (i.e., airplane/FCS only), as well as "inferred" closed-loop deficiency parameters more indicative of pilot equalization requirements and similar to Neal's simplified criterion (Ref. 28). Table 7 lists the various forms considered, excluding the final successful form which is of the "inferred" deficiency type.

This initial evaluation effort served primarily to point out the inadequacies of the "open-loop" response forms as well as certain shortcomings of Neal's criterion. Basically, the open-loop forms were inadequate because of one or more of the following reasons:

1. Required different parameters depending on the characteristics of the θ/δ_s or θ/F_s transfer function.
2. Strongly interacting phugoid and short-period modes made it difficult to measure or apply the criterion parameters.
3. Would not work where unstable roots were present in the θ/δ_s or θ/F_s response.

TABLE 7
CRITERIA FORMS CONSIDERED

OPEN-LOOP RESPONSE

- ω and $\xi\omega$ as functions of $1/T_{\theta 2}$ and/or n_{α}
- Time response parameters
 - Effective time constant
 - Time response parameters, $f(\theta, \dot{\theta})$
- Effective bandwidth, ω_{BW} at $\Phi = -135$ deg
- $d\Phi/d\omega$ vs. ω_{BW} ; both at $\Phi = -135$ deg
- $d\Phi/d\omega$ vs. Φ ; both at $\omega = 1.0$ rad/sec

"INFERRED" CLOSED-LOOP DEFICIENCIES

- Neal and Smith's: $dA/d\Phi$ vs. $\Delta\Phi$; $\omega_{BW} = 1.2$ rad/sec

Needless to say, it was also true that the open-loop forms did not implicitly or explicitly cover the pilot-centered attitude control aspects previously listed.

The "inferred" closed-loop deficiency form, i.e., Neal's criterion (Ref. 28), did however appear to have merit; although some specific problems were evident, in general related to its application as listed below:

- Not precise (application rather artistic)
- Parameters "blow up"
- No rules for applying to non-minimum phase systems
- Application to augmented forms questionable (e.g., compensation limits, outer-loop effects)

The artistic aspect and consequent lack of precision were also inferred in the correlations made in Ref. 28. There it was noted that knowing where to pick the effective bandwidth, and thus the frequency range over which to measure the amplitude phase slope, required some knowledge of the piloting task. In particular, Ref. 28 noted that to obtain the best correlation it was often necessary to vary the effective bandwidth, ω_0 , slightly from one data source to another.

The artistic nature is also apparent from Fig. 16a, where the question is whether to define the phase angle increment, $\Delta\phi$ (in our notation), using the first peak difference or to use the alternative $\omega_0 + 90^\circ$ definition. The difference is significant, since using the first peak definition infers a satisfactory rating level; whereas the converse is true if the $\omega_0 + 90^\circ$ definition is applied. Neither of these definitions provide an accurate indication of the actual rating (i.e., PR = 5.5). However, the $\omega_0 + 90^\circ$ would imply a conservative unacceptable estimate (e.g., PR = 6.5), since $\Delta\phi$ is large (i.e., $\Delta\phi = 110^\circ$).

The problem of "blowup" is a practical aspect of using the "average" slope, $dA/d\phi$, as the companion parameter of $\Delta\phi$. This slope is compounded of the ratio of the amplitude ($dA/d\omega$) and phase ($d\phi/d\omega$) frequency response characteristics. Since either of these individual slopes may be zero for systems of practical interest, their ratio is quite sensitive, and potentially widely variable, for relatively small changes in the transfer function.

A more basic difficulty is the inapplicability of the current rules (see Table 8) to non-minimum phase systems, that is, to systems where unstable

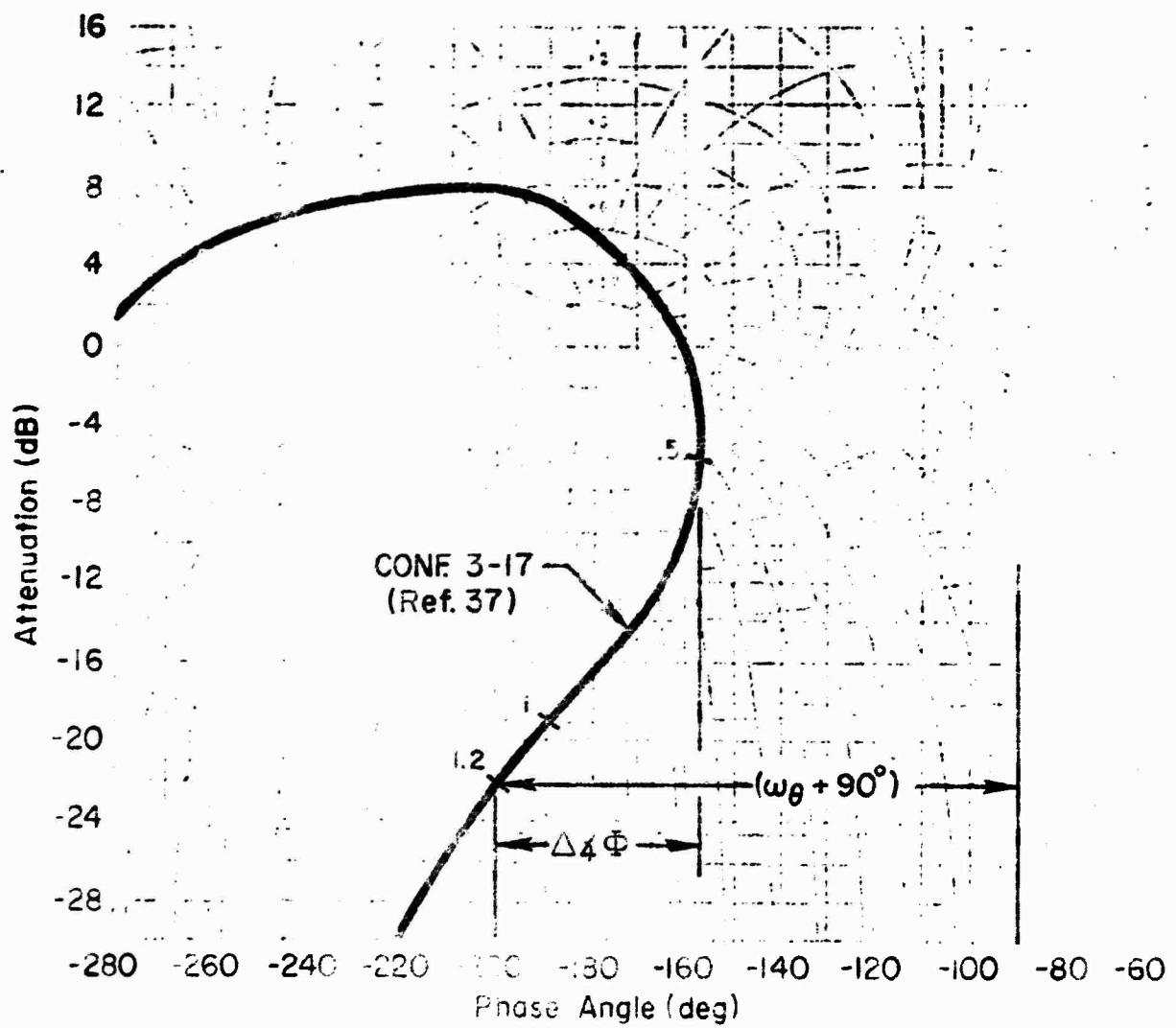


Figure 1.1. Example 1.1. Indicating Deficiency in Definition of ω_g for Newell's Criterion

TABLE 8. DEFINITIONS AND RULES OF APPLICATION (REF. 28 CRITERION)

$\left(\frac{\Delta A}{\Delta \phi}\right)_\theta$	A parameter measured from the combined frequency response of pitch attitude to elevator control force and a 0.3 second time delay. If the amplitude of $[\theta(j\omega)/F_s(j\omega)] \times \exp(-0.3j\omega)$ is plotted versus the phase, $(\Delta A/\Delta \phi)_\theta$ is the most negative average slope between the reference frequency, ω_0 , and any frequency from low frequencies up to $\omega_0 + 0.3$ (see Fig. 16b). Units are dB/deg.
$\Delta \phi_\theta$	A parameter measured from the amplitude phase curve of $[\theta(j\omega)/F_s(j\omega)] \times \exp(-0.3j\omega)$. It is the phase at ω_0 minus the first local phase maximum. If no well-defined local phase maximum exists, $\Delta \phi_\theta = (\text{phase at } \omega_0 + 90)$. Units are degrees.
ω_0	The reference frequency used for the maneuver response measurements of 3.2.2.1, rad/sec.
$\left \frac{\ddot{\theta}}{F_s}\right _{\max}$	Pitch control sensitivity. The peak frequency response amplitude of $ \ddot{\theta}(j\omega)/F_s(j\omega) $, (rad/sec ²)/lb.

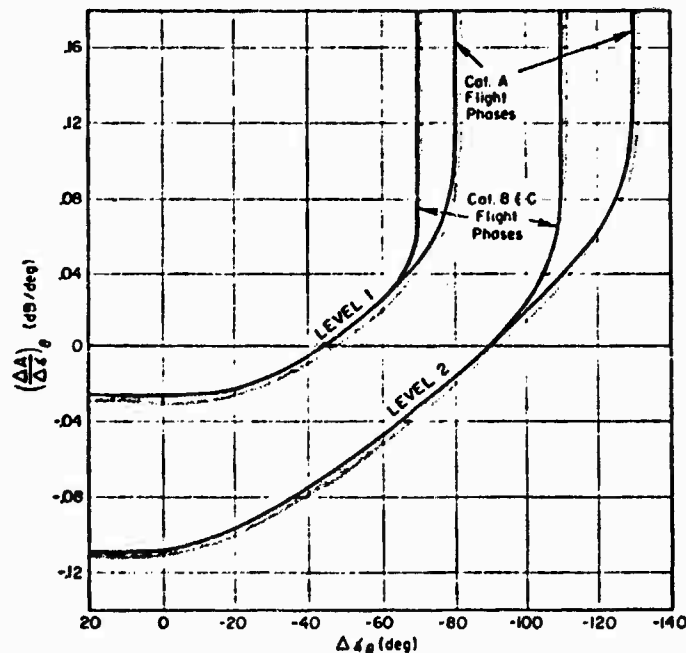


Figure 16b. Longitudinal Maneuver Response Requirements

control roots are present in the θ transfer functions. This deficiency stems directly from the fact that the criterion was developed using only data for which the short-period approximation applied, i.e., no unusual or strong (unstable) phugoid and short-period interactions.

The final "deficiency" relates to the criterion's apparent inapplicability to high gain augmentation concepts. Such difficulties can involve the "blowup" of the $dA/d\phi$ parameter previously cited. However, a more basic problem may be that the criterion is based on an attitude loop closed by the pilot, whereas such closure may already be effected by a high gain command augmentation system. Under such circumstances, the pilot may simply command attitude directly (without inner-loop complications) to control flight path.

Many of the "problems" cited above could presumably be overcome with modified "rules" and/or reference points for the parameters involved, and their application to a broader, more inclusive, data base. Such possibilities were considered but rejected in favor of developing the simpler recommended criterion.

Justification of the Recommended Criterion

The departure point for the recommended criterion is the same as that for Neal's (Ref. 28), namely, using the open-loop θ/F_s or θ/δ_s transfer function plus an effective time delay of 0.30 second. However, to overcome some of the problems inherent in the Ref. 28 criterion, only the phase properties of θ/F_s or θ/δ_s response are used. These properties are the phase angle, ϕ , and the phase gradient, $d\phi/d\omega$, as previously defined.

Background Considerations. Phase characteristics were specifically selected for consideration because our previous studies (Refs. 31 and 38) had shown a strong correlation between phase measures and rating trends. Also, phase parameters are implicitly a measure of several of the pilot-centered qualities previously defined. The only quality not specifically indicated by the phase characteristics is the static gain level.

Initial consideration as to the proper definition and use of phase properties was based on a "standard" control element form for which the correspondence between rating level and pilot equalization was well known and justifiable from

both theoretical and empirical viewpoints. The phase parameters selected were to be indicative not only of the desired region, but also of departures therefrom.

The standard control element was the simple rate system:

$$\frac{\theta}{\delta} = \frac{K}{s(s + 1/T_{sp})}$$

where

$$1/T_{sp} = 1 \text{ rad/sec}$$

For this system, pilot equalization is a lead to essentially cancel the lag due to $1/T_{sp}$. This allows the pilot to extend the bandwidth to approximately 2.5 rad/sec, which is desired for compensatory tracking tasks. The lead requirement of 1 rad/sec is approximately the minimum value for which the pilot will give a satisfactory rating (i.e., Level 1). Thus, simply knowing the phase at a reference frequency near 1 rad/sec infers the equalization needs of the pilot and the approximate pilot rating level. In effect, this almost supplies a single-point definition of the effective airframe.

To complete the picture, the gradient of the phase curve, $d\phi/d\omega$, is used to further describe the characteristics of the effective airframe. Note that when the phase angle is -135 degrees, the slope, $d\phi/d\omega$, will be -26 deg per rad/sec, and the effective airframe corresponds to the rate system with a 1 rad/sec time constant. Departures from this slope are indicative of the effectiveness of the pilot compensation, since for $d\phi/d\omega < -26$ deg per rad/sec simple lead equalization may not be adequate for desired closures. The value of the slope also provides an indication of the sensitivity of the closed-loop characteristics to changes in pilot compensation. Finally, recognizing the implicit relationship between phase and amplitude slope for minimum phase systems (e.g., Ref. 6), it serves to indicate the available gain margin.

Correlation With Available Data. To obtain some indication of the trends for the Level 1 (PR = 3.5) and Level 3 (PR = 6.5) boundaries given by the selected parameters, semi-empirical data from a variety of sources (e.g., Refs. 31, 39, 41-42) were first examined. These data cover a spread in dynamic

characteristics ranging from simple rate response to rate command and attitude command systems. Tables 9 and 10 summarize, respectively, the Levels 1 and 3 boundaries derived from these sources.

Figure 17 shows the trends established by these data as they relate to the recommended Levels 1 and 3 boundaries. Note that the Level 1 boundary is basically described by the requirement for the extremes of second-order-type system. That is, the upper level is defined primarily by the phase gradient associated with the periodic (i.e., oscillatory) form, while the limiting phase angle is tied to the aperiodic form.

The Level 3 boundary appears to be dominated by the requirement for a time-to-double amplitude greater than about 5 seconds. In other words, the divergence (i.e., unstable response) time appears to be the roughly governing factor regardless of the exact nature of the response. The third-order element from Ref. 31 also helps define the Level 3 boundary. In this case, the pilot's major complaint centers on the sluggish response and corresponding excessive lead required to stabilize the system.

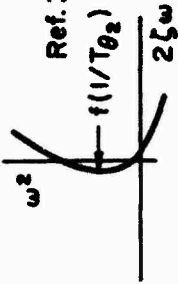
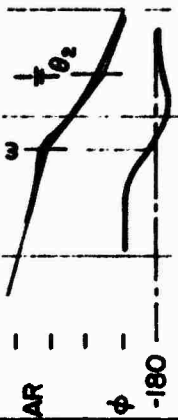
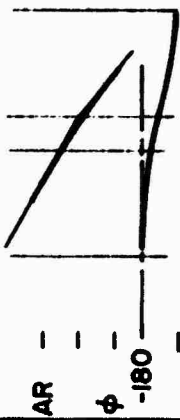
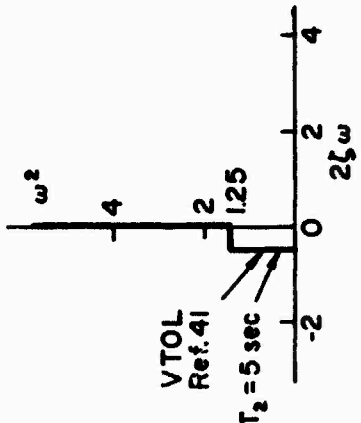
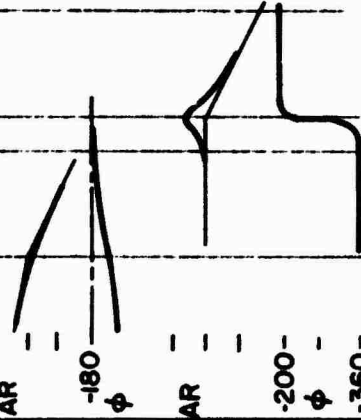
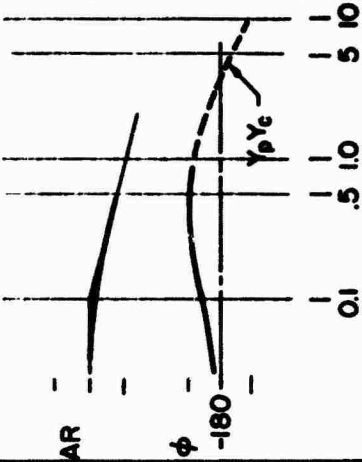
Figure 18 provides the final correlation obtained with the Table 6 representative group of handling quality data. It is apparent that the boundaries, which are a compromise between the data points shown and the semi-empirical boundaries mapped in Fig. 17, are reasonably well supported by the combined data. Furthermore, as either phase angle or phase gradient increases, there is essentially a linear deterioration in the rating. A clearer indication of this feature is given by the typical cross section plot of Fig. 19. The variability and justifications for the final compromise boundaries are evident. Additional crossplots are given in Appendix D.

Returning to Fig. 18 again, we find that the Level 1 boundary is fairly well defined by the data shown except for a single point at $d\phi/d\omega = -23.5 \text{ deg}/(\text{rad}/\text{sec})$ and $\phi = -140 \text{ deg}$. This point represents a rate-command/attitude-hold system tested in the PA-30 aircraft at NASA Flight Research Center (Ref. 40). The rating given (5.0+) corresponds to the average that was achieved in a slightly turbulent environment. There are apparently two reasons why this system is downrated. First, the aircraft is gust sensitive (i.e., M_α and Z_α are large) even with a relatively high bandpass rate-command/attitude-hold system. This is indicated by the trends and the data variability shown in Fig. 20 as a

TABLE 9. SEMI-EMPIRICAL LEVEL 1 BOUNDARIES DERIVED FROM VARIOUS SOURCES

CLASSIFICATION	TRANSFER FUNCTION	LEVEL 1 (PR = 3.5) REQUIREMENT	BODE CHARACTERISTICS
Rate Response Systems	$Y_c = \frac{\theta}{\delta} = \frac{K}{s(s + 1/T_{sp})}$	$1.0 \leq T_{sp} \leq 1.25$ Refs. 31, 42	
Attitude Response System	$\frac{\theta}{\delta} = \frac{K}{[s^2 + 2\zeta\omega s + \omega^2](s + 1/T_{sp1})(s + 1/T_{sp2})}$		
Rate Command Attitude Hold System	$\frac{\theta}{\delta} = \frac{K}{s[s^2 + 2\zeta\omega s + \omega^2](s + 1/T_1)(s + 1/T_2)}$		

TABLE 10. SEMI-EMPIRICAL LEVEL 3 BOUNDARIES DERIVED FROM VARIOUS SOURCES

CLASSIFICATION	TRANSFER FUNCTION	LEVEL 3 (PR = 6.5) REQUIREMENT	BODE CHARACTERISTICS
Conventional Airframe	$\frac{\theta}{\delta} = \frac{M\delta(s + 1/T_{\theta 2})}{s[s^2 + 2\zeta\omega s + \omega^2]}$ <p>where $\omega_{sp} \ll 1/T_{\theta 2}$</p>		
Third Order	$\frac{\theta}{\delta} = \frac{K}{s^2(s + 1/T_{sp})}$	$1/T_{sp} \doteq 1$ <p>Ref. 31</p>	
Unstable Second Order a) aperiodic b) periodic	$\frac{\theta}{\delta} = \frac{K}{s(s - \lambda)}$ $\frac{\theta}{\delta} = \frac{K}{[s^2 - 2\zeta\omega s + \omega^2](s - \lambda_1)(s + \lambda_2)}$		
Unstable First Order	$\frac{\theta}{\delta} = \frac{K}{s - \lambda}$	$\lambda = 0.1 \rightarrow 0.21$ $T_2 = 5-6 \text{ sec}$ <p>Ref. 41</p>	

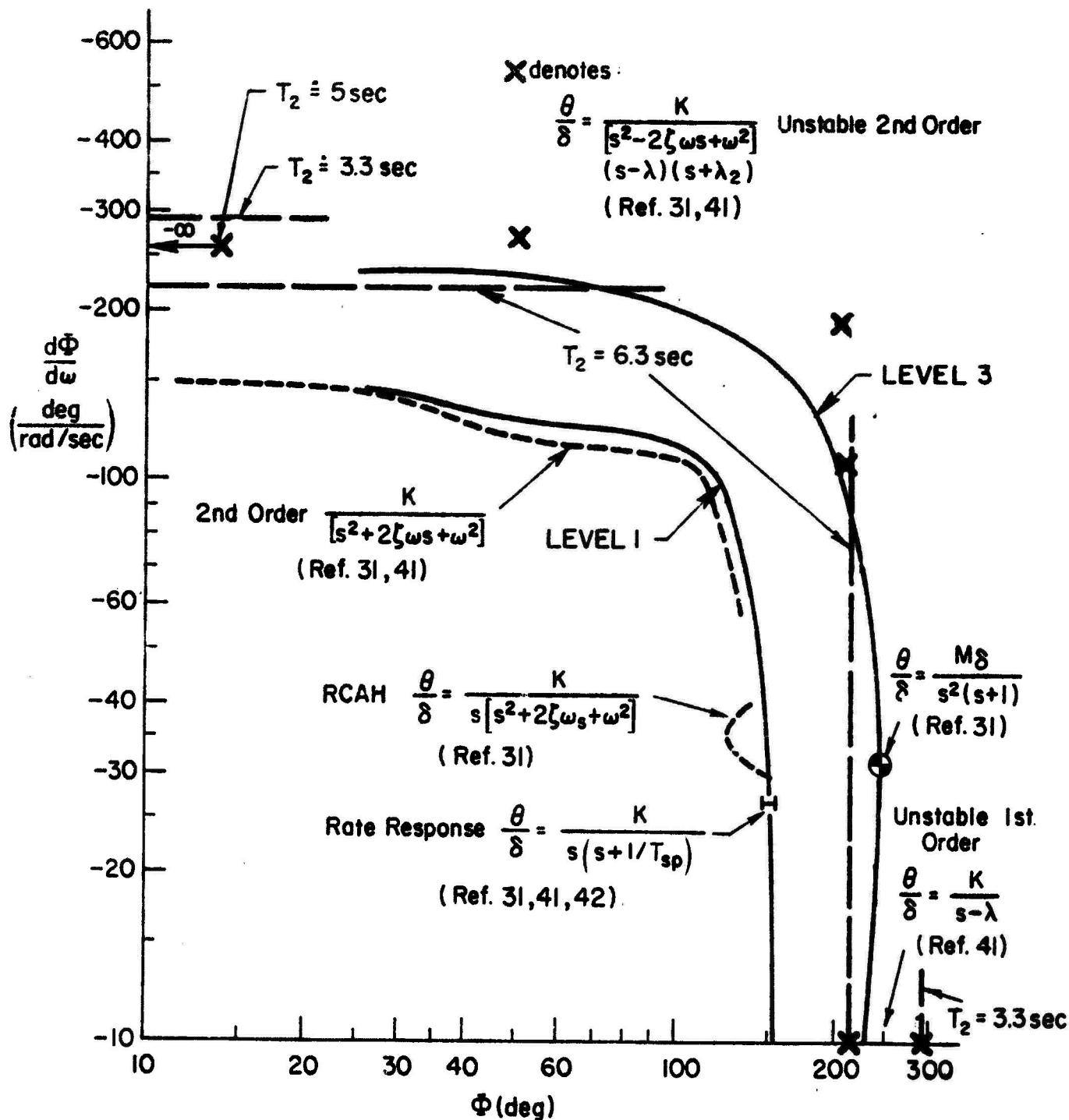


Figure 17. Comparison With Other Semi-Empirical Boundaries

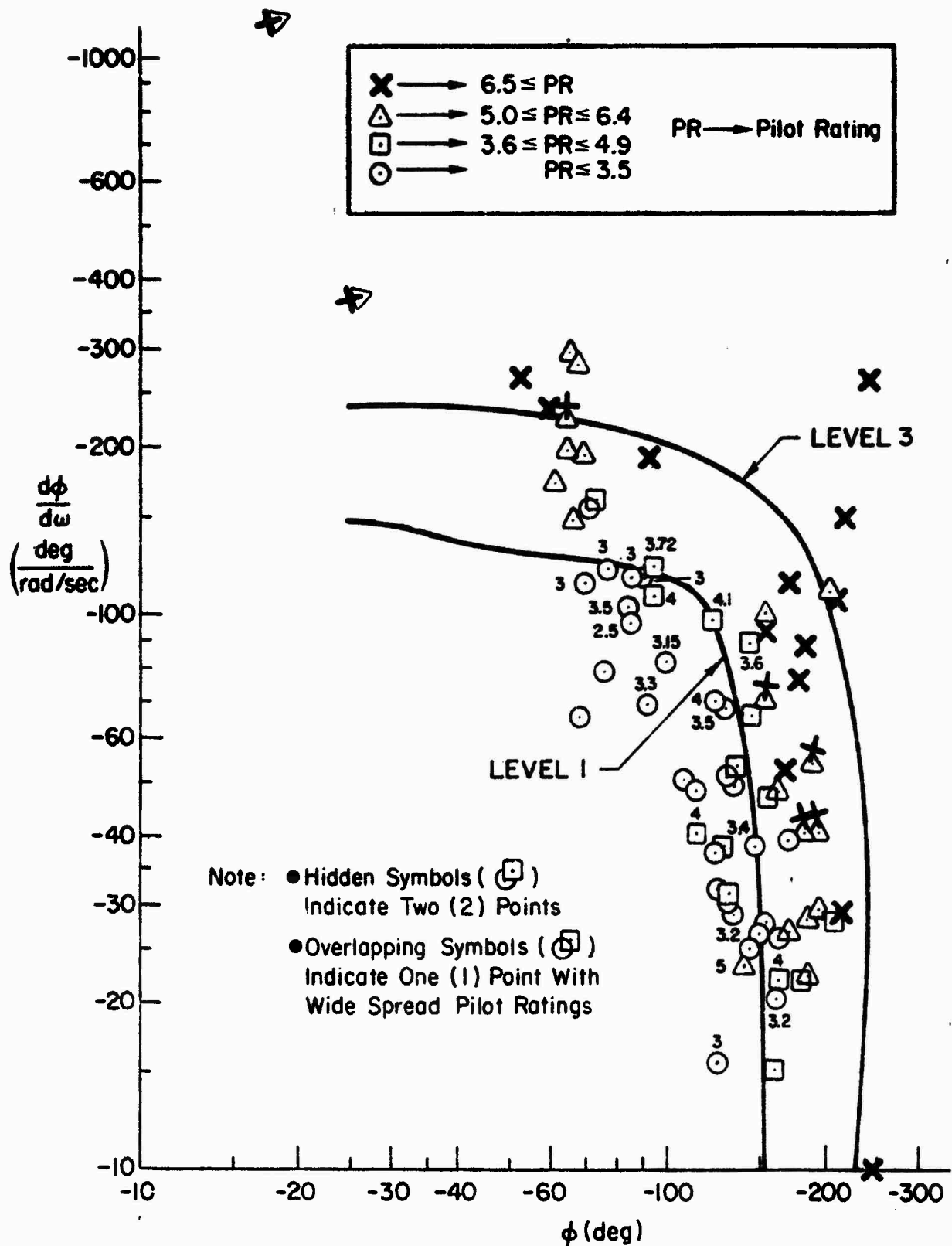


Figure 18. Correlation of Criterion With Available Data

Cross Section

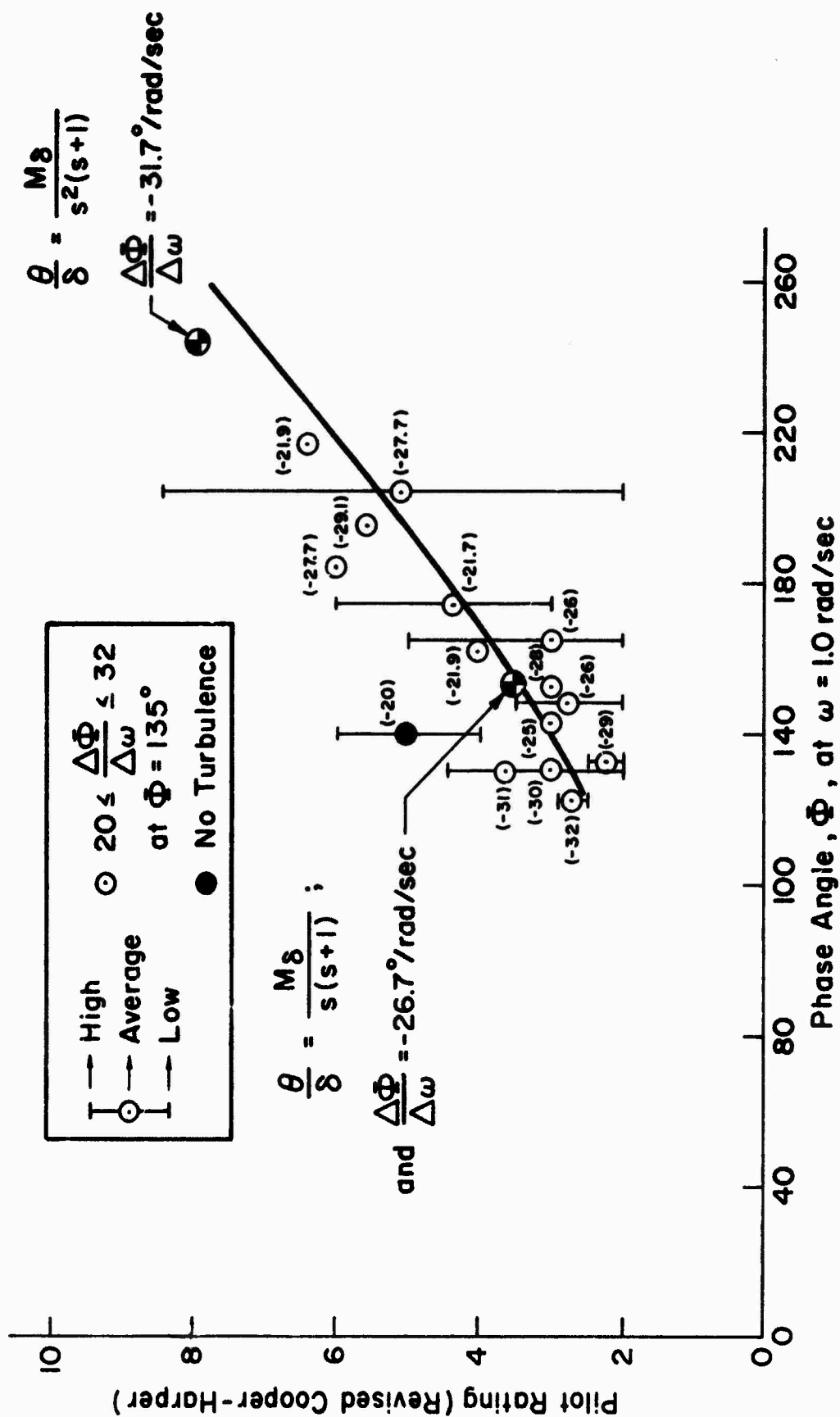


Figure 19. Typical Crossplots in the Region of Rate Response System

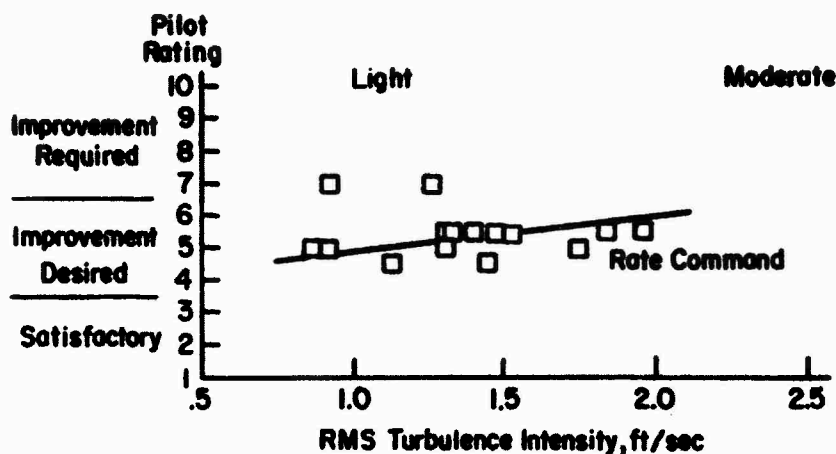


Figure 20. Pilot Ratings of ILS Approach Task;
Basic and Rate Command Control (Ref. 40)

function of gust intensity level. Second, the ability of the pilot to increase the attitude bandwidth to improve flight path control is severely limited. For example, note from the frequency response diagram of Fig. 21 that the phase angle of the basic θ/δ response is limited to somewhat less than $2\frac{1}{2}$ rad/sec if the pilot introduces no lead equalization. However, if lead equalization is introduced (as shown illustratively), there is an improvement in the phase margin but the gain margin essentially disappears. A better choice of the lead equalization time constant would compromise these counteracting effects, i.e., provide somewhat better phase margin at less gain margin reduction. The point is, though, that the situation is one of incipient performance reversal, and the pilot is compelled to accept the airplane more or less as is; he cannot easily compensate for any deficiencies that arise. In a sense, he is "locked in" to a given role and resulting performance which may or may not be satisfactory for the atmospheric conditions and disturbances that he encounters.

A final point (of general importance, as well as of specific interest for the data point in question) concerns the detailed features of a rate command concept. In this concept the stick commands attitude rate and must be held at neutral to hold a given attitude. This feature means that the low-frequency characteristics are significantly changed, since there is no correspondence between stick position and attitude. In a sense, attitude control is degraded from that of a conventional airplane, particularly in a disturbance environment,

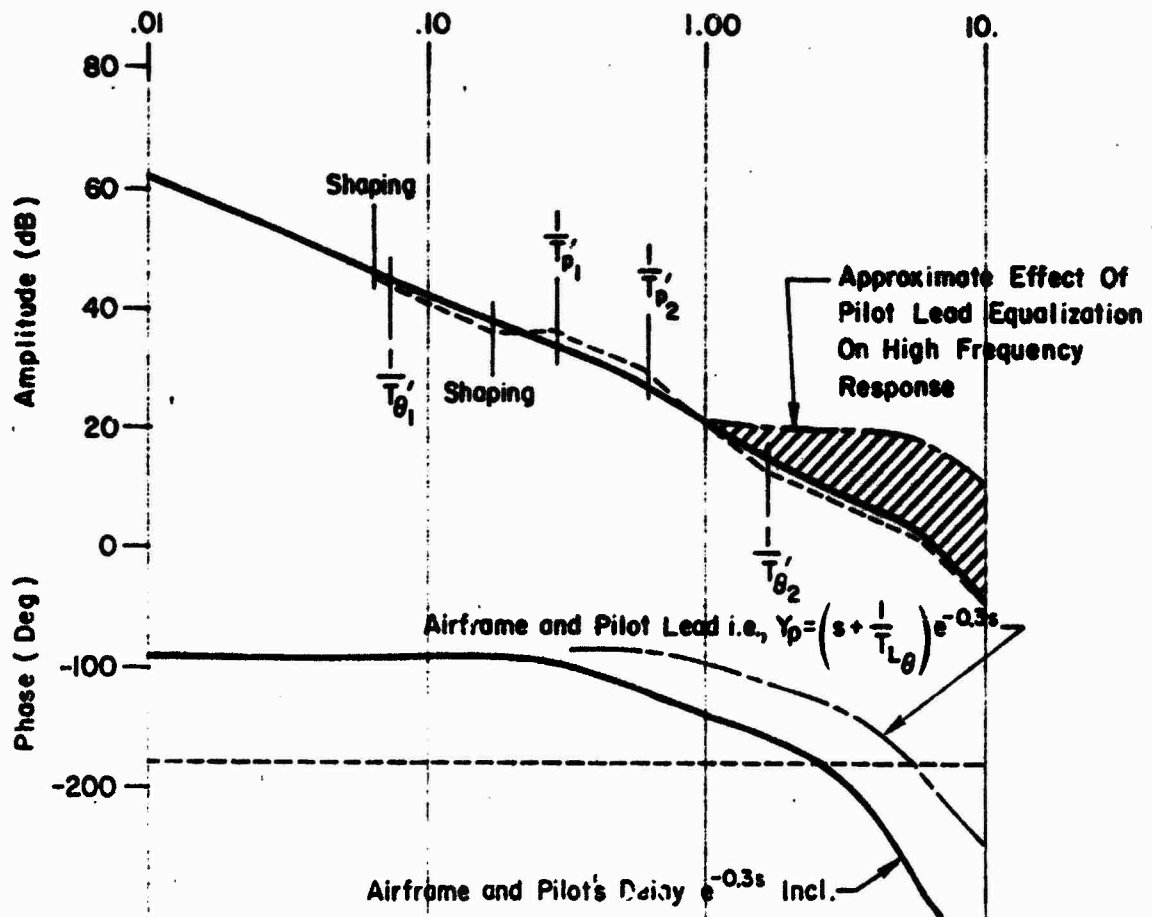


Figure 21. Effects of Pilot Equalization on Attitude Closure With a Rate Command System

because the attitude will appear to drift, thus upsetting the trim speed and flight path. This increases the pilot's workload and, consequently, degrades his opinion. This conclusion is consistent with the Ref. 40 pilots' preference for the attitude command system, where they specifically commented on the desirability of having a solid attitude reference (i.e., no drift) when controlling in turbulence.

Thus, we conclude that the basic difficulty encountered with this system is not totally related to "basic" attitude control alone, but appears to be due to a combination of path control and turbulence factors.

REFERENCES

1. Drake, Douglas, E., Robert A. Berg, Gary L. Teper, and W. Allen Shirley, A Flight Simulation Study of STOL Transport Lateral Control Characteristics, FAA-RD-70-61, Sept. 1970.
2. Flying Qualities of Piloted Airplanes, MIL-F-8785B(ASG), 7 Aug. 1969.
3. Hoh, R. H., and H. R. Jex, Effect of Sideslip on Precise Lateral Tracking, Systems Technology, Inc., Working Paper No. 189-3, Nov. 1969.
4. Stapleford, Robert L., Richard H. Klein, and Roger H. Hoh, Handling Qualities Criteria for the Space Shuttle Orbiter During the Terminal Phase of Flight, Systems Technology, Inc., Tech. Rept. No. 1002-1, Aug. 1971.
5. Doetsch, K-H., Jr., D. G. Gould, and D. M. McGregor, A Flight Investigation of Lateral-Directional Handling Qualities for V/STOL Aircraft in Low Speed Maneuvering Flight, AFFDL-TR-69-41, Mar. 1970.
6. McRuer, Duane, Dunstan Graham, and Irving Ashkenas, Aircraft Dynamics and Automatic Control, Princeton, N. J., Princeton Univ. Press, 1972.
7. Stapleford, R. L., D. T. McRuer, R. H. Hoh, D. E. Johnston, and R. K. Heffley, Outsmarting MIL-F-8785B(ASG), the Military Flying Qualities Specification, Systems Technology, Inc., Tech. Rept. No. 190-1, Aug. 1971.
8. Magdaleno, R. E., and D. T. McRuer, Experimental Validation and Analytical Elaboration for Models of the Pilot's Neuromuscular Subsystem in Tracking Tasks, NASA CR-1757, Apr. 1971.
9. McRuer, Duane, Dunstan Graham, Ezra Krendel, and William Reisener, Jr., Human Pilot Dynamics in Compensatory Systems — Theory, Models, and Experiments with Controlled Element and Forcing Function Variations, AFFDL-TR-65-15, July 1965.
10. Stapleford, Robert L., Donald E. Johnston, Gary L. Teper, and David H. Weir, Development of Satisfactory Lateral-Directional Handling Qualities in the Landing Approach, NASA CR-239, July 1965.
11. Seckel, Edward, James A. Franklin, and George E. Miller, Lateral-Directional Flying Qualities for Power Approach Influence of Dutch Roll Frequency, Princeton Univ. Dept. of Aero. and Mech. Sciences Rept. 797, Sept. 1967.

12. Hall, G. Warren, and Edward M. Boothe, An In-Flight Investigation of Lateral-Directional Dynamics for the Landing Approach, AFFDL-TR-70-145, Oct. 1970.
13. Ellis, David R., Flying Qualities of Small General Aviation Airplanes. Part 2: The Influence of Roll Control Sensitivity, Roll Damping, Dutch-roll Excitation, and Spiral Stability, FAA-RD-70-65 Part 2, Apr. 1970.
14. Meeker, James I., and G. Warren Hall, In-Flight Evaluation of Lateral-Directional Handling Qualities for the Fighter Mission, AFFDL-TR-67-98, Oct. 1967.
15. Creer, B. Y., D. R. Heinle, and R. C. Wingrove, "Study of Stability and Control Characteristics of Atmosphere-Entry Type Aircraft Through Use of Piloted Flight Simulators," Inst. of the Aero. Sci. Paper 59-129, presented at 7th Anglo-American Aeronautical Conf., New York, Oct. 5-7, 1959.
16. Chalk, C. R., T. P. Neal, T. M. Harris, et al., Background Information and User Guide for MIL-F-8785B(ASG), "Military Specification - Flying Qualities of Piloted Airplanes", AFFDL-TR-69-72, Aug. 1969.
17. Faye, Alan E., Jr., Attitude Control Requirements for Hovering Determined Through the Use of a Piloted Flight Simulator, NASA TN D-792, Apr. 1961.
18. Dander, Capt. Vernon A., An Evaluation of Four Methods for Converting Single Axis Pilot Ratings to Multi-Axis Pilot Ratings Using Fixed Base Simulation Data, (Thesis), Air Force Inst. of Tech. GE/EE/62-4, Dec. 1962.
19. White, Maurice D., Richard F. Vomaske, et al., A Preliminary Study of Handling-Qualities Requirements of Supersonic Transports in High-Speed Cruising Flight Using Piloted Simulators, NASA TN D-1888, May 1963.
20. Klein, Richard H., FWJSRA Flight Director Simulation Program, STI WP-1015-8, March 1972. (To be included in final NASA CR-).
21. McDonnell, John D., Pilot Rating Techniques for the Estimation and Evaluation of Handling Qualities, AFFDL TR-68-76, Dec. 1968.
22. Madill, D. R., Lead Discussion, AGARD Conference Proceedings No. 79, North Atlantic Treaty Organization, Advisory Group for Aerospace Research and Development, Simulation, January 1971, pp. 8-4, 8-12.
23. Teper, Gary L., An Assessment of the "Paper Pilot" — An Analytical Approach to the Specification and Evaluation of Flying Qualities, AFFDL-TR-71-174, Nov. 1971.

24. Taylor, Lawrence W., Jr., and Kenneth W. Iliff, Fixed-Base Simulator Pilot Rating Surveys for Predicting Lateral-Directional Handling Qualities and Pilot Rating Variability, NASA TN D-5358, Aug. 1969.
25. Gedeon, Jozsef, "The Statistical Treatment of Pilot-Opinions on Flying Qualities," The Sixth Congress of the International Council of the Aeronautical Sciences, Deutsches Museum, Munchen, Germany, 9-13 Sept. 1968, ICAS Paper No. 68-17.
26. Klein, R. H., et al., XC-142 Vehicle Analyses, Pilot Workload Models, Disturbance Characteristics, and Lateral-Directional Requirements Pertinent to the Design of a STOL Flight Director, Systems Technology, Inc., Interim Tech. Rept. 1011-1, Section VI, 1 June 1971.
27. Ashkenas, Irving L., and Samuel J. Craig, Multiloop Piloting Aspects of Longitudinal Approach Path Control, ICAS Paper No. 72-46, August 28-September 2, 1972.
28. Neal, T. Peter, and C. R. Chalk, Revision of Military Specification MIL-F-8785B(ASG), Flying Qualities of Piloted Airplanes, Cornell Aeronautical Lab., Flight Research Dept., CAL FRM No. 462, 23 July 1971.
29. Greif, Richard K., Emmett B. Fry, Ronald M. Gerdes, and Terrence D. Gossett, Effect of Stabilization on VTOL Aircraft in Hovering Flight, NASA TN D-6900, Aug. 1972.
30. Miller, G. E., and E. Seckel, Flight Evaluation of the Effects of Short Period Frequency and Normal Acceleration Response in Carrier Approach, Princeton University Report No. 882, Nov. 1969.
31. Craig, S. J., and I. L. Ashkenas, Background Data and Recommended Revisions for MIL-F-8785B(ASG), "Military Specification — Flying Qualities of Piloted Airplanes", Systems Technology, Inc., Tech. Rept. 189-1, June 1970.
32. Shooter, K. L., and J. L. Lockenour, TPA 145 Advanced Vehicle Flying Qualities Studies — Task 0001 — Carrier Approach Characteristics, Status Report, North American Aviation, Inc., Rept. NA67H-791, Mar. 1969.
33. Smith, R. E., J. V. Lebacqz, and J. M. Schuler, Flight Investigation of Various Longitudinal Short-Term Dynamics for STOL Landing Approach Using the X-22A Variable Stability Aircraft, Cornell Aeronautical Lab., TB-3011-F-2, Jan. 1973.
34. Miller, G. E., and R. L. Traskos, Flight Evaluation of Engine Response, Flight Path Stability, Tail Lift, and Direct Lift Control, Princeton University Report No. 888, Aug. 1971.
35. Neal, T. Peter, and Rogers E. Smith, An In-Flight Investigation to Develop Control System Design Criteria for Fighter Airplanes, AFFDL-TR-70-74, Vol. I, Dec. 1970.

36. Eney, John A., Comparative Flight Evaluation of Longitudinal Handling Qualities in Carrier Approach, Princeton University Report No. 777, May 1966.
37. Mocij, Herman A., Flight Evaluation of Direct Lift Control and Its Effect on Handling Qualities in Carrier Approach, Princeton University Report No. 811, Dec. 1967.
38. Craig, Samuel J., Anthony Campbell, and R. H. Klein, Analysis of VTOL Handling Qualities Requirements. Part II: Lateral-Directional Hover and Transition, AFFDL-TR-67-179, Part II, Feb. 1970.
39. Rediess, Herman A., Donald L. Mallick, and Donald T. Berry, Recent Flight Test Results on Minimum Longitudinal Handling Qualities for Transport Aircraft, presented at the FAUSST VIII Meeting, Washington, D. C., Jan. 1971.
40. Gee, S. W., M. R. Barber, and T. C. McMurtry, A Flight Evaluation of Curved Landing Approaches, presented at STOL Technology Conf., NASA Ames Research Center, Oct. 1972.
41. Chalk, Charles R., David L. Key, John Kroll, Jr., et al., Background Information and User Guide for MIL-F-83300 — Military Specification. Flying Qualities of Piloted V/STOL Aircraft, AFFDL-TR-70-88, Mar. 1971.
42. Ashkenas, I. L., A Study of Conventional Airplane Handling Qualities Requirements. Part I: Roll Handling Qualities, AFFDL-TR-65-138, Part I, Nov. 1965.
43. Franklin, James A., and Robert C. Innis, Longitudinal Handling Qualities During Approach and Landing of a Powered Lift STOL Aircraft, NASA TM X-62,144, Mar. 1972.
44. Stapleford, Robert L., and Irving L. Ashkenas, "Longitudinal Short-Period Handling Quality Requirements," Section IV of Analysis of Several Handling Quality Topics Pertinent to Advanced Manned Aircraft, AFFDL-TR-67-2, June 1967, pp. 119-166.
45. Weir, D. H., R. H. Klein, and D. T. McRuer, Principles for the Design of Advanced Flight Director Systems Based on the Theory of Manual Control Displays, NASA CR-1748, Mar. 1971.
46. McRuer, D. T., D. H. Weir, and R. H. Klein, "A Pilot-Vehicle Systems Approach to Longitudinal Flight Director Design," J. Aircraft, Vol. 8, No. 11, Nov. 1971, pp. 890-897.
47. Stapleford, Robert L., Samuel J. Craig, and Jean A. Tennant, Measurement of Pilot Describing Functions in Single-Controller Multiloop Tasks, NASA CR-1238, Jan. 1969.
48. Stapleford, R. L., D. T. McRuer, and R. Magdaleno, Pilot Describing Function Measurements in a Multiloop Task, NASA CR-542, Aug. 1966.

49. Cromwell, C. H., and I. L. Ashkenas, A Systems Analysis of Longitudinal Piloted Control in Carrier Approach, Systems Technology, Inc., Tech. Rept. 124-1, June 1962.
50. McRuer, D. T., I. L. Ashkenas, and H. R. Pass, Analysis of Multiloop Vehicular Control Systems, ASD-TDR-62-1014, Mar. 1964.
51. Craig, Samuel J., Robert F. Ringland, and I. L. Ashkenas, An Analysis of Navy Approach Power Compensator Problems, AIAA Paper No. 72-124, Jan. 1972.
52. Neumark, S., Problems of Longitudinal Stability Below Minimum Drag Speed, and Theory of Stability Under Constraint, Aeronautical Research Council R and M No. 2983, July 1953.
53. McRuer, D. T., and H. R. Jex, "A Review of Quasi-Linear Pilot Models," IEEE Trans., Vol. HFE-8, No. 3, Sept. 1967, pp. 231-249.
54. Ashkenas, I. L., "Summary and Interpretation of Recent Longitudinal Flying Qualities Results," J. Aircraft, Vol. 8, No. 5, May 1971, pp. 324-328.
55. Craig, Samuel J., Irving L. Ashkenas, and Robert K. Heffley, Pilot Background and Vehicle Parameters Governing Control Techniques in STOL Approach Situations, FAA RD 72-69, June 1972.
56. Stapleford, Robert L., and Irving L. Ashkenas, "Effects of Manual Altitude Control and Other Factors on Short-Period Handling Quality Requirements," J. Aircraft, Vol. 5, No. 1, Jan.-Feb. 1968, pp. 41-48.
57. Ashkenas, I. L., Some Open- and Closed-Loop Aspects of Airplane Lateral Directional Handling Qualities, AGARD Rept. 533, May 1966.
58. Anderson, Ronald O., A New Approach to the Specification and Evaluation of Flying Qualities, AFFDL-TR-69-120, June 1970.
59. Ashkenas, I. L., and D. T. McRuer, "A Theory of Handling Qualities Derived from Pilot-Vehicle System Considerations," Aerospace Engineering, Vol. 21, No. 2, Feb. 1962, pp. 60, 61, 83-102.
60. Craig, Samuel J., and Anthony Campbell, Analysis of VTOL Handling Qualities Requirements. Part I: Longitudinal Hover and Transition, AFFDL TR-67-179, Oct. 1968.
61. Walton, R. P., I. L. Ashkenas, and C. P. Shortwell, Analytical Review of Military Helicopter Flying Qualities, Systems Technology, Inc., Tech. Rept. 143-1, Nov. 1965.
62. Chen, R. T. N., A Preliminary Analysis on the Pilot-STOL Aircraft System in Landing Approach, Cornell Aeronautical Lab., Inc., Flight Research Dept., VTOL H.Q. TM-30, Feb. 11, 1972.

63. McRuer, Duane, and David H. Weir, "Theory of Manual Vehicular Control," Ergonomics, Vol. 12, No. 4, July 1969, pp. 599-633.
64. Giles, Richard F., "An Analytical Investigation of Short-Period Flying Qualities," J. Aircraft, Vol. 9, No. 2, Feb. 1972, pp. 103-107.
65. Ashkenas, I. L., and T. S. Durand, "Simulator and Analytical Studies of Fundamental Longitudinal Control Problems in Carrier Approach," AIAA Simulation for Aerospace Flight Conference, A Volume of Technical Papers Presented Aug. 26-28, 1963, Columbus, Ohio, AIAA, New York, 1963, pp. 16-34.
66. Wasicko, Richard J., Application of Approach Speed Criteria Derived from Closed-Loop Pilot-Vehicle Systems Analyses to an Ogee Wing Aircraft, NASA CR-579, Sept. 1966.
67. Drinkwater, Fred J., III, and L. Steward Rolls, Flight Experience with the Ogee Wing at Low Speed, AIAA Paper No. 65-782, Nov. 1965.

APPENDIX A

CALCULATION OF μ

The following example is given to illustrate a typical computation of the rudder shaping parameter, μ . The example configuration is taken from the variable stability in-flight simulation of Ref. 5 (Configuration LH70+20+37). Given the basic stability derivatives, the sideslip numerators are computed and substituted into Eqs. 3 and 5 as follows:

$$Y'_{CF} = \frac{N_{\delta_{rc}} \delta_{rc}}{L_{\delta_{ac}} \delta_{ac}} = - \frac{N'_{\delta_{rc}}}{L'_{\delta_{ac}}} \frac{N_{\delta_{ac}}^{\beta}}{N_{\delta_{rc}}^{\beta}} = \frac{.19(.102)(-.922)(605.18)^{*}}{(-.057)(5.60)(109.93)} \quad (A-1)$$

As discussed in the text, the roots outside the frequency range of interest (0.333 to 6 rad/sec) are eliminated by considering the high-frequency roots as part of the leading coefficient and the low-frequency roots to be at zero. The following expression results:

$$Y'_{CF} = \frac{1.042(-.922)}{(5.6)} \quad (A-2)$$

Figure 22 presents the rudder time history to a unit step aileron obtained from Eq. A-2. The rudder shaping parameter, μ , is obtained from Eq. 12.

$$\mu = \left[\left(-\frac{.17}{1.042} - 1 \right) \frac{1}{1 - e^{-3 \times 5.6}} \right] = -1.165 \quad (A-3)$$

The frequency response for the aileron rudder shaping considered in the present example is given in Fig. 23 and is seen to have the same

*Nomenclature is $(1/T) = s + 1/T$.

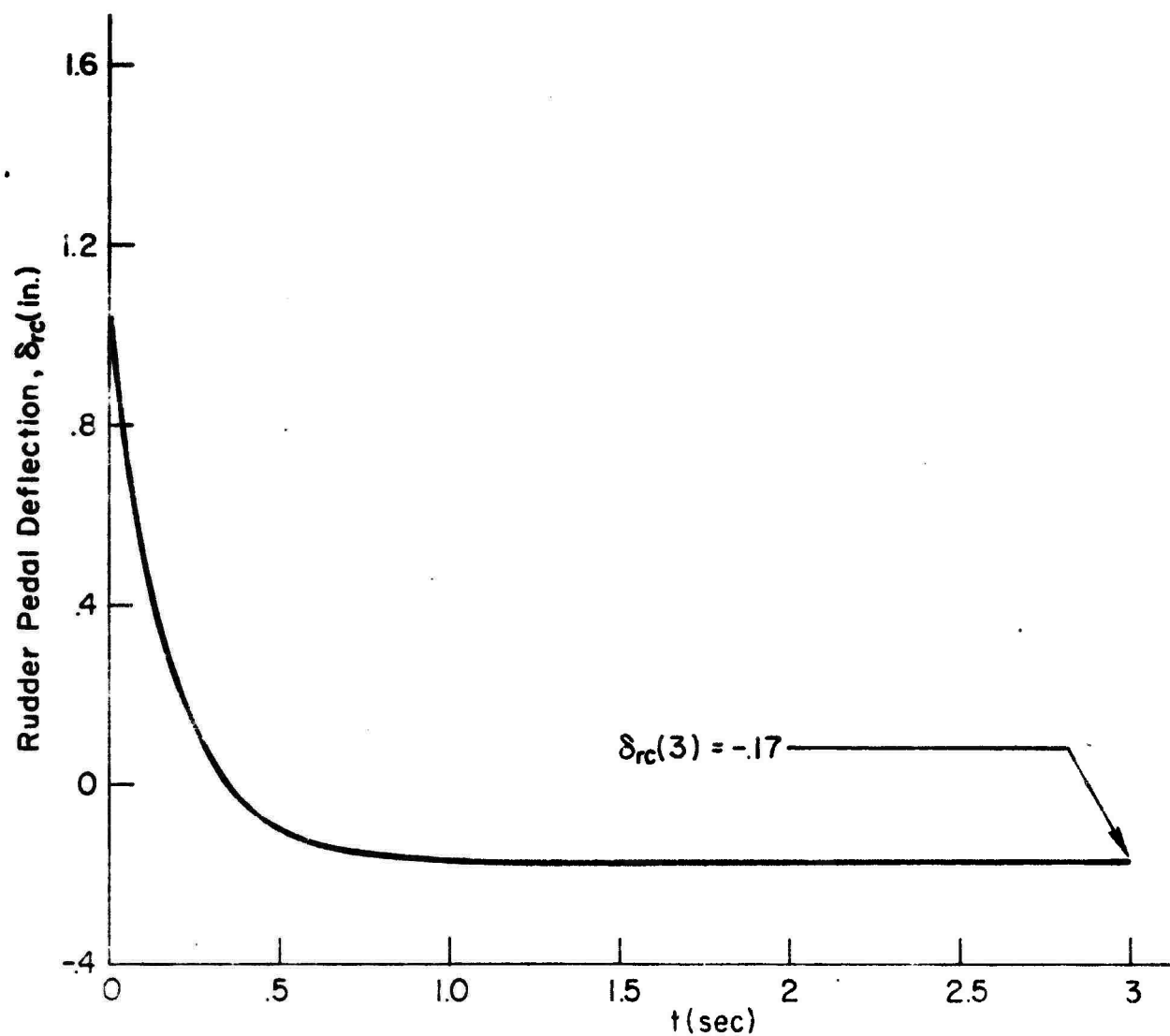


Figure 22. Required Rudder Time Response to Coordinate a Unit Step Aileron Input

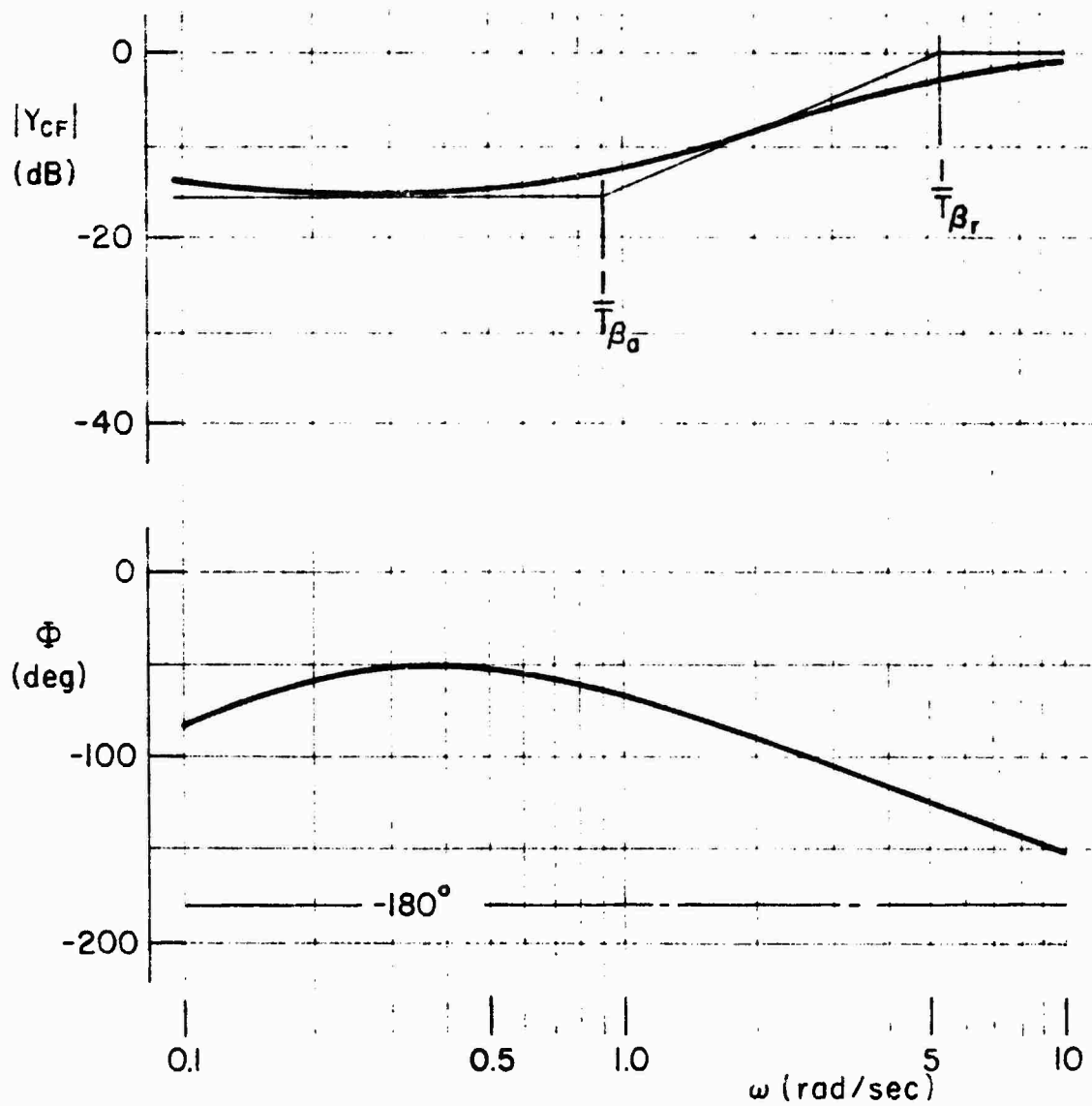


Figure 23. Frequency Response for Aileron-Rudder Crossfeed (Ref. 5, Configuration LH70+20+37)

asymptote form as shown in Fig. 3 for $\mu < 0$. Using these frequency characteristics, μ is computed from Eq. 7 as follows:

$$\mu = \frac{T_{\beta r}}{T_{\beta a}} - 1 = -\frac{.922}{5.6} - 1 = -1.165 \quad (A-4)$$

It should be remembered that when the actual crossfeed does not match the first-order model as well as this example, it is considerably more straightforward to compute μ based on the time response (Eq. 12) than to compute an equivalent system in the frequency domain.

Finally, it is of some interest to look at the effects of eliminating the low- and high-frequency modes from Eq. A-1. Figure 24 presents a comparison of the time responses for Eqs. A-1 and A-2. The very-high-frequency rudder activity discussed in the text is quite evident from the plot of Eq. A-1. Comparison of the two time responses shows very little difference from 0.05 sec to 3.0 sec.

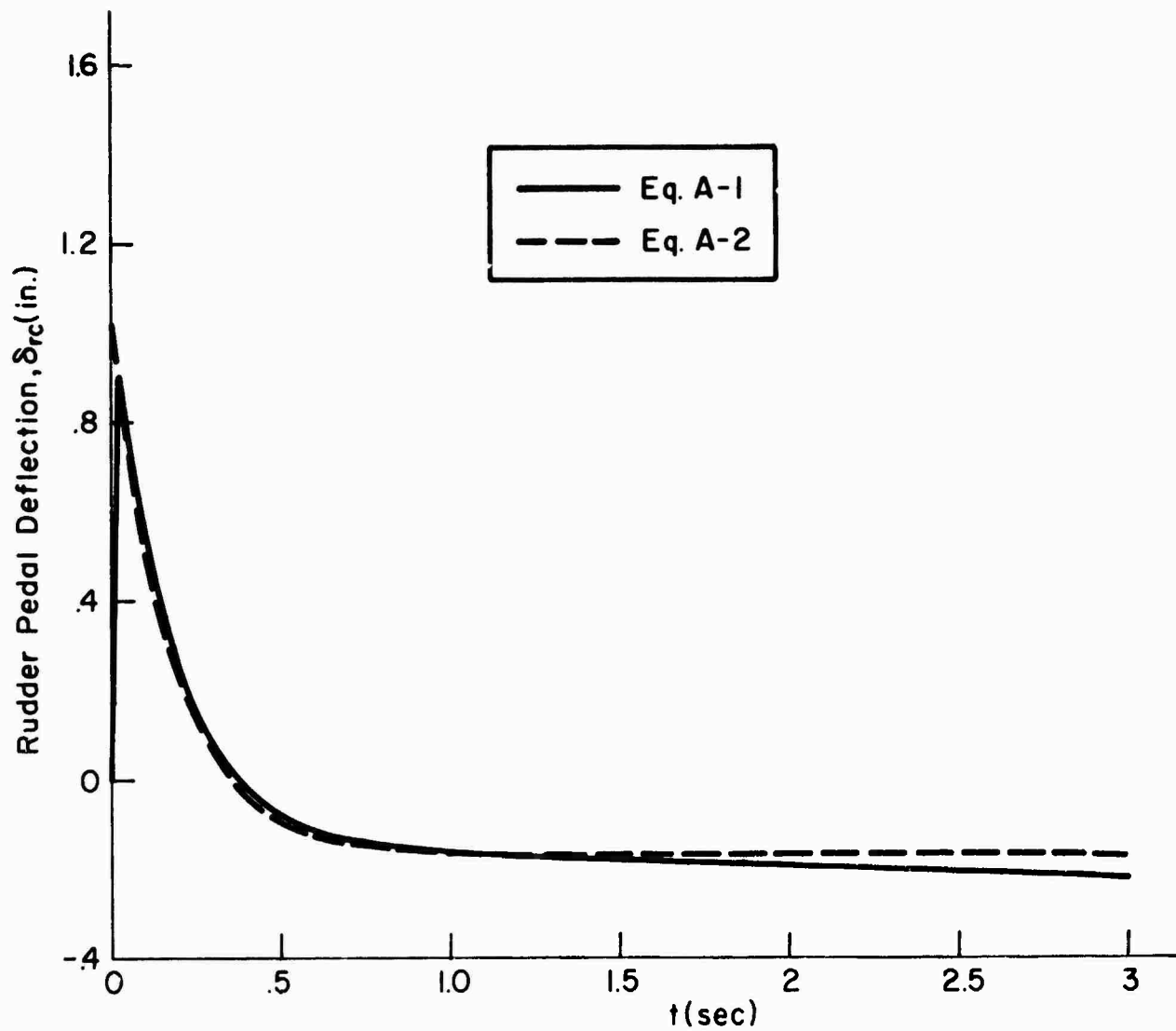


Figure 24. Comparison of Eq. A-1 and Eq. A-2

APPENDIX B

SUMMARY OF DATA USED IN HEADING CONTROL CORRELATIONS

REFERENCE 12 DATA (Δ)

EXECUTIVE JET AND MILITARY CLASS II

RUN ID	$\frac{1}{T_R}$	ω_d	ξ_d	$\left \frac{\phi}{\beta}\right _d$	$\frac{N'_{\delta_{ac}}}{L'_{\delta_{ac}}}$	μ	$\frac{N'_{\delta_{rc}}}{L'_{\delta_{ac}}} \delta_{rc}(3)$	AVG. POR (Cooper-Harper)
2P2	2.5	1.98	0.10	1.71	0.0016		-0.03	2.5
3A3		2.01	0.24	1.50	-0.252	0.153		2.5
3A2					-0.200	0.193		3.0
3NO					-0.098	0.407		2.0
3P2					0.0016		-0.04	1.5
3P3					0.051	-0.81		1.5
4P2		2.02	0.10	3.14	0.0016		-0.046	3.0
7A1		1.01	0.29	1.48	-0.149	0.568		2.5
7NO					-0.098	0.873		2.0
7P1					-0.048	1.81		2.0
12A2		0.98	0.34	0.24	-0.20	0.415		3.0
12A1					-0.149	0.565		2.5
12P1					-0.048	1.80		2.0
12P2					0.0016		-0.08	2.0
12P3					0.051	-1.75		1.5

REFERENCE 5 DATA (C)

(STOL)

Avg Pilots B, C, D, E

RUN ID	$\frac{1}{T_R}$	ω_d	ζ_d	$\left \frac{\Phi}{\beta}\right _d$	$\frac{N_{\delta_{ac}}}{L_{\delta_{ac}}}$	μ	$\frac{N_{\delta_{rc}}}{L_{\delta_{ac}}} \delta_{rc}(3)$	AVG. POR (Cooper-Harper)
LH100+20+50	4.0	1.0	0.2	0.2	2.45	-0.932		7.25
LH77+20+40					2.00	-1.14		6.5
LH70+20+37					1.88	-1.17		6.0
LH112+20+44					2.00	-0.838		6.25
LH100+20+40					1.70	-0.986		6.00
LH94+20+38					1.55	-1.08		6.00
LH81+20+34					1.30	-1.29		4.75
LH73+20+31					1.12	-1.49		6.0
LH121+20+35					1.41	-0.642		7.0
LH111+20+33					1.1	-0.812		4.75
LH100+20+30					0.81	-1.12		3.0
LH91+20+28					0.595	-1.52		4.0
LH76+20+24					0.277	-3.26		4.75
LH111+20+22					0.152	0.126		4.0
LH100+20+20					-0.133	-0.145		2.5
LH86+20+18					-0.473	-0.041		4.75
LH76+20+17					-0.675	-0.029		6.25
LH123+20+17					0.035		0.63	6.0
LH111+20+16					-0.318	-1.70		5.0
LH100+20+15					-0.533	-0.927		4.75
LH90+20+14					-0.823	-0.657		4.75
LH115+20+11					-0.630	-1.60		6.25
LH100+20+10					-1.03	-0.976		6.5
LH90+20+10					-1.26	-0.798		5.5
LH100+30+30		↓	0.30		-0.200	-0.076		2.0
LM50+29+29		0.50	0.29		-0.100	-0.70		3.5
LH100+30+40		1.0	0.30		0.720	-1.15		2.0
LH100+30+20		1.0	0.30		-1.10	-0.808		3.75
LM50+30+40		0.5	0.30		0.517	-1.12		2.5
LM50+30+20	↓	0.5	0.30	↓	-1.27	-0.927		7.00

REFERENCE 13 DATA (Δ)

(LIGHT AIRCRAFT)

RUN ID	$\frac{1}{T_R}$	ω_d	ζ_d	$\left \frac{\Phi}{\beta}\right _d$	$\frac{N_{\delta_{ac}}}{L_{\delta_{ac}}}$	μ	$\frac{N_{\delta_{rc}}}{L_{\delta_{ac}}} \delta_{rc}(5)$	AVG. POR (Cooper-Harper)
H-93-11	4.0	2.3	0.1	1.65	-0.043	0.665		3.0
H-106-05	↓	↓	↓	1.36	-0.009		0.06	3.0
H-113-09	↓	↓	↓	1.46	0.078	0.055		3.5
H-120-07	↓	↓	↓	1.43	-0.112	0.314		4.5
H-132-06	↓	↓	↓	1.43	0.215	0.164		6.5
H-142-06	↓	↓	↓	1.43	0.302	0.117		7.0
H-96-14	↓	↓	↓	1.88	0		-0.10	3.0

REFERENCE 11 DATA (Δ)

(JET FIGHTER — CARRIER APPROACH)

RUN ID	$\frac{1}{T_R}$	ω_d	ζ_d	$\left \frac{\Phi}{\beta}\right _d$	$\frac{N'_{\delta_{ac}}}{L'_{\delta_{ac}}}$	μ	$\frac{N'_{\delta_{rc}}}{L'_{\delta_{ac}}} \delta_{rc}(3)$	AVG. FOR (Cooper-Harper)
2	4.0	1.8	0.1	1.1	0	NA	-0.069	2.8
6	4.0	1.8	0.1	2.2	↓	↓	-0.080	2.8
7	2.0	1.9	0.1	4.0			-0.135	2.6
104	4.0	1.8	0.1	1.99			-0.216	2.3
109	↓	1.8	0.4	0			-0.193	2.6
128		1.8	0.1	0			-0.057	3.4
201		1.3	0.1	0			-0.046	3.0
202		1.3	0.1	1.96			-0.018	2.7
203		1.3	0.1	3.25			-0.023	2.9
204		1.3	0.4	0			-0.143	3.0
205		1.3	0.4	1.89			-0.149	2.8
206		1.3	0.4	3.6			-0.200	2.9
225		1.3	0.2	1.82			-0.062	2.5
226		2.3	0.2	1.13			-0.102	2.9
231		2.3	0.1	1.13			-0.068	3.2
232		2.3	0.1	1.7			-0.088	3.1
240		2.3	0.4	0			-0.240	2.9
241		2.3	0.4	0.88			-0.230	2.7
242		2.3	0.4	1.96			-0.245	2.6
243		3.0	0.4	0			-0.310	3.4
244		3.0	0.4	1.41			-0.334	3.1
245		3.0	0.4	2.73			-0.362	3.3

REFERENCE 4 DATA (□)

(SPACE SHUTTLE CONFIGURATIONS — LANDING)

RUN ID	$\frac{1}{T_R}$	ω_d	ζ_d	$ \frac{\phi}{\beta} _d^*$	$\frac{N_{\delta_{ac}}}{L_{\delta_{ac}}}$	μ	$\frac{N_{\delta_{rc}}}{L_{\delta_{ac}}} \delta_{rc}(3)$	AVG. POR (Cooper-Harper)
1	1.5	1.0	0.2		-0.378	-0.742		4.5
2					0.0012		0.30	4.5
3					-0.358	0.048		5.5
4					-0.020		-0.015	2.1
5					0.379	-0.045		4.5
6					0.067	-4.99		4.0
7					0.389	-0.863		4.75
8					-0.071	-0.662		1.75
9					-0.0025		0.04	2.40
10					-0.070	0.091		1.5
11					0.01		0.00	1.5
12					0.061	-0.18		3.0
13					-0.011		-0.095	2.5
14					0.044	-2.86		4.0
1A					-0.207	-1.51		3.0
1B					-0.077	-1.46		1.5
1C					-0.037	-1.47		1.0
1D					-0.023		0.01	2.0
2A					-0.40	-0.132		5.5
2B					-0.147	-0.038		4.0
2C					-0.083	0.029		2.0
2D					-0.057	0.171		2.5
3A					0.402	-0.144		5.8
3B					0.115	-0.146		3.5
3C					0.047	-0.41		1.75
3D					0.022		-0.03	2.25

(continued on next page)

* $|\phi/\beta|_d$ is not a factor since turbulence was not simulated in these experiments.

REFERENCE 4 DATA (concluded)

RUN ID	$\frac{1}{T_R}$	ω_d	ζ_d	$\left \frac{\Phi}{\beta}\right _d$	$\frac{N'_{\delta_{ac}}}{L'_{\delta_{ac}}}$	μ	$\frac{N'_{\delta_{rc}}}{L'_{\delta_{ac}}} \delta_{rc}(3)$	AVG. POR (Cooper-Harper)
4B	1.5	1.0	0.2		0.185	-1.83		3.75
4C	↓	↓	↓		0.037		-0.15	2.25
4D	↓	↓	↓		-0.004		-0.12	2.0
5A	↓	↓	0.40		-0.434	-0.086		4.5
5B	↓	↓	↓		-0.171	-0.006		3.5
5D	↓	↓	↓		-0.075	0.450		2.75
6A	↓	↓	↓		0.285	-0.124		5.0
6B	↓	↓	↓		0.038	-1.45		3.75
6D	↓	↓	↓		-0.024		-0.19	3.25
9A	↓	2.0	0.20		-0.260	0.288		3.25
9C	↓	↓	↓		-0.087	1.21		1.5
10A	↓	↓	↓		0.238	-0.335		3.0
10B	↓	↓	↓		0.111	-0.661		1.5
10C	↓	↓	↓		0.062	-1.4		1.75

REFERENCE 1 DATA (□)

(SPOL CONFIGURATIONS)

RUN ID	$\frac{1}{T_R}$	ω_d	ζ_d	$\left \frac{\Phi}{\beta}\right _d$	$\frac{N'_{\delta_{ac}}}{L'_{\delta_{ac}}}$	μ	$\frac{N'_{\delta_{rc}}}{L'_{\delta_{ac}}} \delta_{rc}(3)$	AVG. POR (Cooper-Harper)
15	2.5	0.78	0.37		0.033		-0.205	3.25
16	↓	0.4	0.38		0.127	-2.78		3.9
17	↓	0.4	0.71		-0.092	2.90		4.5
18	↓	1.2	0.24		0.033		-0.194	4.0
19	↓	1.2	0.37		0.033		-0.24	3.0
20	↓	0.77	0.36		-0.178	0.887		3.0
21	↓	0.39	0.38		0.033			4.5

* $\left|\frac{\Phi}{\beta}\right|_d$ is not a factor since turbulence was not simulated in these experiments.

APPENDIX C

MULTIPLE/SINGLE-AXIS RATING DATA

Presented herein are the experimental data points considered and used in the Fig. 15 correlations.

Ref. 17 — "Attitude Control Requirements for Hovering Determined Through the Use of a Piloted Flight Simulator," NASA TN D-792.

The Ref. 17 two- vs. one-axis faired plots for "harmonized" controls are reproduced below.

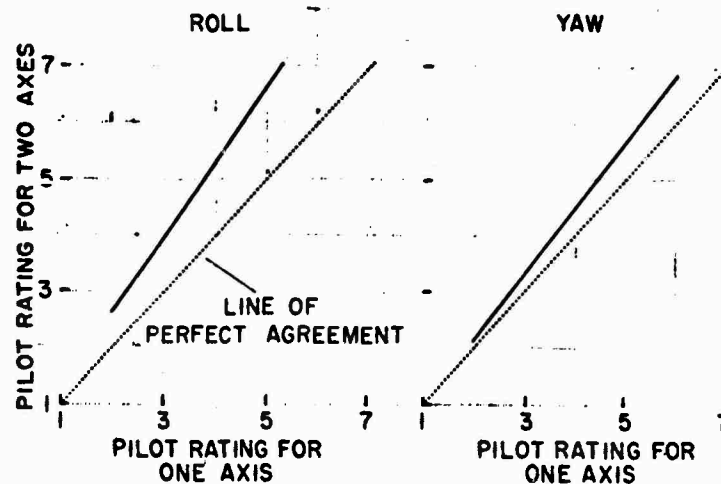


Figure 25
Comparison of Pilot Rating of Controllability
for One and Two Axes: Optimum Ratio
(Fig. 9 of Ref. 17)

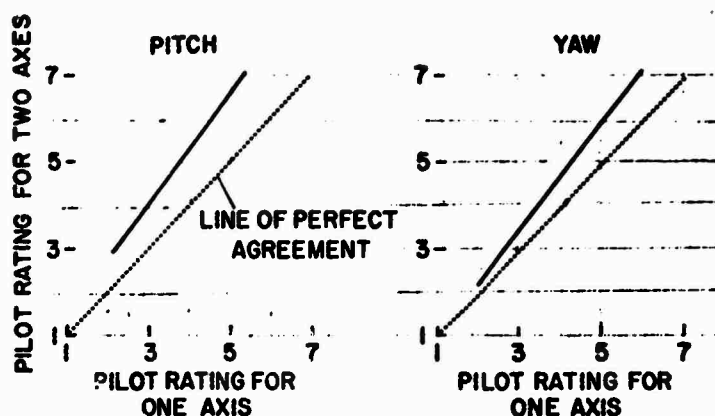


Figure 26
Comparison of Pilot Rating of Controllability
for One and Two Axes: Optimum Ratio
(Fig. 11 of Ref. 17)

The axis combinations used in the motion simulator were roll-yaw and pitch-yaw, the latter being coupled by an unspecified (horizontal engine) gyroscopic angular momentum. Figure 25 is for roll-yaw axes; Fig. 26 for pitch-yaw. The tasks involved no disturbance inputs. The pilot was required to make attitude changes rapidly and with minimum overshoot. The maximum attitude changes amounted to about 15 deg in pitch or roll and 30 deg in yaw. When two axes were controlled simultaneously, attitude changes were made about a "primary" axis while attempting to maintain a fixed attitude about the other. The "primary" axes for the plots above are reflected in the labeling of each (e.g., Roll, Yaw, Pitch).

Picking values off the plots for given levels of one-axis ratings results in the following tabulation, which also includes the computed

ONE-AXIS RATING	TWO-AXIS RATINGS				R _m
	ROLL (YAW)	PITCH (YAW)	YAW		
			(ROLL)	(PITCH)	
2	2.6	2.8	2.1	2.3	2.28
3	3.9	4.1	3.4	3.4	4.10
4	5.3	5.4	4.5	4.8	5.67
5	6.6	6.7	5.7	6.1	6.99
6	7.9	8.0	6.9	7.1	8.07

(Eq. 25) value of R_m . The two-axis ratings where yaw was the primary axis are not considered especially applicable to the airplane-centered problem, (i.e., yaw is usually a secondary axis) and were not used in the final Fig. 15 correlations.

Ref. 18 — "An Evaluation of Four Methods for Converting Single Axis Pilot Ratings to Multi-Axis Pilot Ratings Using Fixed Base Simulation Data," AFIT GE/EE/62-4.

The task(s) involved fixed base simulation requiring regulation about one, two or three axes in the presence of random disturbance(s). Three basic levels of dynamics about each axis, corresponding to high, medium and low levels of augmentation (labeled H, M, L, respectively) were tested. The tabulated raw data and averaged values presented in Ref. 4 are reproduced below (Tables 11 through 15).

Examination of the averaged 2-axis ratings, Table 13 and the corresponding single-axis ratings in Table 12 shows that the majority of the 2-axis ratings are less than one of the pertinent single-axis ratings. Because of this inconsistent result all 2-axis data were rejected in the final, Fig. 15, correlations. Nevertheless the four (out of nine) configurations where the 2-axis ratings are greater than the highest single-axis ratings do correlate reasonably well with Eq. 25, as indicated by the tabulation below.

CONFIGURATION	SINGLE-AXIS RATINGS	2-AXIS RATING	COMPUTED R_m
HL	2.9 , 5.8	6.2	6.41
ML	3.5 , 5.8	6.8	6.71
LH	3.8 , 3.3	4.0	5.00
LL	3.8 , 5.8	7.0	6.86

For the 3-axis data, in addition to computing (and plotting) the average 3-axis ratings based on average 1-axis data (Tables 14 and 15), the spreads shown in Fig. 15 were obtained by averaging separate run series; i.e., first and second sets of one-axis ratings used to compute and compare, respectively, with first and second sets of 3-axis ratings. The values used for these comparisons and computations are tabulated in Table 16.

TABLE 11

RAW DATA FOR ALL DATA RUNS
(Table C-I of Ref. 18)

Three Axis Experiment

Data Run #1
Single Axis - 120 seconds

Run Configuration Pilot Rating				Run Configuration Pilot Rating				
	Θ	ϕ	β		Θ	ϕ	β	
1	M			4.0	12	H		3.0
2	L			6.5	13	L		7.0
3		H		2.5	14	H		2.5
4		L		6.0	15	M		4.5
5			M	4.0	16		M	3.5
6			H	3.5	17		L	5.5
7	L			8.0	18		H	3.0
8	H			2.5	19		H	3.5
9			M	4.5	20		L	7.0
10			L	7.0	21		M	3.0
11		M		4.0				

Data Run #2
Three Axis - 120 seconds

Run Configuration Pilot Rating				Run Configuration Pilot Rating					
	Θ	ϕ	β		Θ	ϕ	β		
22	H	L	H	-*	24	M	M	M	-
23	H	L	H	9.0	25	M	M	M	8.0

* Pilot exercised re-run option

TABLE 11 (Continued)

Run Configuration Pilot Rating				Run Configuration Pilot Rating					
	Θ	ϕ	β		Θ	ϕ	β		
26	L	M	M	-	49	L	H	M	10.0
27	L	M	M	9.0	50	M	H	H	6.5
28	H	H	L	-	51	H	H	M	6.5
29	H	H	L	10.0	52	L	L	L	-
30	L	L	M	-	53	L	L	L	-
31	L	L	M	10.0	54	L	L	L	10.0
32	H	L	M	-	55	H	M	H	6.0
33	H	L	M	8.0	56	L	L	H	-
34	M	L	L	-	57	L	L	H	9.5
35	M	L	L	10.0	58	L	H	H	-
36	H	M	L	-	59	L	H	H	10.0
37	H	M	L	9.0	60	H	L	L	-
38	H	H	H	6.0	61	H	L	L	9.5
39	L	M	H	-	62	M	L	M	-
40	L	M	H	9.0	63	M	L	M	9.5
41	M	H	M	8.0	64	L	H	L	-
42	M	M	H	7.5	65	L	H	L	10.0
43	L	M	L	-	66	M	M	L	-
44	L	M	L	9.5	67	M	M	L	9.0
45	M	H	L	-	68	H	M	M	7.0
46	M	H	L	9.5	69	M	L	H	-
47	L	H	M	-	70	M	L	H	8.5
48	L	H	M	-	71	H	H	H	5.5

TABLE 11 (Continued)

Data Run #3

Three Axis Repeated Runs - 120 seconds

Run Configuration Pilot Rating Run Configuration Pilot Rating

	Θ	ϕ	ψ			Θ	ϕ	ψ	
72	H	L	H	-	90	H	H	L	9.0
73	H	L	H	7.0	91	L	L	H	-
74	L	H	H	-	92	L	L	H	8.5
75	L	H	H	9.0	93	M	L	H	8.0
76	L	M	L	-	94	H	M	M	6.0
77	L	M	L	9.0	95	H	H	L	-
78	M	H	H	6.5	96	H	H	L	10.0
79	L	L	M	-	97	M	H	L	-
80	L	L	M	-	98	M	H	L	-
81	L	L	M	9.0	99	M	H	L	9.0
82	M	H	M	7.5	100	H	M	L	-
83	H	H	H	6.0	101	H	M	L	-
84	M	M	M	7.0	102	H	M	L	8.0
85	H	H	M	6.0	103	H	M	H	5.0
86	L	H	M	-	104	M	H	M	6.5
87	L	H	M	8.5	105	M	H	H	5.5
88	H	H	L	-	106	H	M	H	5.5
89	H	H	L	-	107	H	H	H	6.0

TABLE 11 (Continued)

Data Run #4

Single Axis Repeated Runs - 60 seconds

Run Configuration Pilot Rating			Run Configuration Pilot Rating			
Θ	ϕ	ρ	Θ	ϕ	ρ	
108	M	4.0	120	L	6.0	
109	L	5.0	121	H	3.0	
110		M	122	M	5.0	
111		H	123	H	3.0	
112	M	4.5	124	H	4.0	
113	L	6.0	125	M	4.5	
114		L	126	M	5.0	
115		M	127	L	6.5	
116	M	5.0	128		L	5.0
117	H	4.0	129		H	3.5
118	H	3.0	130		H	3.0
119	M	5.0	131		M	4.0

Two Axis Experiment

Data Run #5

Single Axis - 60 seconds

Run Configuration Pilot Rating			Run Configuration Pilot Rating		
Θ	ϕ		Θ	ϕ	
132	H	3.0	136	H	3.0
133	M	3.5	137	M	3.5
134	L	4.0	138	H	3.0
135	L	3.5	139	H	2.5

TABLE 11 (Concluded)

Run Configuration Pilot Rating			Run Configuration Pilot Rating		
	Θ	ϕ		Θ	ϕ
140	L	4.0	145	H	3.0
141		H 3.0	146	H	4.0
142		M 4.5	147	L	6.0
143		M 5.0	148	L	5.5
144		L 6.5	149	L	5.0

Data Run #6
2 Axis - 120 seconds

Run Configuration Pilot Rating				Run Configuration Pilot Rating			
	Θ	ϕ			Θ	ϕ	
150	M	M	4.0	165	L	L	7.0
151	H	M	3.0	166	H	M	4.0
152	H	H	2.0	167	H	H	3.0
153	M	H	3.5	168	M	M	4.0
154	L	H	4.0	169	M	M	5.0
155	M	L	6.5	170	L	L	7.0
156	L	M	4.0	171	M	H	3.0
157	L	L	7.0	172	H	H	3.5
158	H	L	6.0	173	L	M	4.0
159	H	M	4.0	174	L	M	5.0
160	H	H	3.0	175	H	L	6.5
161	M	H	3.0	176	L	H	4.0
162	L	H	4.0	177	M	L	7.0
163	H	H	3.0	178	H	L	6.0
164	M	L	7.0				

TABLE 12
AVERAGED VALUES OF SINGLE AXIS RUNS
FOR TWO AXIS EXPERIMENT
(Table C-II of Ref. 18)

Pitch	Bank
H - 2.9	H - 3.3
M - 3.5	M - 4.8
L - 3.8	L - 5.8

TABLE 13
AVERAGED VALUES FOR TWO AXIS RUNS
(Table C-III of Ref. 18)

Configuration		Pilot Rating	Configuration		Pilot Rating
Θ	ϕ		Θ	ϕ	
H	H	2.9	M	L	6.8
H	M	3.7	L	H	4.0
H	L	6.2	L	M	4.3
M	H	3.2	L	L	7.0
M	M	4.3			

TABLE 14
AVERAGED VALUES OF SINGLE AXIS RUNS
FOR THREE AXIS EXPERIMENT
(Table C-IV of Ref. 18)

Pitch	Bank	Sideslip
H - 2.8	H - 3.3	H - 3.4
M - 4.6	M - 4.3	M - 4.1
L - 6.7	L - 5.8	L - 6.2

TABLE 15

AVERAGED VALUES OF THREE AXIS RUNS
(Table C-V of Ref. 18)

Configuration			Pilot Rating	Configuration			Pilot Rating
Θ	ϕ	β		Θ	ϕ	β	
H	H	H	5.9	M	M	L	9.0
H	H	M	6.2	M	L	H	8.2
H	H	L	9.7	M	L	M	9.5
H	M	H	5.5	M	L	L	10.0
H	M	M	6.5	L	H	H	9.5
H	M	L	8.5	L	H	M	9.2
H	L	H	8.0	L	H	L	10.0
H	L	M	8.0	L	M	H	9.0
H	L	L	9.5	L	M	M	9.0
M	H	H	6.2	L	M	L	9.2
M	H	M	7.3	L	L	H	9.0
M	H	L	9.2	L	L	M	9.5
M	M	H	7.5	L	L	L	10.0
M	M	M	7.5				

TABLE 16. REFERENCE 18 DATA USED IN FIGURE 15 CORRELATIONS

SINGLE AXIS AVERAGE RATINGS

CONFIGURATION										FIRST SET	SECOND SET
H	2.5	3.0
H	2.8	4.0
H	3.5	3.3
M	4.3	4.8
M	3.8	4.6
M	3.8	4.3
L	7.1	6.0
L	5.8	5.8
L	7.0	5.5

THREE-AXIS AVERAGE RATINGS*

CONFIGURATION										FIRST SET	SECOND SET
HHH	5.7	6.0
M	6.5	6.0
L	10.0	9.5
HMH	6.0	5.3
M	7.0	6.0
L	9.0	8.0
HLH	9.0	7.0
M	8.0	-
L	9.5	-
MHH	6.5	6.0
M	8.0	7.0
L	9.5	9.0
MMH	7.5	-
M	8.0	7.0
L	9.0	-
MLH	8.5	8.0
M	9.5	-
L	10.0	-
LHH	10.0	9.0
M	10.0	8.5
L	10.0	-
LMH	9.0	-
M	9.0	-
L	9.5	9.0
LLH	9.5	8.5
M	10.0	9.0
L	10.0	-

* Overall three-axis average ratings are those in Table 15.

It should be noted, finally, that the 3-axis ratings for Configuration HHL were rejected entirely because the ratings are worse than those for Configuration HML whereas they should, logically, be better.

Ref. 19 — "A Preliminary Study of Handling-Qualities Requirements of Hypersonic Transports in High-Speed Cruising Flight Using Piloted Simulators, NASA TN D-1888.

The "data point" applicable to the present study is contained in a single paragraph quoted as follows:

"Effects of multiple failures of stability augmenters. — It is noteworthy that, in general, the ratings developed in this study are strongly dependent on the values assigned to derivatives other than those varied. Thus, the values plotted in figures 5, 6, and 7 are, strictly speaking, appropriate only with all other derivatives at completely satisfactory levels (PR 1-1/2). This limitation of the data was demonstrated forcibly by some incidental tests in which the values of derivatives that were individually rated 3-1/2 were tested in combination. The resulting configuration was rated at 6-1/2 to 7, definitely unacceptable. ..."

Ref. 20 — "AWJSRA Flight Director Simulation Program," STI WP-1015-8.

Table 17 (Appendix D of Ref. 20) contains the combined axis ratings of interest, obtained incidental to a moving base simulation of a Category II STOL approach. Of the data shown only four sets, Configurations 3, 4, 6, and 8, are more or less complete; 8, as shown, is incomplete but the Longitudinal Flight Director (FD) off rating can be inferred from Sets 3 and 4 as $R = 4 \frac{1}{2}$. Also, the overall rating(s) shown for 8 have been expanded to reflect the drastic differences between IFR and "partial" IFR (the pilot could on some runs partially see the simulated visual scene earlier than on others). Finally, for Configuration 6 the lateral rating shown, $5 \frac{1}{2}$, was shaded to $5-5 \frac{1}{2}$ to be consistent with the overall rating for Configuration 2. The "sets" used in the Fig. 15 correlations are, therefore:

CONFIGURATION	INDIVIDUAL AXIS RATINGS	MULTIPLE RATING
3	4 - $4\frac{1}{2}$; $4\frac{1}{2}$	$5\frac{1}{2}$
4	2 - $2\frac{1}{2}$; $4\frac{1}{2}$	5
6	5 - $5\frac{1}{2}$; $4\frac{1}{2}$	$5\frac{1}{2}$ - 6
8	7 ; $4\frac{1}{2}$	7 - 10

TABLE 17

PILOT RATINGS FOR INDIVIDUAL AXES AND OVERALL SYSTEM FOR
COMBINATIONS OF FLIGHT DIRECTOR AND SAS CONFIGURATIONS
(Appendix D of Ref. 20)

Gust Inputs: 4 FPS RMS

Pilot: Bob Innis

Date: 2/7/72

<u>CONFIGURATION</u>				<u>POR</u>
1.	LAT	SAS	ON	No overall given 2-2 1/2 IAT 2 1/2 LONG
	LAT	FD	ON	
	LONG	FD	ON	
2.	LAT	SAS	OFF	5-5 1/2 overall No individual given
	LAT	FD	ON	
	LONG	FD	ON	
3.	LAT	SAS	ON	5 1/2 overall 4-4 1/2 IAT 4 1/2 LONG
	LAT	FD	OFF	
	LONG	FD	OFF	
4.	LAT	SAS	ON	5 overall 2-2 1/2 IAT 4 1/2 LONG
	LAT	FD	ON	
	LONG	FD	OFF	
5.	LAT	SAS	ON	No overall given 4-4 1/2 IAT 2 1/2 LONG
	LAT	FD	OFF	
	LONG	FD	ON	
6.	LAT	SAS	OFF	5 1/2 - 6 overall 5 1/2 IAT 4 1/2 LONG
	LAT	FD	ON	
	LONG	FD	OFF	
7.	LAT	SAS	OFF	No overall given 7 IAT 3 LONG
	LAT	FD	OFF	
	LONG	FD	ON	
8.	LAT	SAS	OFF	7 overall [(partial IFR); 10 (pure IFR)]* 7 IAT Can't rate LONG — lateral too hard
	LAT	FD	OFF	
	LONG	FD	OFF	

* added to reflect (Ref. 20) Table 8 data.

APPENDIX D

SUMMARY OF DATA ANALYZED FOR ATTITUDE RESPONSE REQUIREMENTS

This appendix contains a listing of the handling quality data compiled in the development of the attitude response criterion given in Section IV. Where appropriate, aerodynamic stability and control data and augmentation system block diagrams have been included.

Tables 18 through 27 contain the basic handling quality rating data, attitude transfer functions, and criterion parameters ($\Delta\phi/\Delta\omega$ and ϕ).

EFFECTS OF TURBULENCE

As noted in the text, the turbulence had a significant effect in the handling quality rating level. Figure 27 shows the trend which was typically exhibited with and without turbulence. Note that at the lower phase gradient (e.g., $\Delta\phi/\Delta\omega$) this crossplot shows an improvement of about 1.5 rating points without moderate turbulence.

Additional crossplots used to establish the boundaries are given in Figs. 28 through 31. Figures 32 through 34 provide a block diagram schematic of the pitch attitude augmentation concepts evaluated in Refs. 43 and 40, respectively.

TABLE 18
REFERENCE 31 DATA

CONF. NO.	CASE NO.	PILOT RATING (CHR)	ATTITUDE TRANSFER FUNCTION $\frac{\theta}{\delta_{ES}/\Delta}$	ϕ at 1 rad/sec	$\frac{\Delta\phi}{\Delta\omega}$ at $-135^\circ \phi$
1	7-2	3.6	$\frac{400(.1)(.47)}{[.17, .33][.412, .911][.7, 20.]}$	-145	- 87.36
2	7-4	6.5	$\frac{400(.1)(.47)}{[.17, .33][.44, .586][.7, 20.]}$	-185	- 87.10
3	7-6	7.3	$\frac{400(.1)(.47)}{[.17, .33][.928, .536][.7, 20.]}$	-168	- 54.5
4	7-8	3.5	$\frac{400(.1)(.47)}{[.17, .33][.4, 1.57][.7, 20.]}$	- 85	-100.2
5	8-1	6.5	$\frac{9.6(.075)(2.1)}{[.1, .3][.1, 3.][.8, 15.1]}$	- 94	-189.4
6	8-2	3.72	$\frac{9.6(.075)(2.1)}{[.1, .3][.2, 3.][.8, 15.1]}$	- 95	-124.7
7	8-3	3.15	$\frac{9.6(.075)(2.1)}{[.1, .3][.3, 3.][.8, 15.1]}$	-100	- 81.7
8	8-23	6.4	$\frac{9.6(.075)(2.1)}{(-.38)(3.2)[.1, .3][.8, 15.1]}$	-217	- 23.8
9	14-6	3.0	$\frac{225(.04)(1.1)}{[.17, .1][.28, 1.98][.7, 15.]}$	- 90	-115.
10	14-7	4.0	$\frac{225(.04)(1.1)}{(.475)(1.9)[.17, .1][.7, 15.]}$	-162	- 21.9
11	14-38	3.5	$\frac{225(.04)(1.1)}{[.17, .1][.45, 1.3][.7, 15.]}$	-130	- 67.6

TABLE 19
REFERENCE 40 DATA

CONF. NO.	CASE NO.	PILOT RATING (CHR)	ATTITUDE TRANSFER FUNCTION	ϕ at 1 rad/sec	$\frac{\Delta\phi}{\Delta\omega}$ at $-135^\circ \phi$
1	BASIC PA 30 A/F	(TURBULENCE EFFECT) 6 4 5	$\frac{.02(.076)(1.632)}{[.140, .203][.784, 5.486]}$	-92 TURNS	-60
2	RATE SYSTEM	7 4.5 5	$\frac{.46 \times 10^6(1.635)(.076)(.17)}{(0)(.0636)(.29)(.619)[.507, 6.68][.707, .383]}$	-140	-20
3	ATTITUDE HOLD	3 2 2.5	$\frac{.934(.076)(.50)(1.635)}{(.0696)(4.213)(21.43)[.721, .578][.594, 2.972]}$	-68	-65

TABLE 20
REFERENCE 34 DATA

CONF. NO.	CASE NO.	PILOT RATING (CHR)	ATTITUDE TRANSFER FUNCTION	ϕ at 1 rad/sec	$\frac{\Delta\phi}{\Delta\omega}$ at $-135^\circ \phi$
A41	1	4.5 2.5 3.6	$\frac{.204(.133)(.493)}{[-.032, .267][.736, .925]}$	-31	-130
A51	2	4.5 2.0 3.0	$\frac{.204[.839, .374]}{[-.042, .254][.703, .970]}$	-30	-130
B41	3	3.5	$\frac{.16(.133)(.493)}{[-.034, .177][.745, .605]}$	-15	-160
B51	4	3.0	$\frac{.16[.839, .374]}{[-.037, .204][.688, .657]}$	-20	-160

TABLE 21
REFERENCE 33 DATA

CONF. NO.	CASE NO.	PILOT RATING (CHR) Avg.	ATTITUDE TRANSFER FUNCTION $\frac{\theta}{N_{ES}/\Delta}$	ϕ at 1 rad/sec	$\frac{\Delta\phi}{\Delta\omega}$ at $-135^\circ \phi$
1		7D	$\frac{.49(.22)(.50)}{[.447, .251][.0262, 2.557]}$	-53	-265
2		5B	$\frac{.41(.220)(.500)}{[.446, .246][.0948, 2.568]}$	-56.9	-223.9
3		2.5B	$\frac{.49(.22)(.50)}{[.445, .240][.185, 2.548]}$	-62.1	-170.9
4		2B	$\frac{.49(.22)(.5)}{[.445, .228][.243, 2.363]}$	-67.1	-145.2
5		1.5B	$\frac{.49(.22)(.5)}{[.447, .229][.340, 2.565]}$	-70.3	-113.7
6		6B	$\frac{.49(.22)(.5)}{[.438, .215][.0757, 1.914]}$	-60.1	-232.5
7		6F	$\frac{.33(.220)(.50)}{[.440, .208][.129, 1.896]}$	-65.0	-195.8
8		3B	$\frac{.44(.220)(.500)}{[.445, .202][.217, 1.940]}$	-71.4	-154.6
9		3B	$\frac{.49(.220)(.500)}{[.454, .189][.301, 1.921]}$	-78.3	-125.
10		2.5C	$\frac{.41(.220)(.500)}{[.470, .181][.450, 2.013]}$	-85.8	-96.0
11		8D	$\frac{.33(.220)(.500)}{[.433, .251][.0694, 1.501]}$	-65.1	-224.8
12		6E	$\frac{.39(.220)(.500)}{[.431, .244][.123, 1.479]}$	-69.5	-192.5
13		2B	$\frac{.36(.220)(.500)}{[.434, .245][.333, 1.622]}$	-85.9	-116.4

TABLE 21. (CONCLUDED)

CONF. NO.	CASE NO.	PILOT RATING (CHR) Avg.	ATTITUDE TRANSFER FUNCTION $\frac{\theta}{\delta_{ES}/\Delta}$	ϕ at 1 rad/sec	$\frac{\Delta\phi}{\Delta\omega}$ at -135° ϕ
14		3D-4B	$\frac{.35(.220)(.500)}{[-.1007)(.197)[.550, 1.385]}$	- 69.2	-123.0
15		8F	$\frac{.19(.220)(.500)}{[.384, .234][.276, .890]}$	-170.0	-112.5
16		7C	$\frac{.44(.220)(.500)}{(-.0207)(.117)[.341, .997]}$	-153.0	- 92.2
17		2.5B	$\frac{.36(.220)(.500)}{[.426, .202][.558, 1.009]}$	-145.0	- 65.3
18		2D	$\frac{.44(.22)(.5)}{[.430, .223][.788, 1.179]}$	-131.8	- 50.7
21		5.5D	$\frac{.34(.13)(.68)}{[.324, .165][.155, 2.433]}$	- 70.2	-177.4
22		2D	$\frac{.34(.13)(.68)}{[.333, .157][.246, 2.452]}$	- 74.5	-139.0
23		3C	$\frac{.46(.13)(.68)}{[.332, .164][.320, 2.645]}$	- 77.1	-118.1
24		3.5A	$\frac{.34(.13)(.68)}{[.335, .147][.152, 2.229]}$	- 71.7	-184.2
25		2A	$\frac{.39(.13)(.68)}{[.495, .0816][.267, 1.980]}$	- 83.0	-126.3
26		2A	$\frac{.34(.13)(.68)}{[.307, .158][.187, 1.423]}$	- 89.5	-149.0
27		4A	$\frac{.39(.13)(.68)}{[.325, .156][.333, 1.632]}$	- 95.0	-106.5
28		7C	$\frac{.34(.13)(.68)}{[.292, .119][.366, .841]}$	-179.0	- 75.5
29		7B	$\frac{.41(.13)(.68)}{[.784, .0551][.653, .810]}$	-170.0	- 39.0

TABLE 22

ESTIMATED STABILITY DERIVATIVES OF THE
EVALUATION CONFIGURATIONS
(Table II-5 of Ref. 33)

A - 65 Kt

$x_u = -0.22 \text{ sec}^{-1}$

$z_u = -0.25 \text{ sec}^{-1}$

$x_w = 0.0 \text{ sec}^{-1}$

$z_w = -0.50 \text{ sec}^{-1}$

$x_{\delta_{E5}} = 0.0 \text{ ft/sec}^2/\text{inch}$

$z_{\delta_{E5}} = 0.0 \text{ ft/sec}^2/\text{inch}$

CONFIG.	M_u , rad/ft-sec	M_w , rad/ft-sec	$M_{\dot{\eta}}$, 1/sec
1 ✓	-0.009	-0.0611	+0.362
2 ✓	-0.009	-0.060	+0.013
3 ✓	-0.009	-0.057	-0.437
4 ✓	-0.009	-0.0478	-0.629
5 ✓	-0.009	-0.054	-1.23
6 ✓	-0.009	-0.0345	+0.242
7 ✓	-0.009	-0.0329	+0.047
8 ✓	-0.009	-0.0327	-0.30
9 ✓	-0.009	-0.0304	-0.61
10 ✓	-0.009	-0.0304	-1.26
11 ✓	-0.0037	-0.0222	+0.294
12 ✓	-0.0037	-0.0209	+0.146
13 ✓	-0.0024	-0.0216	-0.572
14 ✓	-0.009	-0.0116	-0.899
15 ✓	-0.0017	-0.00775	+0.06
16 ✓	-0.0048	-0.00816	0.057
17 ✓	-0.00112	-0.00654	-0.579
18 ✓	+0.0006	-0.00655	-1.33

COL

B - 80 Kt

$x_u = -0.13 \text{ sec}^{-1}$

$z_u = -0.24 \text{ sec}^{-1}$

$x_w = 0.0 \text{ sec}^{-1}$

$z_w = -0.68 \text{ sec}^{-1}$

$x_{\delta_{E5}} = 0.0 \text{ ft/sec}^2/\text{inch}$

$z_{\delta_{E5}} = 0.0 \text{ ft/sec}^2/\text{inch}$

CONFIG.	M_u , rad/ft-sec	M_w , rad/ft-sec	$M_{\dot{\eta}}$, 1/sec
21	-0.009	-0.0437	-0.051
22	-0.009	-0.042	-0.50
23	-0.009	-0.0468	-0.99
24	-0.009	-0.0370	+0.035
25	-0.009	-0.0271	-0.330
26	-0.0037	-0.016	+0.18
27	-0.0037	-0.0178	-0.38
28	-0.0017	-0.00575	+0.124
29	-0.0010	-0.00290	-0.335

COL

TABLE 23

DATA SUMMARY FOR EVALUATION CONFIGURATIONS
(Table II-1 of Ref. 33)

CONFIGURATION NUMBER	FLIGHT NO.	V_T/γ kt/deg	PILOT	WIND kt	ω_{ST} rad/sec	ζ_{ST} —	$2\zeta_{ST}\omega_{ST}$ rad/sec	M_{ESS} rad/sec ² m.	M_{FSS} rad/sec ² lb	F_{ES} $\frac{n_y}{lb/g}$	PILOT RATING AND TURBU- LENCE RATING	
											VFR	OVERALL
1	40F-24	65/9	A	10	2.6	0.04	0.21	0.34	0.045	86	7D	7D
2	43F-27	65/9	A	8	2.8	0.10	0.52	0.54	0.072	56	4.5C	5B
3 (M) *	36F-22	65/9	A	11	2.8	0.20	1.04	0.41	0.055	70	6D	6E
3	41F-25	65/9	A	5	2.8	0.20	1.04	0.41	0.055	70	3B	2.5B
3	43F-27	65/9	A	11	2.8	0.20	1.04	0.54	0.072	54	3C	3C
4 (M)	39F-23	65/9	A	10	2.8	0.24	1.25	0.32	0.043	52	5D	5E
4	43F-27	65/9	A	5	2.8	0.24	1.25	0.40	0.065	61	2B	—
4 (M)	51F-31	65/6	A	20	2.8	0.24	1.25	0.36	0.048	82	4D	5D
4 (M)	54F-33	65/9	B	14	2.8	0.24	1.25	0.44	0.059	67	4C	4C
5	40F-24	65/9	A	14	2.8	0.35	1.82	0.40	0.065	61	2B	1.5B
5 (M)	42F-26	65/9	A	15	2.8	0.35	1.82	0.54	0.072	55	2C	3E
6 (M)	39F-23	65/9	A	11	2.0	0.09	0.36	0.32	0.043	54	6.5F	7F
6 (M)	42F-26	65/9	A	15	2.0	0.09	0.36	0.40	0.065	35	6F	7F
6	49F-29	65/9	A	6	2.0	0.09	0.36	0.44	0.059	39	5B	6B
7 (M)	50F-30	65/9	A	14	2.0	0.16	0.64	0.33	0.044	52	5E	6F
8	41F-25	65/9	A	9	2.0	0.23	0.92	0.44	0.050	38	2B	3B
9 (M)	51F-31	65/6	A	17	2.0	0.23	0.92	0.39	0.052	43	2D	2.5D
9 (M)	54F-33	65/9	B	15	2.0	0.23	0.92	0.39	0.052	43	4D	4D
9	40F-24	65/9	A	13	2.0	0.31	1.24	0.40	0.065	34	3B	—
10	36F-21	65/9	A	10	2.1	0.44	1.85	0.41	0.055	47	3C	2.5C
11 (M)	38F-22	65/9	A	20	1.5	0.09	0.27	0.34	0.045	30	6D	6F
11	48F-29	65/9	A	12	1.5	0.09	0.27	0.33	0.044	31	6D	9D
11 (M)	51F-31	65/6	A	20	1.5	0.09	0.27	0.35	0.045	29	—	6F
12 (M)	50F-30	65/9	A	15	1.5	0.14	0.42	0.39	0.052	25	4D	6E
13	41F-25	65/9	A	5	1.7	0.34	1.16	0.36	0.048	34	2B	2B
13 (M)	42F-26	65/9	A	12	1.7	0.34	1.16	0.39	0.052	32	4E	3E
13 (M)	51F-31	65/6	A	10	1.7	0.34	1.15	0.36	0.048	34	3.5D	3E
13 (M)	54F-33	65/9	B	17	1.7	0.34	1.16	0.32	0.043	38	3C	3C
14 (M)	39F-23	65/9	A	12	1.4	0.55	1.54	0.36	0.048	26	3C	3D
14	43F-27	65/9	A	9	1.4	0.55	1.54	0.35	0.047	25	4B	4B
15 (M)	38F-22	65/9	A	12	0.9	0.30	0.54	0.29	0.039	13	7F	8F
15	43F-27	65/9	A	8	0.9	0.30	0.54	0.19	0.025	19	7C	9C
16	48F-29	65/9	A	8	1.0	0.36	0.72	0.44	0.050	10	6C	7C
17 (M)	30F-23	65/9	A	12	1.0	0.57	1.14	0.32	0.043	15	3D	4E
17	41F-25	65/9	A	9	1.0	0.57	1.14	0.36	0.048	13	2B	2.5B
18	40F-24	65/9	A	14	1.2	0.79	1.90	0.44	0.059	14	3C	4C
16 (M)	42F-26	65/9	A	12	1.2	0.79	1.90	0.35	0.047	18	2D	2D
18 (M)	50F-30	65/9	A	12	1.2	0.79	1.90	0.36	0.048	19	3.5D	4E
* * 19	48F-29	65/9	A	12	—	—	—	0.36	0.048	—	7D	9D
* * 20 (M)	50F-30	65/9	A	12	—	—	—	0.36	0.048	—	6E	6F
21	59F-38	80/7	B	10	2.4	0.16	0.77	0.34	0.045	45	5.5A	—
22	57F-36	80/7	B	9	2.5	0.25	1.25	0.34	0.045	46	2A	2A
23 (M)	56F-35	80/7	B	22	2.6	0.32	1.66	0.46	0.061	39	3C	3C
24	57F-36	80/7	B	10	2.2	0.16	0.70	0.34	0.045	38	3A	3.5A
25	57F-36	80/7	B	9	2.0	0.28	1.12	0.39	0.052	26	2A	2A
26	57F-36	80/7	B	10	1.4	0.20	0.56	0.34	0.045	15	2A	2A
27 (M)	55F-35	80/7	B	17	1.7	0.37	1.26	0.39	0.052	18	4C	4C
27	59F-38	80/7	B	10	0.37	1.26	0.30	0.040	24	24	4.5A	4A
28 (M)	56F-35	80/7	B	20	0.9	0.38	0.68	0.34	0.045	6	5C	7C
29	57F-36	90/7	B	10	0.8	0.67	1.07	0.41	0.055	4	5A	7B

* (M) - Moderate Turbulence

** Short-Term Dynamics Could Not be Identified

TABLE 24
REFERENCE 43 DATA

COMP. NO.	CASE NO.	PILOT RATING (CHR)	ATTITUDE TRANSFER FUNCTION	ϕ at 1 rad/sec	$\frac{\Delta\phi}{\Delta\omega}$ at $-135^\circ \phi$
1		2-2.5	$\frac{106.6(.216)(.300)(1.0)}{(0)(.927)(3.025)(17.54)[.812, .277]}$	-132	-29
2		3	$\frac{106.6(.216)(.300)(2.0)}{(0)(.927)(3.025)(17.54)[.812, .277]}$	-153	-28
3		4	$\frac{106.6(.216)(.300)(0.50)}{(0)(.927)(3.025)(17.54)[.812, .277]}$	-100	-40
4		2.5-3.0	$\frac{106.6(.216)(.300)(1.00)}{(0)(.952)(4.589)(15.93)[.874, .272]}$	-124	-32
6		3.0	$\frac{106.6(.216)(.300)(2.0)}{(0)(.952)(4.589)(15.93)[.874, .272]}$	-143	-25
7		4.0	$\frac{106.6(.216)(.300)(0.50)}{(0)(.952)(4.589)(15.93)[.874, .272]}$	-106	-48
9		4.0	$\frac{106.6(.216)(.300)(0.50)}{(0)(.857)(1.854)(18.86)[.660, .284]}$	-128	-38

TABLE 25. REFERENCE 39 DATA

CONF. NO.	CASE NO.	PILOT RATING: (CHR)	ATTITUDE TRANSFER FUNCTION	ϕ at 1 rad/sec	$\frac{\Delta\phi}{\Delta\omega}$ at $-135^\circ \phi$
1	39B	6.0	$\frac{2950. (.02015) (.9717) (-13.3) (-13.3)}{(-.1263) (13.3) (13.3) [.469, .141] [.7, 20.]}$	-184	-27.67
2	42B	6.5	$\frac{2950. (.02015) (.9717) (-13.3) (-13.3)}{(-.5923) (2.4506) (13.3) (13.3) [.0922, .0974] [.7, 20.]}$	-211	-108.3
3	39H	5.6	$\frac{2950. (.02015) (.9717) (-13.3) (-13.3)}{(13.3) (13.3) [.0377, .0657] [.781, .571] [.7, 20.]}$	-194	-29.12
4	39H	7.2	$\frac{2950. (.02015) (.9717) (-13.3) (-13.3)}{(-.4802) (1.3488) (13.3) (13.3) [.108, .0849] [.7, 20.]}$	-218	-149.0
5	25Z	5.5	$\frac{2950. (.02015) (.9717) (-13.3) (-13.3)}{(13.3) (13.3) [.0457, .0833] [0., 2.3353] [.7, 20.]}$	-66	-289.8
6	30Z	5.25	$\frac{2950. (.02015) (.9717) (-13.3) (-13.3)}{(13.3) (13.3) [.0411, .086] [0., 1.7544] [.7, 20.]}$	-68	-279.4
7	35Z	7.0	$\frac{2950. (.02015) (.9717) (-13.3) (-13.3)}{(13.3) (13.3) [.0142, .104] [.0018, .834] [.7, 20.]}$	-242	-253.1
8	37Z	8.1	$\frac{2950. (.02015) (.9717) (-13.3) (-13.3)}{(-.0654) (.0901) (.4787) (-.5003) (13.3) (13.3) [.7, 20.]}$	-245	$\frac{d\phi}{d\omega}$ at $\omega = 1$ rad/sec 5.355

TABLE 26
REFERENCE 36 DATA

CONF. NO.	CASE NO.	PILOT RATING (CHR) High Low Avg.	ATTITUDE TRANSFER FUNCTION	ϕ at 1 rad/sec	$\frac{\Delta\phi}{\Delta\omega}$ at -135°
13		5 3.0 2	$\frac{38.4(.075)(2.0)}{(.7)(2.42)[-0.02, .24][.3, 15.1]}$	-165	-26° at 1 rad/sec
14		4.9 4.1 3.0	$\frac{38.4(.075)(2.0)}{[.03, .43][.25, 1.55][.3, 15.1]}$	-124	- 96.5
15		6 4.3 3	$\frac{38.4(.075)(2.0)}{(.455)(2.665)[-0.06, .20][.3, 15.1]}$	-175	- 21.7
19		8 5.1 4	$\frac{38.4(.075)(2.0)}{[-0.08, .5][.36, 1.20][.3, 15.1]}$	-155	- 71.0
20		6.4 5.1 3	$\frac{38.4(.075)(2.0)}{[-.16, .6][.4, 1.1][.3, 15.1]}$	-190	- 54
22		8.4 4.2 2	$\frac{38.4(.075)(2.0)}{[-.4, .4][.73, .90][.3, 15.1]}$	-205	- 27.7 at 1 rad/sec
23		8.4 6.0 4.0	$\frac{38.4(.075)(2.0)}{(-.38)(3.2)[.2, .3][.3, 15.1]}$	-205	-108.7
24		3.5 2.7 2.0	$\frac{38.4(.075)(2.0)}{(-.10)(.26)(.62)(1.2)[.3, 15.1]}$	-148	- 26.2

TABLE 27. REFERENCE 37 DATA

CONF. NO.	CASE NO.	PILOT RATING (CR) High Low Avg.	ATTITUDE TRANSFER FUNCTION	ϕ at 1 rad/sec	$\frac{\Delta\phi}{\Delta\omega}$ at $-135^\circ \phi$
1	1	$\bar{CR} = 3.50$ 5 3 3.92	$\frac{13.0(.093288)(.57871)}{[.070535, .20169][.58009, .87362][.3, 15.1]}$	-155	-46
	5	$\bar{CR} = 3.20$ 3.5 3 3.13	$\frac{13.0(.093288)(1.1)}{[.070535, .20169][.58009, .87362][.3, 15.1]}$	-170	-39
2	7	$\bar{CR} = 3.1$ 4 2 2.88	$\frac{13.0(.093288)(.57871)}{[.148, .21655][.60165, 2.9983][.3, 15.1]}$	-76	-78
	11A	$\bar{CR} = 3.1$ 3.5 2.5 3.0	$\frac{13.0(.093288)(2.4)}{[.148, .21655][.60165, 2.9983][.3, 15.1]}$	-113	-48
3	13	$\bar{CR} = 5.2$ 7 4 5.67	$\frac{13.0(.081645)(1.1904)}{[-.087554, .32854][.66055, .87002][.3, 15.1]}$	-180	-38
	17	$\bar{CR} = 4.0$ 7 4 5.50	$\frac{13.0(.081645)(1.85)}{[-.087554, .32854][.66055, .87002][.3, 15.1]}$	-190	-38
3A	13A	$\bar{CR} = 3.3$ 3.3 3.3 3.3	$\frac{13.0(.081645)(1.1904)}{[.084888, .24175][.60332, 1.3422][.3, 15.1]}$	-134	-49
	17A	$\bar{CR} = 3.4$ 3.4 3.4 3.4	$\frac{13.0(.081645)(2.14)}{[.084888, .24175][.60332, 1.3422][.3, 15.1]}$	-147	-38
4	19	$\bar{CR} = 3.3$ 4 2.5 3.38	$\frac{31.92(.081645)(1.1904)}{[.16028, .20736][.59944, 2.999][.3, 15.1]}$	-92	-68
	22	$\bar{CR} = 2.7$ 4 2 2.9	$\frac{31.92(.081645)(2.1)}{[.16028, .20736][.59944, 2.999][.3, 15.1]}$	-108	-50
	23B	$\bar{CR} = 3.0$ 3.0 3.0 3.0	$\frac{31.92(.081645)(4.7)}{[.16028, .20736][.59944, 2.999][.3, 15.1]}$	-123	-37.1

Note: \bar{CR} is the rating listed as the mean in the Reference, however, the average value as computed from the listed rating data was added here.

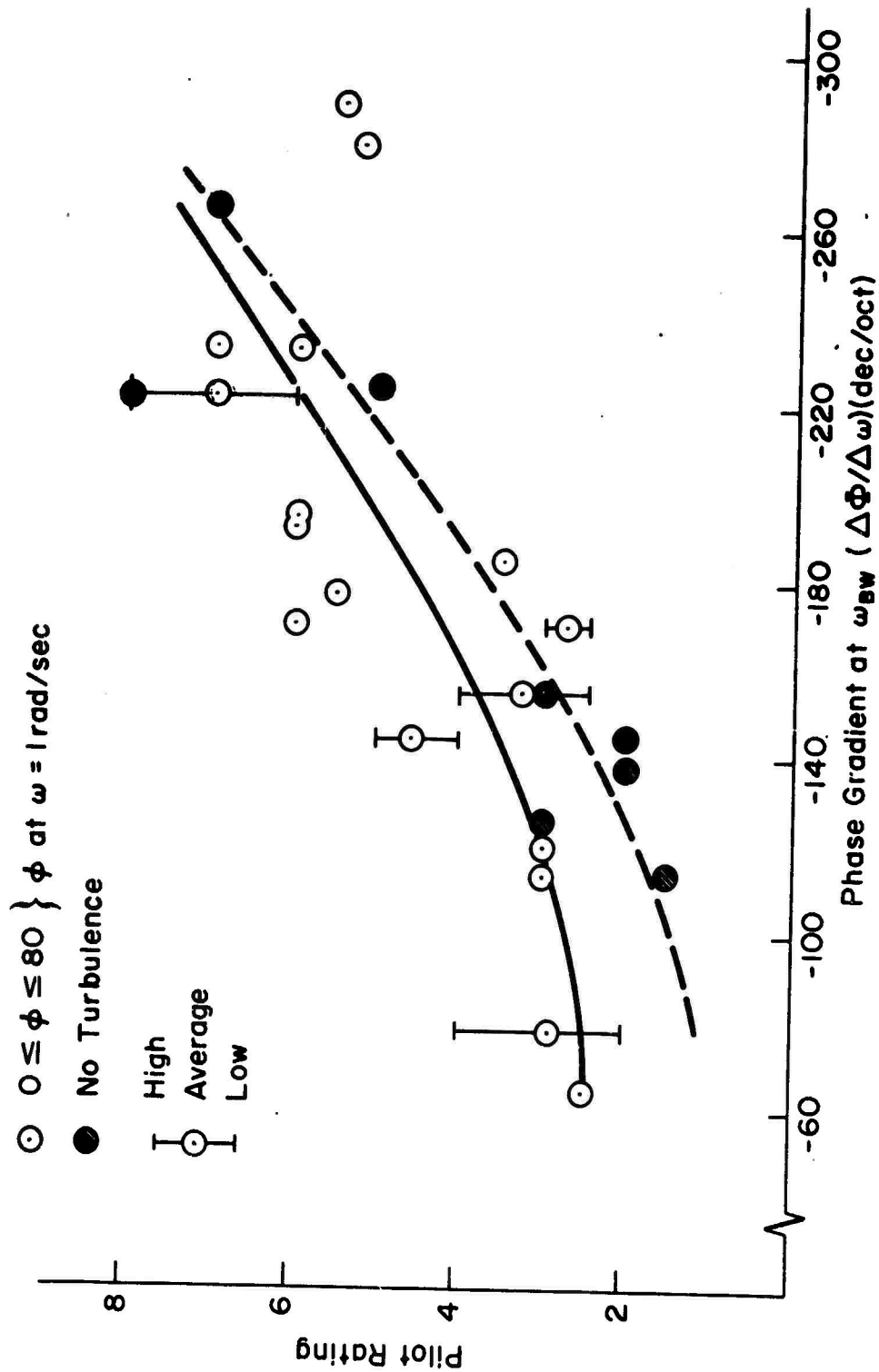


Figure 27. Effect of Turbulence on Rating Trends

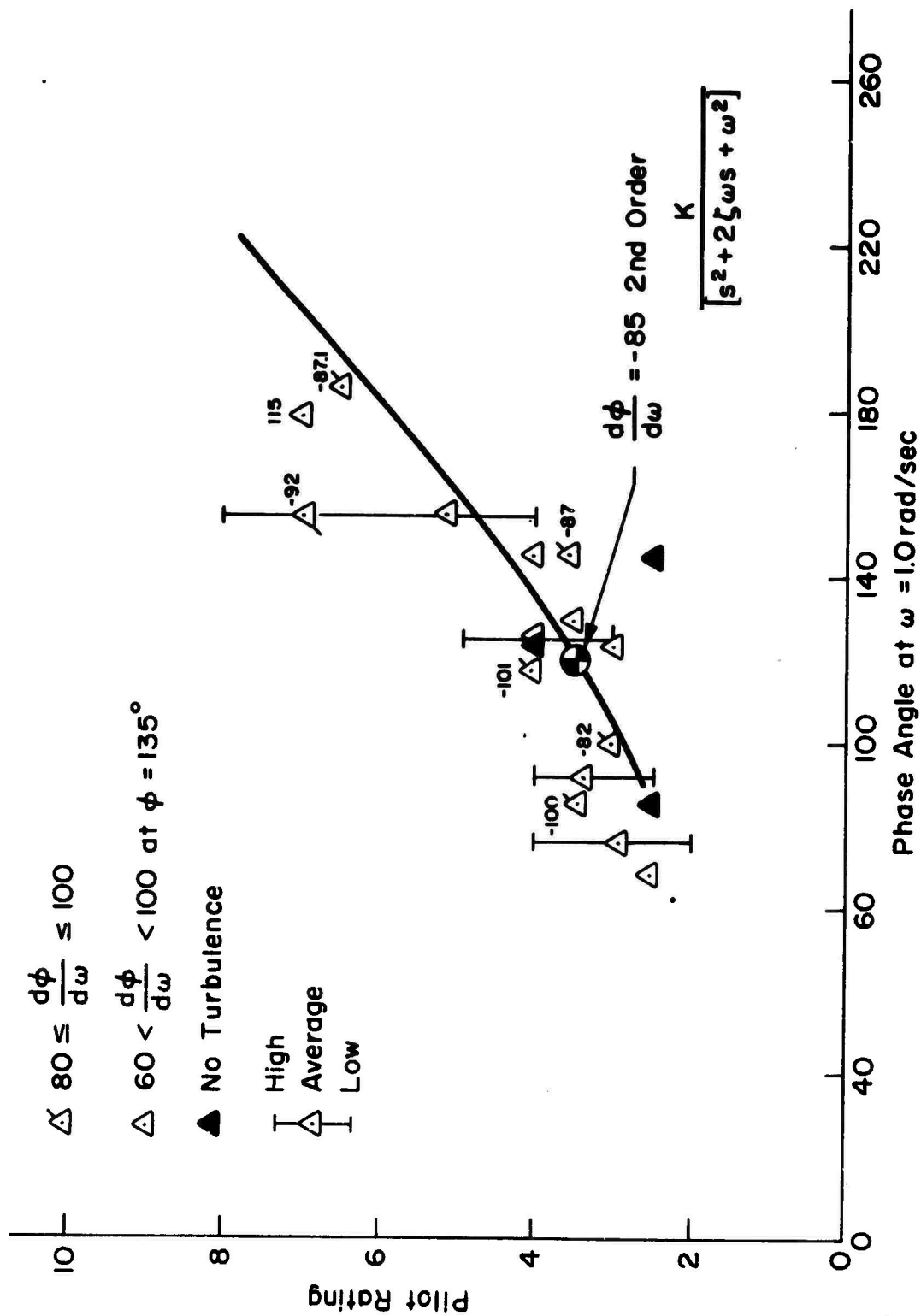


Figure 28. Crossplot for Constant Phase Gradient

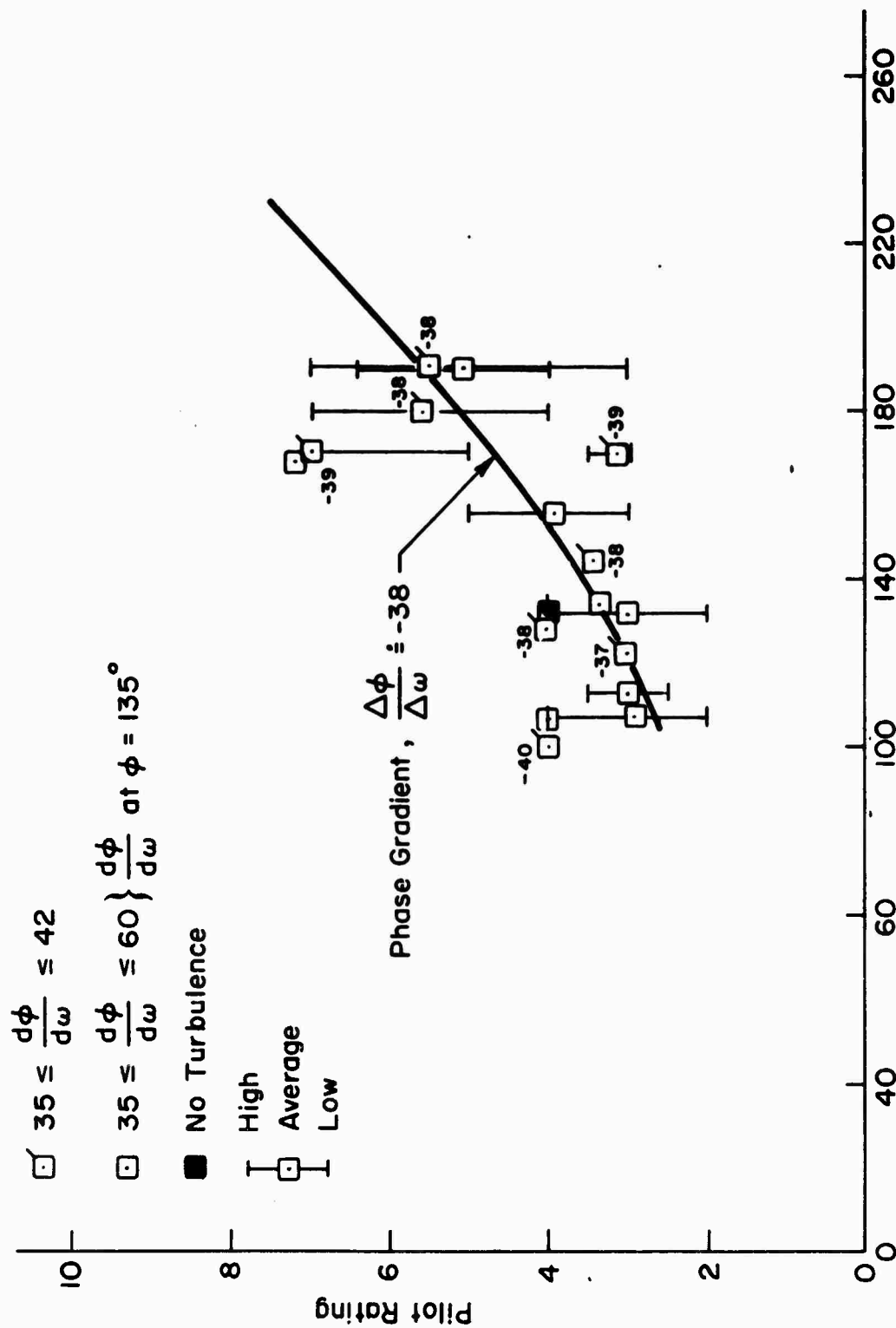


Figure 29. Crossplot for Constant Phase Gradient

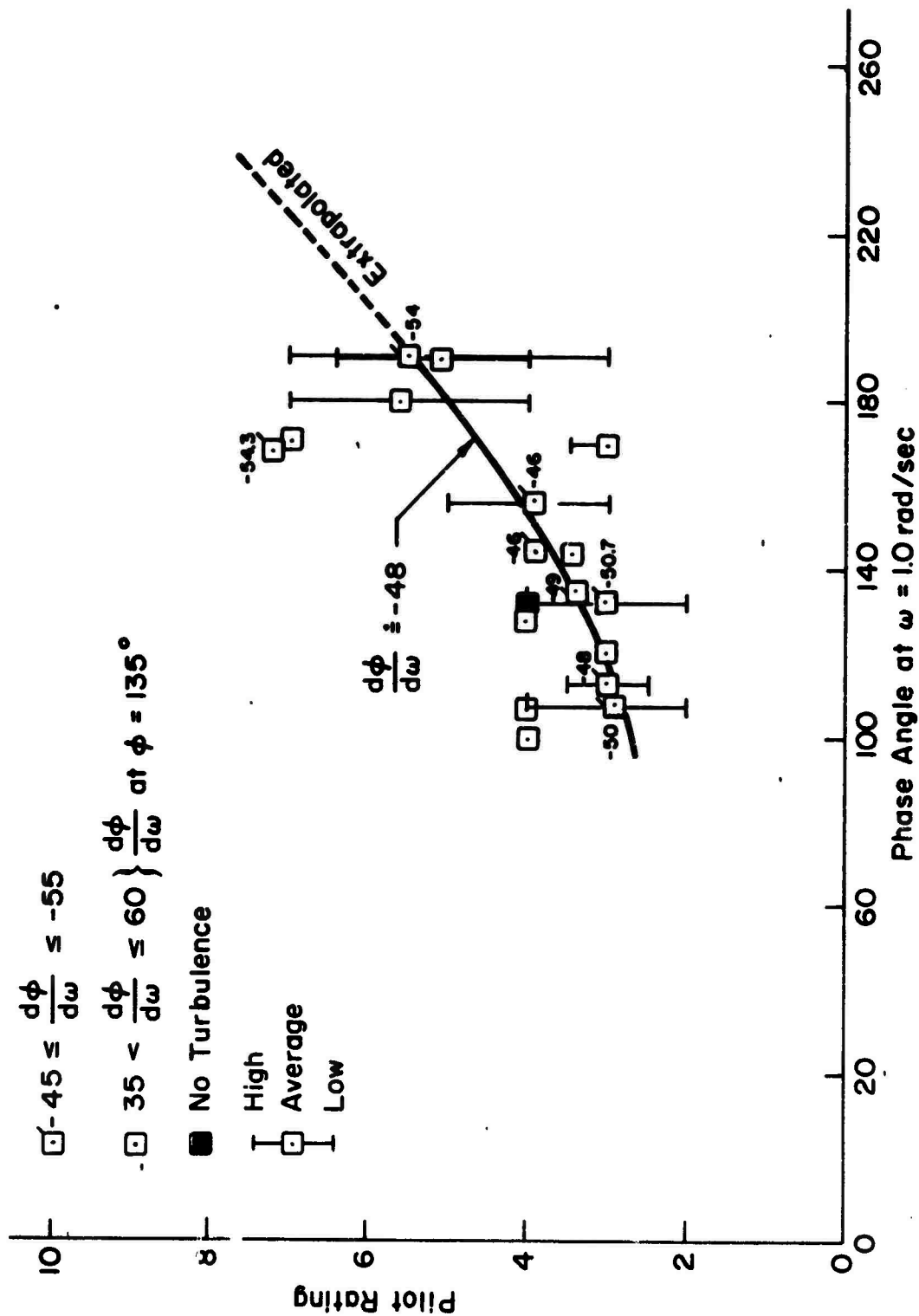


Figure 30. Crossplot for Constant Phase Gradient

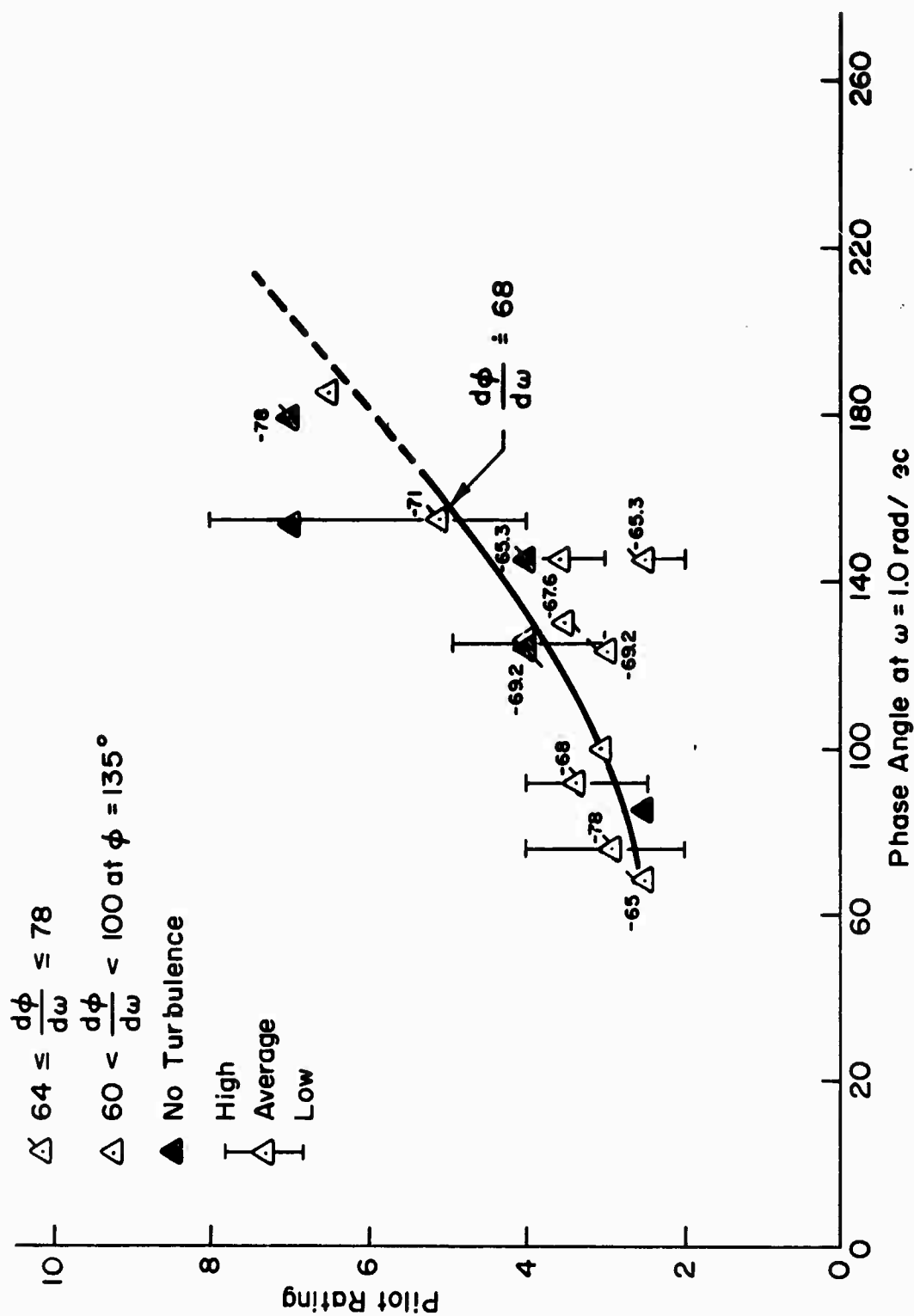


Figure 31. Crossplot for Constant Phase Gradient

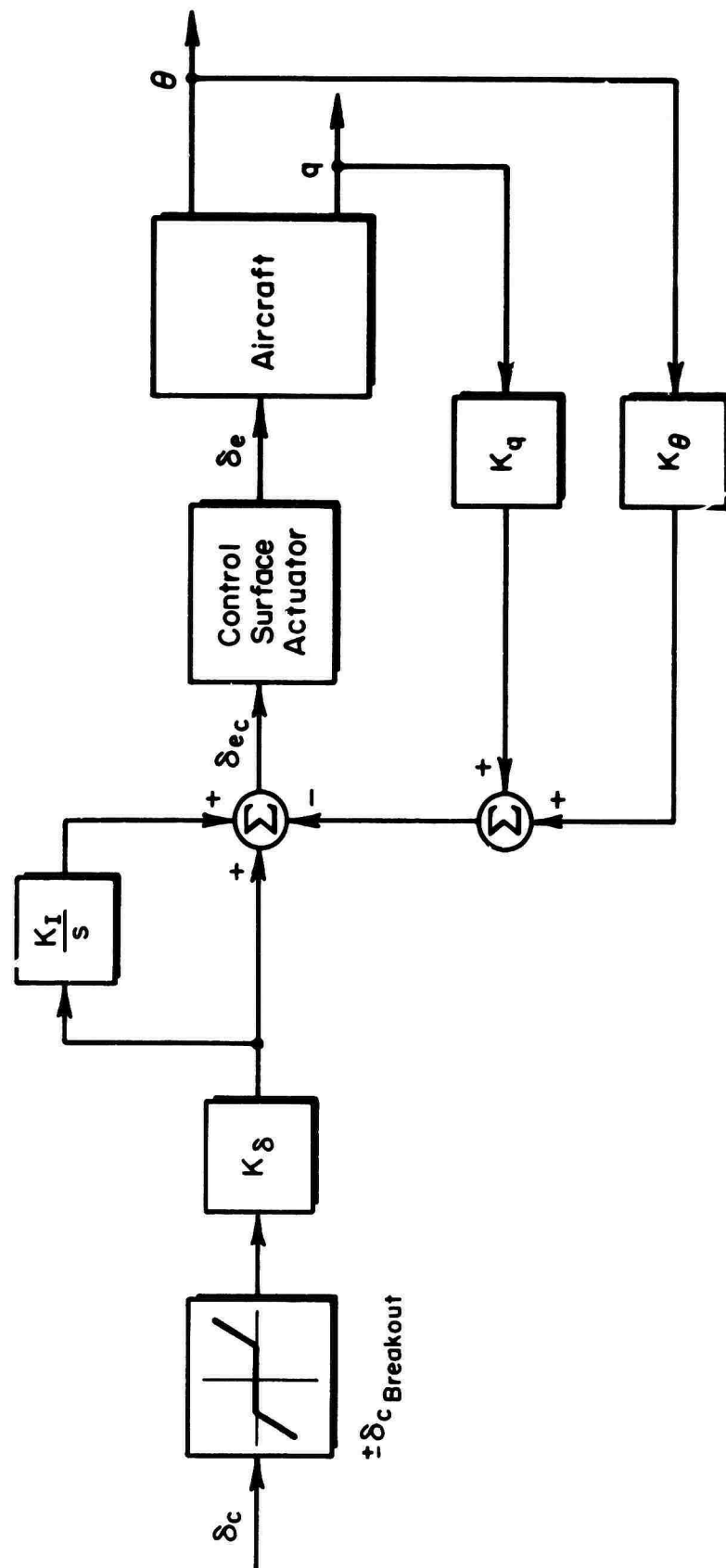


Figure 32. Block Diagram of Pitch Rate Command/Attitude Hold Control System (Ref. 43)

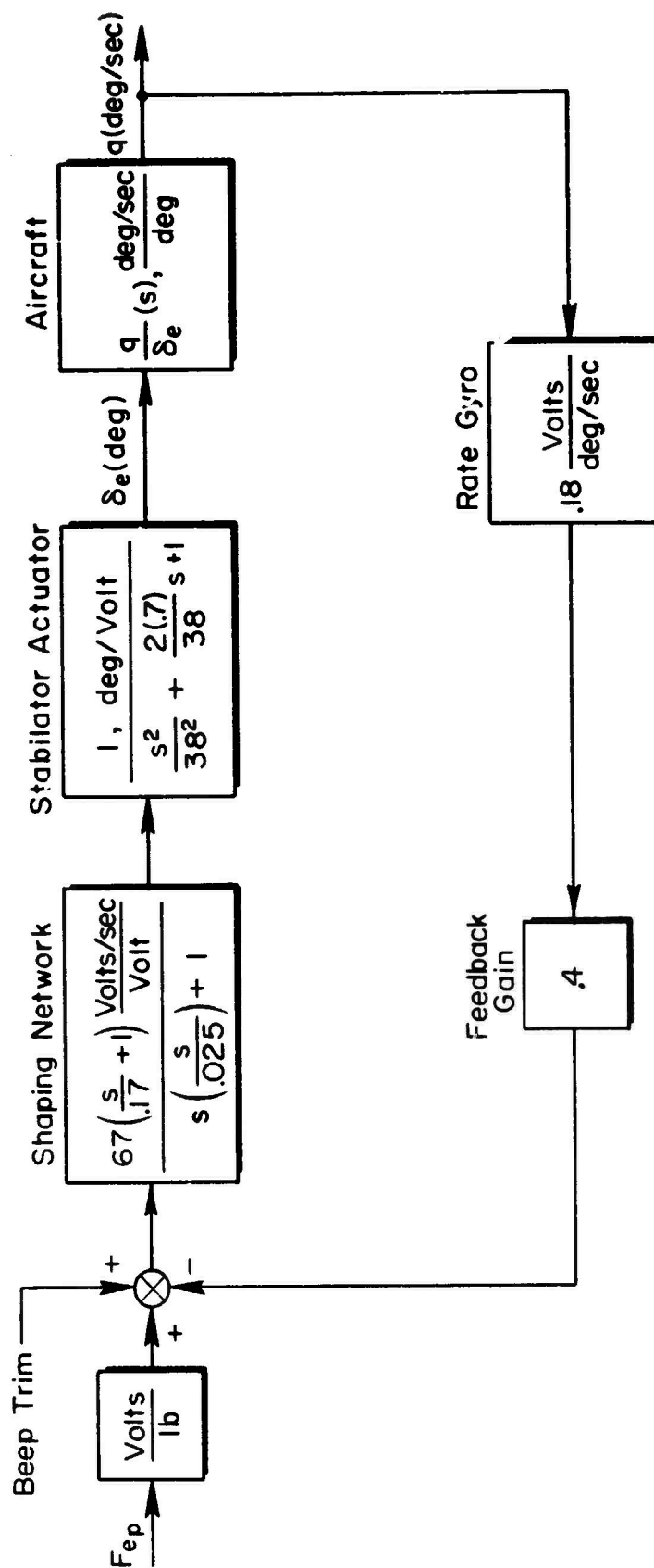


Figure 32. Block Diagram of Pitch Rate Command System (Ref. 40)

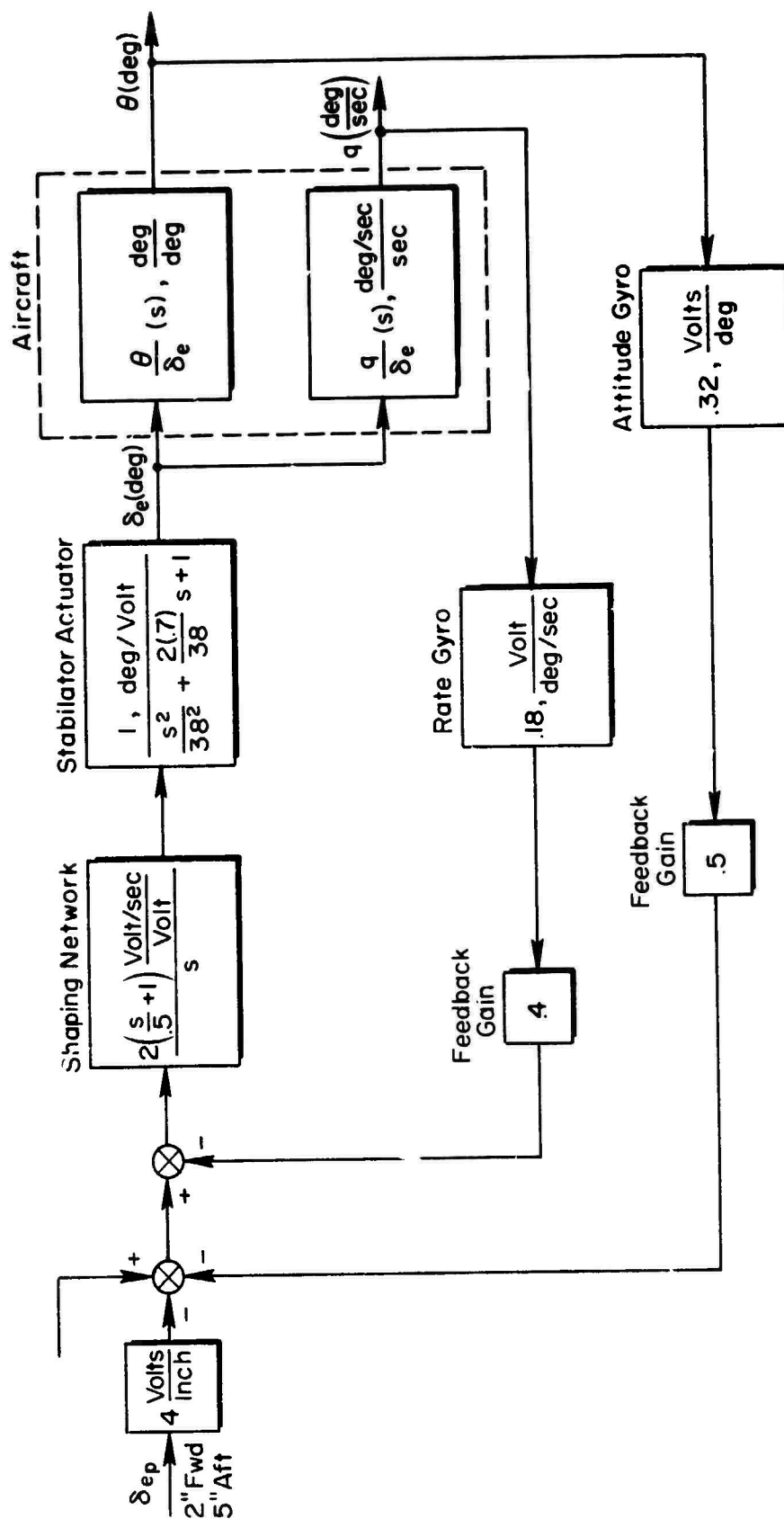


Figure 34. Block Diagram of Pitch Attitude Command System (Ref. 40)

APPENDIX E*

MULTILOOP PILOTING ASPECTS OF LONGITUDINAL APPROACH PATH CONTROL

INTRODUCTION

The title and subject of this appendix may appear somewhat mundane relative to conventional aircraft which generally seem to impose no more than standard difficulties on the pilot during the approach and landing flight phase. However, even for such aircraft, especially when they are required to approach at speeds below that for minimum thrust, flight path control problems can arise which must be handled by the pilot or circumvented by the automatic throttle system designer. Also, otherwise "conventional" aircraft are sometimes fitted with direct lift or drag devices, and proper integration of such devices into the flight control system, or selective use by the pilot, is not clearcut; nor is the question of when such devices are necessary, fully resolved.

When we turn to powered STOL and VTOL aircraft, the problems and concerns increase. Now the approach speed will, almost inevitably, be below the minimum thrust speed. Also, there will be a rich variety of available controls akin to those for a "conventional" aircraft with direct lift and drag, only more so. That is, lift and drag changes may, for example, be accomplished by either, or combinations of, change in power, thrust-line tilt, nozzle deflection, flap setting, boundary layer control bleed, or angle of attack. It is quite often very difficult to decide which control combination to use, or when to switch to an alternative set, not only at the design stage but sometimes when actually flying the aircraft. Similar questions relative to the design of the flight control system are additionally complicated by considerations of necessary vs. desirable complexity and reliability, and conflicting initial investment and maintenance/availability costs.

The purpose of this Appendix is to outline and illustrate an analytic attack directed at better fundamental understanding of the problems and concerns

*Ref. 27 (see Section I, Introduction).

noted above and possible solutions thereto.* In order to reduce the analytic considerations to their bare essentials, the assumption is made that only two controls are involved, stick and throttle. In essence, it is considered that either of these controls may, for a given aircraft, be whatever appropriate combination of real controls produces the assumed control effectiveness values in terms of the resulting X and Z forces and pitching moments, M. It is a simple matter, once desirable vs. undesirable "stick" and "throttle" control qualities are delineated, to determine the corresponding real control combinations for a particular aircraft.

The generic analytic considerations given in the next section are directed toward identifying transfer function forms and factors indicative of control difficulties. To show the basic origins of the factors (poles and zeros) certain simplifying assumptions are made. Whether or not these assumptions hold does not detract from the general usefulness of the resulting conclusions which are given in terms of the factors themselves, their closed-loop equivalents, or the resulting closed- or open-loop transfer function and time-response properties.

These analytic considerations and resulting conclusions are given a certain amount of substance by reference to pertinent applicable literature. More substance is supplied by the specific examples presented in the section, "Example Analytic Studies of Path Control Problems," which were selected to illustrate certain more important problems and the general applicability of the "rules" for "good" or "bad" flying qualities given in the next subsection.

Both the generic and the specific closed-loop analyses are based on methods and pilot models which have been utilized in similar connections for the past ten years. These methods and models are presented with only rudimentary explanations in deference to exposing more interesting and newer developments; however, liberal reference is made to the basic underlying literature.

*While problems associated with flight director functional design (i.e., suitable mixing, equalization and display of pertinent signals) are not specifically treated, the basic analytic considerations exposed here have proven extremely effective in this regard (e.g., Refs. 45 and 46).

GENERIC LONGITUDINAL PATH CONTROL CONSIDERATIONS

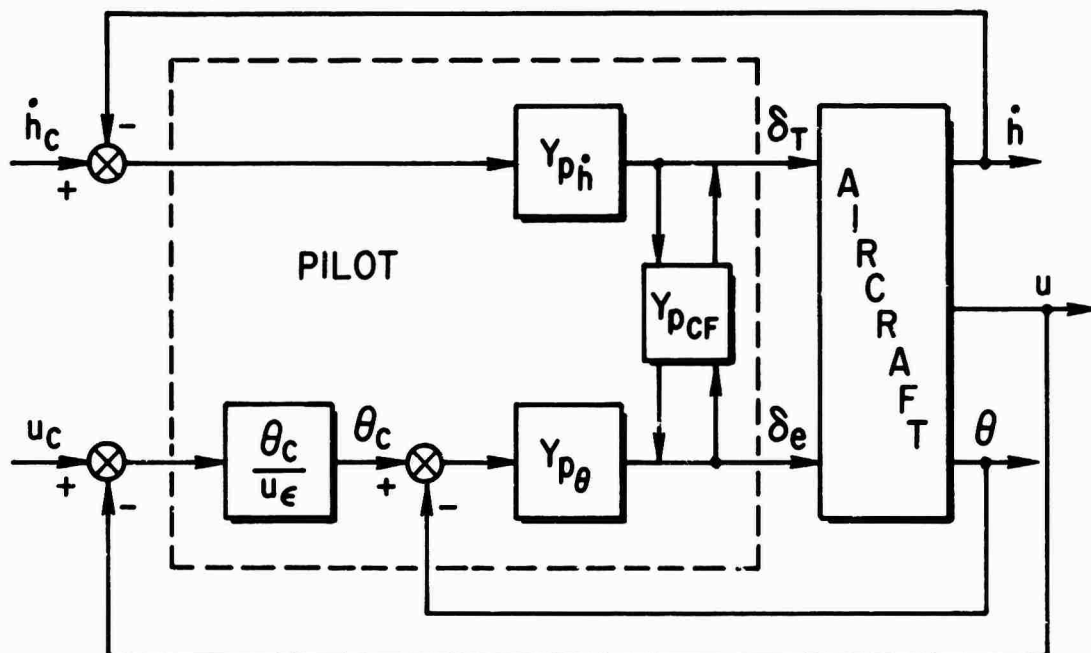
As indicated above we will, for complete generality, consider the classical two-control problem — use of stick and throttle to control air-speed (u) and altitude (h) or rate of climb (\dot{h}) on a landing approach path. The block diagrams of Fig. 35 show two alternative control structures where the specific suitability of either depends upon the intimate details of the aircraft characteristics. Notice that for both alternatives the innermost loop involves control of pitch attitude (θ) with the stick, or elevator (δ_e). This fundamental control is necessary to provide damping (e.g., of the phugoid motions) and other desirable equalization (i.e., faster closed-loop response) of the outer-loop motions. It is also, of course, necessary to control and regulate angle of attack (α), especially in gusty air, and thereby to preserve the stall margin.

The block diagrams are shown with all feedback and feedforward, or crossfeed, elements intact. However, these most general structures are only indicative of the possibilities. As noted above, the use of these possible modes of control depends on the specific aircraft response characteristics involved, and on the nature of the specific piloting task. For example, if the pilot's specific task, at the moment, is to correct an off-nominal air-speed and altitude (or sink rate) condition, the initial portions of such a re-trimming maneuver may well be accomplished open loop, with or without crossfeed. However, as the aircraft nears its nominal condition on target speed and glide slope, the pilot closes the necessary loops to achieve good regulation on the desired path. Thus, we distinguish between regulatory, closed-loop control about a desired operating point and "open"-loop control (with final regulation) to achieve a change in the operating point.

Another distinction resides in the relative priorities assigned to the closed-loop control activities, and generally these follow the speed-of-response properties of the attendant motions. Thus, attitude control which is fast response is usually of highest priority; indeed, as already mentioned, it is generally necessary and implicit regardless of alternative speed and height control activities. The next fastest response is usually in altitude or climb rate; therefore, it receives higher priority than airspeed control

a) "STOL" Technique

$$\begin{aligned} u, \theta &\rightarrow \delta_e \\ \dot{h} &\rightarrow \delta_T \end{aligned}$$



b) "CTOL" (Conventional) Technique

$$\begin{aligned} \dot{h}, \theta &\rightarrow \delta_e \\ u &\rightarrow \delta_T \end{aligned}$$

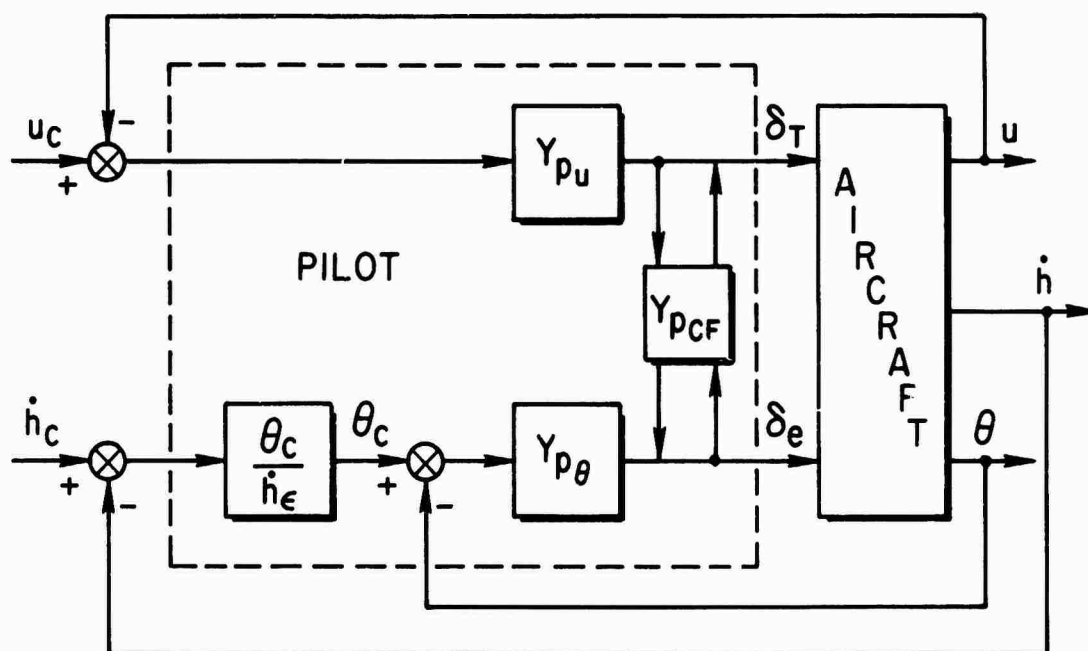


Figure 35. Two Representative Piloting Techniques

which is usually sluggish and slow by comparison. Accordingly, the primary path control input is that used to regulate altitude or its rate, and the secondary input is used to control or to trim airspeed. Thus, referring to the alternative loop structures shown in Fig. 35, the throttle (δ_T) is the primary path control for the "STOL" mode of operation, with secondary attitude (through elevator or stick) inputs to keep airspeed within tolerance. Conversely, for the "CTOL" mode of operation, attitude control of h or \dot{h} is primary, and throttle control of u is secondary.

The foregoing hierarchy of control breaks down, of course, when the pilot's task is to change the operating point. Then the primary consideration is whether the change necessitates an increase or decrease in energy or simply an energy exchange. For instance, in an abort maneuver, the primary input is obviously thrust or throttle to increase the available energy. Similarly, for low and slow (or high and fast) conditions, relative to those desired where total potential and kinetic energy are low (or high), thrust is the primary input. Conversely, for high and slow, or low and fast, where an energy interchange is indicated, attitude is the primary input, and throttle is used to obtain final trim.

The notion of primary and secondary path control inputs serves not only to order the loop-closing sequence but also to provide guidance in selection of the most probable crossfeeds.* Assuming that the pilot finds "coordinating" crossfeeds helpful to "purify" responses, it seems unlikely that he would crossfeed a primary control from a secondary input. Such crossfeeds would superpose lower-frequency (primary) inputs on the basic "high" frequency primary control activity; in this respect, these crossfeeds would appear to be, at best, ineffective and, at worst, confusing. On the other hand, crossfeeding secondary control motions in response to primary inputs provides quicker, effective trimming of the secondary response. However, since trimming is basically a low-frequency process, such higher-frequency crossfeeding in direct response to primary inputs is considered unlikely except on an intermittent basis, e.g., for primary inputs above some threshold level. Based on this reasoning

*Available pilot describing functions, derived from data obtained in two-control multiple-loop situations, are usually based on pure feedback structures (Refs. 23 and 47). However, the data and conclusions of Ref. 48 indicate, but do not specifically quantify, the pilot's selective use of crossfeed.

we hypothesize that crossfeed, if used, will be from primary to secondary control, and will only be active above some threshold level of primary input. The net effect of this hypothesized behavior on regulatory closed-loop activities is to place them somewhere between pure feedback and feedback plus pertinent crossfeeds.

Regulatory Closed-Loop Control

On the basis of the above discussion, the pertinent closed-loop transfer functions can now be written and the generic effects of aircraft characteristics thereon delineated. For generality, the presence and use of a primary-to-secondary control crossfeed is assumed, and the conditions under which such an assumption appears valid are later discussed. Proceeding then from inner to outer loops, neglecting control-system and engine-response dynamics, utilizing standard multiple-loop notation and formulations (Refs. 49-51), and denoting the various pilot transfer functions (more properly, quasilinear describing functions) by $Y_{pi}(s)^*$ where the i subscript is specialized to indicate the particular loop involved:

Elevator (stick) inputs used to command θ :

$$\frac{\theta}{\theta_c} = \frac{Y_{p\theta} N_{\delta_e}^\theta}{\Delta + Y_{p\theta} N_{\delta_e}^\theta} = \Delta' \quad (E-1)$$

$$\frac{\dot{h}}{\theta_c} = \frac{\dot{N}_{\delta_e}^h}{N_{\delta_e}^\theta} \left(\frac{\theta}{\theta_c} \right) = \frac{Y_{p\theta} \dot{N}_{\delta_e}^h}{\Delta'} \quad (E-2)$$

$$\frac{u}{\theta_c} = \frac{N_{\delta_e}^u}{N_{\delta_e}^\theta} \left(\frac{\theta}{\theta_c} \right) = \frac{Y_{p\theta} N_{\delta_e}^u}{\Delta'} \quad (E-3)$$

*The following section discusses the usual simple form of Y_p and provides a background reference.

Throttle inputs in the presence of θ inner loop:

$$\frac{\theta}{\delta_T} = \frac{N_{\delta_T}^{\theta} + Y_{p\theta} N_{\delta_T}^{\theta} \delta_e}{\Delta'} = \frac{N_{\delta_T}^{\theta}}{\Delta'} \quad (E-4)$$

$$\left. \frac{\dot{h}}{\delta_T} \right|_{\theta \rightarrow \delta_e} = \frac{N_{\delta_T}^{\dot{h}} + Y_{p\theta} N_{\delta_T}^{\dot{h}} \delta_e}{\Delta'} \quad (E-5)$$

$$\left. \frac{u}{\delta_T} \right|_{\theta \rightarrow \delta_e} = \frac{N_{\delta_T}^u + Y_{p\theta} N_{\delta_T}^u \delta_e}{\Delta'} \quad (E-6)$$

"Zero error" crossfeeds to purify primary \dot{h} response (i.e., to hold $u = 0$):

$$u = \left(\frac{u}{\delta_T} \right) \delta_T + \left(\frac{u}{\theta_c} \right) \theta_c = 0 \quad ; \quad \theta_{CF}^* \equiv \frac{\theta_c}{\delta_T} \equiv \frac{1}{T_{CF}} \quad (E-7)$$

$$\theta_{CF0} = - \frac{u/\delta_T}{u/\theta_c} = - \frac{N_{\delta_T}^u + Y_{p\theta} N_{\delta_T}^u \delta_e}{Y_{p\theta} N_{\delta_e}^u}$$

"STOL" control mode, with crossfeed:

$$\left. \frac{\dot{h}}{\delta_T} \right|_{\substack{\theta \rightarrow \delta_e \\ \Delta\theta = \theta_{CF} \delta_T}} = \left. \frac{\dot{h}}{\delta_T} \right|_{\theta \rightarrow \delta_e} + \left(\frac{\dot{h}}{\theta_c} \right) \theta_{CF} = \frac{N_{\delta_T}^{\dot{h}} + Y_{p\theta} \left(N_{\delta_T}^{\dot{h}} \delta_e + \theta_{CF} N_{\delta_e}^{\dot{h}} \right)}{\Delta'} \quad (E-8)$$

*The crossfeed details are not specified exactly. The net result of the assumed θ_{CF} is that $\delta_e/\delta_1 = Y_{p\theta} \theta_{CF}$.

$$\left. \frac{\dot{h}}{\delta_T} \right|_{\substack{\theta \rightarrow \delta_e \\ \Delta\theta = \theta_{CF} \delta_T \\ u \rightarrow \delta_e}} = \frac{N_{\delta_T}^{\dot{h}} + Y_{p\theta} \left(N_{\delta_T}^{\dot{h}\theta} + \theta_{CF} N_{\delta_e}^{\dot{h}} \right) + Y_{pu} N_{\delta_T}^{\dot{h}u}}{\Delta' + Y_{pu} N_{\delta_e}^u} \quad (E-9)$$

$$\left. \frac{u}{\theta_c} \right|_{\substack{\theta \rightarrow \delta_e \\ \Delta\theta = \theta_{CF} \delta_T \\ \dot{h} \rightarrow \delta_T}} = \frac{Y_{p\theta} \left\{ N_{\delta_e}^u + Y_{ph} N_{\delta_e}^u \frac{\dot{h}}{\delta_T} \right\}_{\theta_{CF}}}{\Delta' + Y_{ph} \left[N_{\delta_T}^{\dot{h}} + Y_{p\theta} \left(N_{\delta_T}^{\dot{h}\theta} + \theta_{CF} N_{\delta_e}^{\dot{h}} \right) \right]} \quad (E-10)$$

"CTOL" control mode with crossfeed:

$$\left. \frac{\dot{h}}{\theta_c} \right|_{\substack{\theta \rightarrow \delta_e \\ \Delta\delta_T = T_{CF} \theta_c}} = \frac{\dot{h}}{\theta_c} + T_{CF} \left. \frac{\dot{h}}{\delta_T} \right|_{\theta \rightarrow \delta_e} = \frac{Y_{p\theta} N_{\delta_e}^{\dot{h}} + T_{CF} \left(N_{\delta_T}^{\dot{h}} + Y_{p\theta} N_{\delta_T}^{\dot{h}\theta} \right)}{\Delta'} \quad (E-11)$$

$$= \frac{Y_{p\theta} \left(N_{\delta_e}^{\dot{h}} + T_{CF} N_{\delta_T}^{\dot{h}\theta} \right) + T_{CF} N_{\delta_T}^{\dot{h}}}{\Delta'}$$

$$\left. \frac{u}{\delta_T} \right|_{\substack{\theta \rightarrow \delta_e \\ \dot{h} \rightarrow \delta_e \\ \Delta\delta_T = T_{CF} \theta_c}} = \frac{N_{\delta_T}^u + Y_{p\theta} N_{\delta_T}^{u\theta} \Big|_{T_{CF}} + Y_{ph} N_{\delta_T}^{u\dot{h}} \Big|_{T_{CF}}}{\Delta + Y_{p\theta} N_{\delta_e}^{\theta} \Big|_{T_{CF}} + Y_{ph} N_{\delta_e}^{\dot{h}} \Big|_{T_{CF}}}$$

$$= \frac{N_{\delta_T}^u + Y_{p\theta} N_{\delta_T}^{u\theta} \Big|_{T_{CF}} + Y_{ph} N_{\delta_T}^{u\dot{h}} \Big|_{T_{CF}}}{\Delta' + T_{CF} N_{\delta_T}^{\theta} + Y_{ph} \left(N_{\delta_e}^{\dot{h}} + \frac{T_{CF}}{Y_{p\theta}} N_{\delta_T}^{\dot{h}} \right)}$$

(E-12)

The appropriate basic aircraft numerators and the characteristic denominator are of the general forms shown in Table 28, which also displays approximations for the path-dominating poles and zeros in literal form. The approximations, based on the simplifying assumptions:

$$\gamma_0^* = X_{\delta_e} = Z_{\delta_e} = M_{\delta_T} = M_u = 0$$

are useful in establishing relative pole, zero locations and signs in terms of the remaining more basic aircraft derivatives.

Dominant Factors Governing Loop Structure Selection. To more clearly demonstrate path control problems and the dominant effects that influence the choice of control structure, it is convenient to consider situations where the θ loop can easily be, and is in fact, closed quite tightly. Because the resulting $Y_{p\theta}$ characteristics are then of relatively large magnitude, $\theta/\theta_c \doteq 1$ over the frequency band of interest and the \dot{h} and u transfer functions of Eqs. E-2, -3, -5, and -6 are simplified to the ratios of ordinary and coupling numerators (e.g., \dot{h}/δ_T for large $Y_{p\theta} \rightarrow N_{\delta_T}^h \delta_e / N_{\delta_e}$). In effect, the pertinent equations of motion then become those for constrained attitude (Ref. 52), and the path control transfer functions are given rather compactly (invoking the above simplifying assumptions) by the following forms and factors:

Characteristic:

$$\begin{aligned} \Delta' &= N_{\delta_e}^{\theta} = M_{\delta_e} [s^2 + (-Z_w - X_u)s + (Z_w X_u - X_w Z_u)] \\ &= M_{\delta_e} [s^2 + 2\zeta_{\theta}\omega_{\theta}s + \omega_{\theta}^2] \quad , \quad \text{or} \quad (E-13a) \\ &M_{\delta_e} (s + 1/T_{\theta_1})(s + 1/T_{\theta_2}) \end{aligned}$$

*The $\gamma_0 = 0$ initial condition does not detract from the general applicability of these small perturbation relations. Basically, the h responses so computed are equivalent to deviations normal to the flight path stability axis for the usually small values of γ_0 pertinent to approach conditions.

TABLE 28. TRANSFER FUNCTION FORMS AND LITERAL APPROXIMATE FACTORS

FACTORED FORMS	APPROXIMATE FACTORS*
$\Delta(s) = (s^2 + 2\zeta_{sp}\omega_{sp}s + \omega_{sp}^2)(s^2 + 2\zeta_{sp}\omega_{sp}s + \omega_{sp}^2)$ <p style="text-align: center;">or</p> $\left(s + \frac{1}{T_{p1}}\right)\left(s + \frac{1}{T_{p2}}\right)$	$\omega_{sp}^2 \doteq M_q Z_w - M_u$ $2\zeta_{sp}\omega_{sp} \doteq -(Z_w + M_q + M_u)$ $\omega_{sp}^2 \text{ or } \frac{1}{T_{p1}T_{p2}} \doteq \frac{gM_q Z_u}{Z_w M_q - M_u}$ $2\zeta_{sp}\omega_{sp} \text{ or } \left(\frac{1}{T_{p1}} + \frac{1}{T_{p2}}\right) \doteq -X_u$
$N_{\delta_e}^\theta(s) = A_\theta \left(s + \frac{1}{T_{\theta 1}}\right) \left(s + \frac{1}{T_{\theta 2}}\right)$ $[s^2 + 2\zeta_{\theta}\omega_{\theta}s + \omega_{\theta}^2]$	$A_\theta \doteq M_{\delta_e}$ $\frac{1}{T_{\theta 1}} \frac{1}{T_{\theta 2}} = \omega_{\theta}^2 = Z_w X_u - X_w Z_u$ $\frac{1}{T_{\theta 1}} + \frac{1}{T_{\theta 2}} = 2\zeta_{\theta}\omega_{\theta} = -X_u - Z_w$
$N_{\delta_e}^u = A_u \left(s + \frac{1}{T_{u1}}\right) \left(s + \frac{1}{T_{u2}}\right)$	$\frac{A_u}{T_{u2}} \doteq M_{\delta_e}(X_u - g)$ $\frac{1}{T_{u1}} \doteq \frac{gZ_w}{X_u - g}$
$sN_{\delta_e}^h = A_h \left(s + \frac{1}{T_{h1}}\right) \left(s + \frac{1}{T_{h2}}\right) \left(s + \frac{1}{T_{h3}}\right)$	$\frac{A_h}{T_{h2}T_{h3}} \doteq -M_{\delta_e} Z_u$ $\frac{1}{T_{h1}} \doteq -X_u + \frac{Z_u}{Z_u} (X_u - g)$
$N_{\delta_T}^\theta = A_{\theta T} \left(s + \frac{1}{T_{\theta T1}}\right) \left(s + \frac{1}{T_{\theta T2}}\right)$	$\frac{A_{\theta T}}{T_{\theta T2}} \doteq Z_{\delta_T} M_w$ $\frac{1}{T_{\theta T1}} \doteq -X_u + Z_u \frac{X_{\delta_T}}{Z_{\delta_T}}$
$N_{\delta_T}^u = A_{uT} \left(s + \frac{1}{T_{uT}}\right) (s^2 + 2\zeta_{uT}\omega_{uT}s + \omega_{uT}^2)$	$A_{uT}\omega_{uT}^2 \doteq -X_{\delta_T} M_u$ $\frac{1}{T_{uT}} \doteq \frac{g}{U_0} \frac{Z_{\delta_T}}{X_{\delta_T}}$
$sN_{\delta_T}^h = A_{hT} \left(s + \frac{1}{T_{hT}}\right) (s^2 + 2\zeta_{hT}\omega_{hT}s + \omega_{hT}^2)$	$A_{hT}\omega_{hT}^2 \doteq Z_{\delta_T} M_u$ $\frac{1}{T_{hT}} \doteq Z_u \frac{X_{\delta_T}}{Z_{\delta_T}}$
$sN_{\delta_e}^{\theta h} = A_{h\theta} \left(s + \frac{1}{T_{h\theta}}\right)$	$A_{h\theta} \doteq -Z_{\delta_T} M_{\delta_e}$ $\frac{1}{T_{h\theta}} \doteq -X_u + Z_u \frac{X_{\delta_T}}{Z_{\delta_T}}$
$sN_{\delta_e}^{hu} = -sN_{\delta_T}^{hu} = A_{hu} \left(s + \frac{1}{T_{hu1}}\right) \left(s + \frac{1}{T_{hu2}}\right)$	$\frac{A_{hu}}{T_{hu1}T_{hu2}} \doteq -X_{\delta_T} M_{\delta_e} Z_u + Z_{\delta_T} M_{\delta_e} (X_u - g)$
$N_{\delta_e}^{\theta u} = A_{u\theta} \left(s + \frac{1}{T_{u\theta}}\right)$	$A_{u\theta} \doteq X_{\delta_T} M_{\delta_e}$ $\frac{1}{T_{u\theta}} \doteq -Z_w + X_w \frac{Z_{\delta_T}}{X_{\delta_T}}$

 *For $\gamma_0 = X_{\delta_e} = Z_{\delta_e} = M_{\delta_T} = M_u = 0$.

The latter form results if X_w is small or in general if $|X_w Z_u| \ll |Z_w X_u|$, then

$$\Delta' \doteq M_{\delta_e}(s - X_u)(s - Z_w) \quad (E-13b)$$

with $1/T_{\theta_1} \doteq -X_u$ and $1/T_{\theta_2} \doteq -Z_w$.

Elevator Responses:

$$\frac{u}{\delta_e} = -\frac{M_{\delta_e}}{\Delta'} (X_u - g) \left(s + \frac{gZ_w}{X_u - g} \right) = -\frac{M_{\delta_e}}{\Delta'} (X_u - g)(s + 1/T_{u_1}) \quad (E-14)$$

$$\frac{\dot{h}}{\delta_e} = \frac{M_{\delta_e} Z_u}{\Delta'} \left[s - X_u + \frac{Z_u}{Z_w} (X_w - g/U_0) \right] = \frac{M_{\delta_e} Z_u}{\Delta'} (s + 1/T_{h_1}) \quad (E-15)$$

Throttle Responses:

$$\frac{u}{\delta_T} = \frac{M_{\delta_e} X_{\delta_T}}{\Delta'} [s - Z_w + X_w(Z_{\delta_T}/X_{\delta_T})] = \frac{M_{\delta_e} X_{\delta_T}}{\Delta'} (s + 1/T_{u\theta})^* \quad (E-16)$$

$$\frac{\dot{h}}{\delta_T} = -\frac{M_{\delta_e} Z_{\delta_T}}{\Delta'} [s - X_u + Z_u(X_{\delta_T}/Z_{\delta_T})] = -\frac{M_{\delta_e} Z_{\delta_T}}{\Delta'} (s + 1/T_{h\theta})^* \quad (E-17)$$

For conditions on the "frontside" of the thrust-required versus speed curve, and $X_w \ll g/U_0$, the value of:

*As noted above, the u and \dot{h} throttle-response numerators are the coupling numerators which apply when two (or more) control inputs are involved; hence the modified notation which reflects conventional multi-loop practice (Refs. 49, 50, 51).

$$\frac{1}{T_{h1}} \doteq \frac{1}{T_{\theta1}} + \frac{Z_u}{Z_w} \left(X_w - \frac{g}{U_o} \right) \doteq \frac{1}{T_{\theta1}} - \frac{Z_u}{Z_w} \frac{g}{U_o} \quad (E-18)$$

(see Eqs. E-13 and E-15) is positive, and somewhat less than $1/T_{\theta1}$ (because gZ_u/U_oZ_w is always positive); at the same time, $1/T_{u1} \doteq -Z_w \doteq 1/T_{\theta2}$. Accordingly, the $1/T_{h1}$ zero approximately cancels the $1/T_{\theta1}$ pole, and the $1/T_{u1}$ zero approximately cancels the $1/T_{\theta2}$ pole. Then, $\dot{h}/\delta_e \doteq Z_u/(s + 1/T_{\theta2})$ and $u/\delta_e \doteq g/(s + 1/T_{\theta1})$, so that the \dot{h} and u responses are well separated and the \dot{h} response is faster, in keeping with the usual control hierarchy. Under such conditions of favorable pole-zero cancellation, the natural control structure is the CTOL mode with primary control of \dot{h} with elevator (or θ_c) and secondary control of u , as occasionally required (because of sluggish response), with throttle. Notice too that the initial \dot{h}/u response ratio is given by Z_u/g , a handling qualities parameter most often used to characterize short-period response (e.g., see Ref. 16).

It would appear from the above that making $1/T_{h1}$ exactly equal to $1/T_{\theta1}$ would be ideal from the standpoint of pole-zero cancellation and frequency separation. However, if this were attempted by making $X_w = g/U_o$ (e.g., through an angle-of-attack autothrottle) on the basis of Eq. E-18, the effects would not be wholly beneficial. For one thing, the values of $1/T_{\theta1}$ and $1/T_{\theta2}$ would approach each other ($1/T_{\theta1}$ increasing and $1/T_{\theta2}$ decreasing) and might couple to produce an ω_θ oscillation (Eq. E-13 for large X_w); also, the u/δ_e transfer function numerator (Eq. E-14) would be a pure gain, $-gZ_w$. Therefore, the \dot{h}/δ_e response would not necessarily be ideal because of inexact $1/T_{h1}$, $1/T_{\theta1}$ cancellation, and the u/δ_e response would consist of both the $1/T_{\theta1}$ and $1/T_{\theta2}$ aperiodic modes (or be oscillatory if coupled). Under these circumstances, despite the "favorably" positive value of $1/T_{h1}$, the CTOL mode of control would appear to be quite poor. If the STOL mode provided more favorable cancellation, it might be better. However, if coupling were present in the form of a second-order, ω_θ , mode, neither piloting structure would provide cancellation, since all the numerators (Eqs. E-14 through E-17) are first-order. Then the choice of structure would logically depend on possible differences in the magnitude (and time history) of the secondary to primary response ratio, u/\dot{h} .

The most obvious and classical reason for considering a switch from the CTOL to the STOL mode loop structure is a negative value of $1/T_{h_1}$ which occurs on the "backside" of the thrust-required versus speed curve. For such situations, closing the \dot{h}/δ_e transfer function (Eq. E-15), i.e., holding altitude with elevator, results in an aperiodic (speed) divergence characterized by the negative value of T_{h_1} . However, while the STOL mode will normally avoid such difficulties and is the usually preferred "backside" technique (discussed more fully below in the paragraph, "Example Analytic Studies of Path Control Problems"), it may under certain conditions present difficulties warranting a closer examination of the CTOL mode of control.

Suppose, for instance, that $1/T_{h_0}$ (Eq. E-17) approaches $1/T_{\theta_2}$ due to positive thrust inclination (i.e., $X_{\delta_T}/Z_{\delta_T} < 0$) so that $Z_u(X_{\delta_T}/Z_{\delta_T}) \doteq -Z_w$. Then the \dot{h}/δ_T transfer function reduces to $-Z_{\delta_T}/(s + 1/T_{\theta_1})$, which for normal values of $1/T_{\theta_1} \doteq -X_u$ has a relatively slow response. At the same time, the negative value of $X_{\delta_T}/Z_{\delta_T}$ would tend to reduce $1/T_{u_0}$ for normally positive X_w (Eq. E-16), bringing it closer to $1/T_{\theta_1} \doteq -X_u$. The resulting u/δ_T transfer function would then approach $X_{\delta_T}/(s + 1/T_{\theta_2})$, which represents a relatively fast response. Accordingly, not only would \dot{h} control with δ_T be poor because of sluggish response, but the usual primary and secondary response roles would be reversed, i.e., u would respond faster than \dot{h} . However, the steady-state response ratio, u/\dot{h} , given by $-X_{\delta_T}T_{\theta_2}/Z_{\delta_T}T_{\theta_1} \doteq -X_{\delta_T}X_u/Z_{\delta}Z_w$ could conceivably be so small that the u perturbations might not be too troublesome.

The conclusion following from the above discussion is that there is no simple rule which can guarantee the selection of the correct piloting structure. Backsidedness is a primary clue but it must be tempered with dynamic coupling, frequency separation/ordering, and response ratio considerations.

Crossfeed Considerations. The conditions surrounding the selection of the appropriate closed-loop structure require further extension for possible crossfeeds. Still considering situations where the attitude loop is tightly closed, the zero-error crossfeed is given by (Eq. E-7):

$$\theta_{CF_0}(s) = \frac{1}{T_{CF_0}(s)} = -\frac{N_{\delta T \delta e}^u \theta}{N_{\delta e}^u} \doteq -\frac{X_{\delta T} \left(s + \frac{1}{T_{u\theta}}\right)}{(X_\alpha - g) \left(s + \frac{1}{T_{u1}}\right)} \quad (E-19)$$

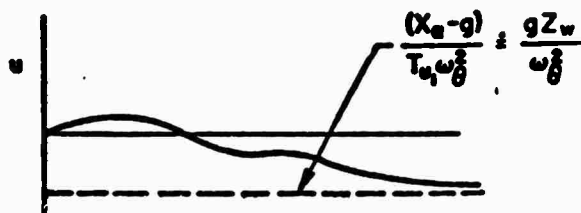
where $\frac{1}{T_{u\theta}} = -Z_w + \frac{Z_{\delta T}}{X_{\delta T}} X_w$

$$\frac{1}{T_{u1}} \doteq \frac{gZ_w}{X_\alpha - g}$$

In general, either or both $1/T_{u\theta}$ and $1/T_{u1}$ can become negative for sufficiently high positive values of X_w (e.g., for an autothrottle utilizing α feedback) and the usually negative sign of $Z_{\delta T}/X_{\delta T}$ (for positive thrust inclination). When $1/T_{u1}$ is negative, $\theta_{CF_0}(t)$, for a step δ_T input increases exponentially (diverges) with time; thus, there is no finite steady-state value. However, another more reasonable interpretation is possible, i.e., multiplying numerator and denominator of Eq. E-19 by $(s - 1/T_{u1})$:

$$\theta_{CF_0}(s) = -\frac{X_{\delta T} \left(s - \frac{1}{T_{u1}}\right) \left(s + \frac{1}{T_{u\theta}}\right)}{(X_\alpha - g) \left(s + \frac{1}{T_{u1}}\right) \left(s - \frac{1}{T_{u1}}\right)} \doteq \frac{X_{\delta T}}{(X_\alpha - g)} \frac{\left(s + \frac{1}{T_{u\theta}}\right)}{\left(s - \frac{1}{T_{u1}}\right)} e^{-2T_{u1}s} \quad (E-20)$$

where the last step utilizes the first-order Padé approximation, $e^{-\tau s} \doteq [s - (2/\tau)][s + (2/\tau)]$, valid only when τ is small relative to the times of interest. For negative T_{u1} , $\theta_{CF_0}(t)$, which is now basically convergent, must, however, start before the δ_T step input by $-2T_{u1}$ sec. This required advancement in start time for the crossed θ_{CF} is consistent with the effective delay in the u/θ_c response when $1/T_{u1}$ is negative, as sketched below. Here, consistent with the large positive values of X_w required to make $1/T_{u1}$ negative, we have assumed that the characteristic, θ numerator, modes are coupled (Eq. E-13), i.e., oscillatory with good damping. Notice that the u response is roughly zero for a time delay



u Response to Step θ_c for Negative $1/T_{u1}$

interval related to $-1/T_{u1}$; hence, the crossfeed θ_c must start earlier to be effective.

Another aspect of the sketched u response is that, initially, u is essentially decoupled (from \dot{h}) for θ_c inputs. Also, although not shown, the value of $1/T_{h1}$ is probably positive, reflecting the large positive value of X_w (see Eq. E-15). It appears, therefore, that the use of throttle as the primary closed-loop control is unwarranted, on the basis of the decoupled u and stable \dot{h} responses to θ_c ; and that the assumed crossfeed and loop structure are probably both incorrect.

A general conclusion afforded by this example is that whenever the zero error crossfeed has a positive pole (negative factor), the assumed loop structure bears careful reconsideration.

A more usual concern is that even for positive values of T_{u0} and T_{u1} the $\theta_{CF0}(t)$ for a step throttle input may vary considerably with time. If this variation is too extreme it is difficult for the pilot to learn and "program" even for discrete maneuvers and doubly so for closed-loop control. Accordingly, we hypothesize that crossfeed will not be used (even intermittently) in closed-loop operations when the ideal crossfeed requires more than a 30 percent change over the time interval from three to ten seconds (following the primary input). The 30 percent value is arbitrary; it reflects the fact that zero percent change (pure gain) is ideally desirable and that pilots are relatively insensitive (from a rating standpoint) to time-invariant gain changes of the order of 50 percent (Ref. 53). The times selected are those consistent with the frequency band of interest for closed-loop \dot{h} and u control, respectively (Refs. 51, 54, 55). This general "rule" for judging the possible efficacy of an assumed crossfeed

also handles situations where the values of $1/T_{u0}$ or $1/T_{u1}$ may be negative but quite small. For positive values it is more convenient and, because of its tentative nature, just as reasonable, to extend the time interval to infinity, i.e., to consider the ratio of the 3 sec and steady-state values.

Pilot-Centered Path Regulation Problem Areas. In order to judge the approach and landing path regulation suitability of a given configuration, it is advisable to catalog some of the more prominent sources of pilots' complaints and difficulties. However, before proceeding in this negative vein, it is appropriate to discuss those properties found desirable. For both discussion and catalog, the assumption, as in the foregoing, that the attitude loop is tightly closed and that such closure does not interfere with path control will not be made, i.e., attitude-loop-related problems will be considered.

Relative to good path regulation properties, the pilot would like:

- **Inner-loop (e.g., attitude) control integrity and equalization potential.** The inner, attitude loop, because it is fundamental to path control regardless of piloting technique, should have response characteristics generally faster, better damped, etc., than the primary path loop. A minimum open-loop crossover frequency capability of the order of 2 rad/sec (Ref. 56) with adequate gain and phase margins and without (or "low") pilot equalization is desirable. The open-loop "dc" gain should be high enough to prevent low frequency attitude "drifting." Closing the inner loop should provide favorable: improvement of the phugoid mode damping to inhibit airspeed fluctuations; and overall path mode equalization, insensitive to and tolerant of the specific θ -loop gains used by the pilot (i.e., "tightness" or "looseness" of attitude control).
- **Adequacy and ordering of path control loop bandwidths.** Basically, the path-mode bandwidth requirements are predicated on good closed-loop performance capabilities and disturbance (i.e., gust and shear) suppression. The \dot{h} -loop (with θ closed) should have faster response than the u -loop by at least a factor of 3; its minimum open-loop crossover capability, with adequate gain and phase margins and without equalization, should be of the order of 0.5 rad/sec (Ref. 54).
- **Uncoupled or complementary control responses.** The \dot{h} and u responses (with θ closed) to the controls should be separated so that they do not interfere. Thus it should be possible to control \dot{h} without exciting excessive excursion in u , and

vice versa. However, if some degree of coupling exists, the responses should be complementary (i.e., the control actions required to regulate one path variable (e.g., \dot{h}) help in the regulation of the other (e.g., u).

- **Minimum depletion of safety margins.** During path regulation and control activities, stall, buffet, control, comfort, etc., boundaries must never be exceeded; and excursions into the available margins should be minimized.
- **Control economy.** Control "economy" refers to the pilot's desire to use as simple, and as easily maintained, a control strategy as possible, e.g., minimum number of nonsensitive feedback loops with little or no equalization and/or cross-feeds. Such "economical" control imposes minimal demands on the pilot's attention and thereby allows him sufficient excess capacity for other functions.
- **Control harmony.** The preceding good qualities have primarily been directed at the dynamic aspects of control, assuming that the pilot loop gains required to achieve control are "comfortable" and "harmonious." An otherwise good airplane (dynamically) can be seriously degraded if control sensitivities are too high or too low, and/or if the relative sensitivities are disproportionate.

Path regulation problem areas will arise in varying degree whenever there are deviations from the "good" properties listed above. However, such generalization is of little utility in pinpointing the specific sources of the pilot's complaint or in suggesting aircraft and/or flight control system modifications to improve pilot acceptance. To enhance appreciation for the particular kinds of problems encountered, the following catalog has been assembled based on past experience. Some of this experience will later be used to illustrate the detailed nature of specific problems. Undoubtedly, other kinds of problems exist to be discovered in the future.

Attitude Control

- **Inadequate bandwidth problems** are often associated with low short-period stiffness where the attitude response is dominated by the phugoid mode. These situations, as noted, e.g., in Refs. 56 and 31, require excessive pilot lead compensation (e.g., $T_{L0} > 1$ sec) to attain the desired crossover frequency range. Increasing T_L is directly associated with degrading (increasing) handling quality ratings; to get a

satisfactory, 3.5, rating, T_L must be less than approximately 1 sec (Refs. 57 and 58).

- **Inner-outer loop equalization conflict** results when pilot lag, T_{θ} , is required in the attitude loop. Reference 56 illustrates how lag equalization in the θ -loop restricts the path mode (i.e., h) bandwidth. Typically, these situations exist where attitude is used to control altitude and the attitude numerator factor, $1/T_{\theta 2}$ (i.e., altitude lag), is much less than one.
- **Low static gain** properties are another manifestation of back-sidness; i.e., from Eq. E-18, for $1/T_{h1} < 0$, $1/T_{\theta 1} < -Z_{u g}/U_0 Z_w \doteq \omega_{\theta}^2 T_{\theta 2}$, and the static gain is then less than the short-period "gain" (Ref. 59). Sufficiently low values of static gain limit the pilot's ability to provide separation of u and h responses. Also, attitude trimmability and the use of attitude as a speed reference are degraded, resulting in increased attentional demands on the pilot (Refs. 23 and 38).
- **Oversensitivity to gain/equalization** occurs when the inner attitude loop or resulting outer-loop crossover frequencies or bandwidths are very sensitive to changes in pilot gain ($K_{p\theta}$) or lead ($T_{L\theta}$). References 49 and 38 illustrate, respectively, situations in which attitude gain and lead equalization sensitivity were the underlying control problems affecting path regulation.

Path Control

- **Performance reversals** occur when increased attention and control activity, i.e., increased pilot gain and/or lead, cause a net loss in performance. Typically, such reversals are multiloop in nature, in that the closure of the innermost loop restricts the path mode bandwidth (Refs. 23 and 49). Other reversal situations involve so-called "boxed-in" conditions (Refs. 38 and 60). In these cases, the pilot is constrained not only to a given control strategy, but also to narrowly confined values of gain and/or lead; increasing or decreasing gain/equalization causes an undesirable performance degradation.
- **Inadequate bandwidth** is primarily an altitude loop (with attitude closed) problem. When the loop crossover frequency is less than about 0.3 to 0.4 rad/sec (Ref. 54), the pilot rating will be unsatisfactory ($PR > 3.5$). Excessive lead equalization, required to achieve desirable bandwidth, will also be unsatisfactory (see above).
- **Inadequate response separation** refers to undesirable "mixing" of u and h responses. As noted above, this can be due to "inherent" coupling when the θ/δ_e numerator is oscillatory, or to thrust inclination effects which produce inadequate

pole-zero cancellations in the appropriate u and \dot{h} transfer functions. If the response in u is faster than that in \dot{h} the "mixing" is especially bad; in general, u responses faster than about half the \dot{h} response (assuming the latter is adequate, as above) are undesirable. Of course, the magnitude (and sign) of u/\dot{h} is also important. For instance, a particularly troubling aspect of "inherent" (ω_0) coupling occurs when the initial u/\dot{h} response to elevator (or θ_c) becomes positive (e.g., due to $X_A > g$, Eqs. E-14 and E-15). Then, since the u/\dot{h} response to thrust is also generally positive, closure of either loop (u or \dot{h}) conflicts with closure of the remaining loop (\dot{h} or u). That is, for a positive \dot{h} response u is (initially, at least) positive; and a secondary control input to reduce u also reduces the desired \dot{h} response. Such conditions tend to limit the pilot's primary regulation activities to the use of a single control; u perturbations are ignored (Ref. 55).

- **Difficult or conflicting crossfeeds** have already been discussed relative to dynamic problems. Additional difficulties arise when the necessary or required control actions are too large, are unnatural (e.g., reversed sign), or when they limit regulation performance (e.g., by reducing effective gain or bandwidth). Regardless of whether or not crossfeeds are actually used by the pilot, inspection of the zero-error crossfeed characteristics (θ_{CF_0} , T_{CF_0}) can provide useful clues in terms of the overall activities (either feedback or crossfeed) required to "purify" responses.
- **Excessive depletion of safety margins** can be caused by any combination of the above noted deficiencies. In general, however, the CTOL mode (controlling \dot{h} with elevator) involves larger α excursions than the STOL mode (\dot{h} with throttle), whereas the latter obviously involves larger thrust excursions. Thus, depending on whether the airplane is closer to a limiting condition on power or stall may dictate the choice of control strategy from a safety standpoint, provided there is no obvious choice from the ease-of-control standpoint.
- **Low (high) effective path gains** are those situations where an otherwise good airplane/flight control system suffers because of overly sensitive, overly sluggish or "disharmonious" control effectiveness. Departures in either direction from desirable gain levels result in degraded ratings and poorer pilot acceptance. Analysis of the regulation control activity in terms of rms control deflections or forces can sometimes provide a clue to degrading gain levels (Refs. 53 and 61).

Open-Loop Changes in Operating Point (Trim Management)

As indicated earlier, the pilot's tasks are not all concerned with closed-loop regulation about a given operating point. He must also readily be able to perform essentially open-loop maneuvers to new operating points, as in: flare and touchdown; correcting off-nominal path and speed, including glide slope acquisition; transitions from cruise to landing configurations; and compensating for steady and sheared winds. All these tasks can be characterized in general by the need to change either airspeed or altitude (or sink rate) or both by a prescribed amount or (for transition) in some easily programmed manner. Assuming that the pilot can comfortably close the attitude loop and that such closure does not "interfere" with path and speed control directs attention back to the attitude-constrained transfer functions of Eqs. E-2, E-3, E-5, and E-6, and the pertinent Table 27 forms and approximations. However, we now consider discrete, rather than continuous, primary and secondary inputs and appropriate crossfeeds and confine our attention to corrections about a near-nominal approach path.

Energy Change. For a trim change requiring an energy increase or decrease, thrust or throttle (δ_T) is the primary input; however, secondary $\theta_c(\delta_e)$ inputs are generally required to rapidly approximate the desired increases or decreases in both speed and altitude (or climb rate). Final achievement of the desired target conditions involves closed-loop regulation, as noted earlier; but the initial maneuver and appropriate pilot strategy involves open-loop coordinated, or crossfed, control inputs. Because both altitude and speed changes are desired, the appropriate crossfeed is not exactly the zero-error form (θ_{CF_0}) previously given. However, scaling θ_{CF_0} up or down directly scales the resulting u response to a throttle input, i.e.:

$$\frac{u}{\delta_T} = \frac{N_{\delta_T}^u + N_{\theta_c}^u K \theta_{CF_0}}{\Delta'} = \frac{N_{\delta_T}^u - K N_{\theta_c}^u \left(\frac{N_{\delta_T}^u}{N_{\theta_c}^u} \right)}{\Delta'} = (1 - K) \frac{N_{\delta_T}^u}{\Delta'} \quad (E-21)$$

Therefore, $K\theta_{CF_0}$ can be taken as indicative of the stick activity required to coordinate a primary throttle input; where K is a constant, appropriate to the airspeed change desired. Note that for the postulated conditions, i.e., thrust input to increase, or decrease, both speed and altitude simultaneously, $1 - K$ is always positive.

As already noted, if $\theta_{CF_0}(t)$ is not roughly constant, it represents a difficult crossfeed for the pilot. Whether or not the rules previously postulated for the permissible time variation of θ_{CF_0} in regulatory tasks also apply to trim change tasks is a moot point. It would seem that for discrete inputs the permissible variations with time could be somewhat larger than those for continuous closed-loop inputs. Nevertheless, it can still be stated that desirable values of $\theta_{CF_0}(t)$ for both tasks are those that remain nearly constant.

The sign and magnitude of θ_{CF_0} are also important. A negative sign, or a very small magnitude, indicates that positive thrust inputs (without crossfeed) tend, respectively, to decrease speed or to produce essentially zero speed change. Since the pilot's intention in applying thrust is to increase both speed and climb (otherwise he would change attitude to effect an energy interchange), positive and reasonably large values of θ_{CF_0} are desirable for trim management. The only surprising aspect of this conclusion is the rejection of $\theta_{CF_0} = 0$ as a desirable condition. Since $\theta_{CF_0} = 0$ represents a "purified" response, i.e., only \dot{h} , it would seem normally desirable, at least from a regulatory standpoint. However, the above considerations suggest that such a condition is somewhat more complex from the trim management standpoint than necessary, i.e., thrust and stick inputs are always required when an energy increase is indicated. For conditions with positive θ_{CF_0} , certain u and \dot{h} energy increases could conceivably involve only thrust inputs. In this regard zero and negative values of θ_{CF_0} infer less economy of control (more workload) than do reasonably positive values. This theoretical consideration needs more specific checking; however, it seems to correlate with the available evidence, as later discussed.

The upper limit on the positive magnitude of θ_{CF_0} is that the resulting α excursions must not be so large that they represent serious depletion of available stall margins.

While θ_{CF_0} appears to have some trim management significance when θ is easily and tightly controlled, the effects of opening this inner loop should also be considered. For example, if there are noticeable thrust-induced pitching moments, both \dot{h} and u responses will depend on the extent to which the attitude-loop closure suppresses such moments. As indicated earlier, the pilot would like some latitude in all loop closure gains; accordingly, large thrust pitching moments are always undesirable (Ref. 43), since they impose a requirement for tight attitude control. However, small pitching moments may have desirable crossfeed consequences in the present context. For instance, when $\theta_{CF_0} = 0$, e.g., for thrust inclination near 90 deg, negative (nose down) pitching moments, if not suppressed by the attitude closure, would produce a positive u response. Then, the zero-error cross-feed, now expressed in terms of stick (positive aft) to throttle, $(\delta_s/\delta_T)_{CF_0}$, would be positive and favorable, rather than zero and possibly questionable. Reference 43 contains some experimental evidence which tends to confirm these considerations, e.g., "some aft thrust line effect was found to improve speed control." Also, "smaller speed excursions and less longitudinal control activity are apparent in the aft offset configuration...."

Generalizing on the above observations: both $(\delta_s/\delta_T)_{CF_0}$ and θ_{CF_0} should be approximately constant (within 30%, say) for times between about 3 and 10 seconds; and either or both should be greater than zero but not so large as to imply excessive α excursions.

Energy Exchange. Turning now to energy exchange conditions, the primary input, as already noted, is θ_c . For backside conditions an increase in attitude will eventually produce both u and \dot{h} decreases. There is no steady-state energy exchange; and this is the essence of the backside problem. Therefore, thrust is always required as a final adjustment to keep \dot{h} and u of opposite sign. The problem is similar to that in regulatory control and little distinction can profitably be made between regulation and energy exchange trim management for backside conditions.

For frontside conditions the desirable energy exchange usually occurs quite predictably with attitude inputs producing monotonic changes of opposite sign in \dot{h} and u . However, if the front-sidedness is due to a large

positive value of X_w (as in some autothrottle-equipped U. S. Navy aircraft), the initial u response is then opposite ($1/T_{u1} < 0^*$) to the final response, which is quite conventional. However, the final response in \dot{h} , although of opposite (conventional) sign to u is quite large. The problem now is that there may be inadequate energy exchange potential because θ_c produces primarily a change in h . If the pilot wants to decrease airspeed with θ_c , he also incurs a large increase in \dot{h} . If he uses thrust to reduce this \dot{h} error he increases airspeed, thereby negating his initially desired airspeed reduction. Formalizing this observation:

$$\text{for } h = 0 \quad \left(\frac{h}{\theta_c}\right)\theta_c + \left(\frac{h}{\delta_T}\right)\delta_T = 0$$

$$\delta_{TCF} \equiv \frac{\delta_T}{\theta_c} = -\frac{(h/\theta_c)}{(h/\delta_T)}$$

$$\begin{aligned} u &= \left(\frac{u}{\theta_c}\right)\theta_c + \left(\frac{u}{\delta_T}\right)\left(\frac{\delta_T}{\theta_c}\right)\theta_c \\ &= \left[\left(\frac{u}{\theta_c}\right) - \left(\frac{u}{\delta_T}\right)\frac{(h/\theta_c)}{(h/\delta_T)}\right]\theta_c \\ &= \left(\frac{u}{\theta_c}\right)\left[1 - \frac{(h/u)\theta_c}{(h/u)\delta_T}\right]\theta_c \end{aligned}$$

Considering steady-state values and "normalizing" with respect to the non-crossfeed case:

$$\frac{\left[\frac{u}{\theta_c}\right]\delta_{TCF}}{\frac{u}{\theta_c}} = 1 - \frac{Z_\alpha X \delta_T}{Z_{\delta_T}(X_\alpha - g)} \frac{T_{u1} T_{h\theta}}{T_{u\theta} T_{h1}} \quad (E-22)$$

*Since $1/T_{u1}$ is a pole in $\theta_{CF0}(s)$, Eq. E-7, the configuration may prove undesirable from the standpoint of divergence $\theta_{CF0}(t)$ characteristics.

If the value of this ratio is small, the θ and α excursions required to effect airspeed trim (without disproportionate \dot{h} excursions) are larger than usual by the inverse of the ratio. A ratio of $1/2$, for example, means that a normal value of $U_0 \theta_c / u_c$, about 0.3 deg for a 1 per cent change in speed, increases to 0.6 deg. Since airspeed fluctuations and usual tolerances approach 10 per cent or so (e.g., 5 kt for a 60 kt nominal approach speed), the resulting α and θ excursions in this example could be as high as 6 deg, an obviously serious incursion into the stall margin.

Thus, the acceptability of a given (Eq. E-22) ratio appears to depend largely on the specifically available stall margin.

Implications for Handling Quality Parameters, Criteria, and Correlations

The large number of parameters involved (e.g., Table 28), the multiple-loop aspects to be considered (e.g., Eqs. E-1 to E-12), and the possible closed- and open-loop problems that can occur present a labyrinthian path to the discovery of universal open-loop airplane-only parameters or criteria which can be used successfully to describe all the effects involved (see also Ref. 62). It may be possible eventually to correlate specific problems and effects with selected airplane parameters, remembering that many of the parameters are connected through basic derivatives. However, the process of examining all potential parameters in the light of correlatable data presents, in view of the dimensions of the problem, an enormous experimental burden.

A more viable alternative, in the authors' opinion, is to apply available and proven open- and closed-loop analysis techniques and general criteria to the development of a design methodology which can be used to discover and rectify fundamental and interacting problem areas. Once confidence in its validity has been established, the method can undoubtedly be reduced to simple computational programs, thereby to streamline the design and specification process (e.g., Ref. 58). In the body of this section we have presented the major considerations and analysis techniques, some already "verified" experimentally, which would form the core of a complete method. In the section to follow we shall further illustrate how certain experimentally-encountered piloting difficulties can be explained by application of these considerations and techniques.

EXAMPLE ANALYTIC STUDIES OF PATH CONTROL PROBLEMS

In the following we present example results of analyses directed at explaining and understanding various rating trends and problems associated with multiple-loop approach control experiments and flight observations. In order to do this most economically, the selected loop closures involved are shown with little or no explanation of the manner in which the parameters comprising the pilot's transfer function,

$$Y_p = \frac{K_p(T_{Ls} + 1)}{(T_{Is} + 1)} e^{-\tau s} \quad (E-23)$$

were individually established for each example. In general, the parameters were set by applying the "adjustment rules" which are an integral part of the complete Pilot Model (Ref. 53). In certain instances, complete adherence to all the adjustment rules is unnecessary and was not used in the interests of a simpler but still revealing analysis. For example, control of the low-frequency path modes is little influenced by the elimination of the time delay (τ) term, because its phase contribution for the frequencies of concern (below 1 rad/sec) is quite small.

The cases of most interest and complexity are those on the "backside" of the thrust-required vs. speed curve; therefore, most of the examples considered have this feature. For more examples of closed-loop analyses pertinent to frontside conditions, the reader is referred to the existing literature (Refs. 54, 56, 59, 63, and 64).

Example 1. Carrier Aircraft Approach-Speed Selection

This first example is also taken from the literature (Refs. 49, 59, 65, and 66) and represents a pioneering effort to apply multiple-closed-loop analyses to the approach path regulation problem. The situation considered was stick and throttle control of approach path and speed on an optical beam; and the analyses were directed at examining those flight test conditions, on a variety of U. S. Navy airplanes, where the pilots reported an "inability

to control altitude or arrest rate of sink." This inability could not, at the time, be ascribed to any of the then-current approach speed selection parameters.

The very complete analyses of Ref. 49 considered both the basic loop structures shown in Fig. 35; angle-of-attack feedbacks to throttle or stick were also considered and analyzed. After many specific and generic loop closure exercises which took account of thrust and angle-of-attack lags it was decided that the probable piloting technique employed was $h \rightarrow \delta_T, \theta, u \rightarrow \delta_e$, corresponding to the so-called STOL mode. This conclusion was supported in part by contacts with Navy pilots and by official Navy "doctrine." In analyzing this control structure it was discovered that, for certain conditions well on the "backside," primary control of altitude was very sensitive to the assumed inner (θ) loop gain. In fact, as airspeed was progressively decreased, increasing the pilot's θ -loop gain became less effective in increasing the outer loop, altitude control, bandwidth; and eventually an increase in gain resulted in a decrease in bandwidth and in altitude control performance.

The speed at which this reversal occurs was postulated as corresponding to incipient "inability to control altitude...." For lower speeds the harder the pilot tries, by tightening attitude control (normally effective in improving altitude response), the more he degrades his altitude performance. The altitude bandwidth sensitivity to attitude gain was computed for seven Navy carrier aircraft for a range of approach speeds; and the speed at which reversal occurred (bandwidth:gain sensitivity = 0) was shown to compare favorably with pilot-selected approach speeds for five of the seven aircraft. The remaining two had other limiting problems, e.g., poor lateral control, forward visibility, etc. Finally, a simplified form of a "reversal criterion," based on assumptions equivalent to those for the Table 28 approximate factors and on the phugoid equations of motion (i.e., neglecting $M_q, M_{\dot{\alpha}}, \ddot{\theta}$ terms) was derived (see also Ref. 59); i.e., reversal occurs when:

$$\frac{1}{T_{\theta_1} T_{\theta_2}} \left(\frac{1}{T_{hT}} - 2\zeta_p \omega_p \right) + \omega_p^2 \left(\frac{1}{T_{\theta_1}} + \frac{1}{T_{\theta_2}} - \frac{1}{T_{hT}} \right) = 0 \quad (E-24)$$

It was later noticed that the "reversed" conditions could be improved by reductions in the static margin. This thesis was tested in a fixed-base simulator experiment with favorable confirmation in the work reported in Ref. 65. In this reference it was also explicitly shown that, for characteristics representative of then-current Navy carrier aircraft, two-loop control of attitude with elevator and altitude with throttle (without $u \rightarrow \delta_e$) caused only small perturbations in airspeed. These were, in fact, considerably smaller than those accompanying the complete three-loop CTOL mode of operation, i.e., $h, \theta \rightarrow \delta_e; u \rightarrow \delta_T$. While the CTOL mode exhibits some potential superiority relative to altitude control (noted and discussed in Ref. 49), it suffers by comparison with the STOL mode on two counts: u dispersions are increased as noted above, and three loops, rather than two (as for acceptable STOL mode performance), must be closed. In the latter sense, the CTOL structure violates the pilot's desire for control economy.

Another effort relative to this subject is reported in Ref. 66. Here the primary purpose of the work was to define a landing approach flight test program for a specific aircraft and to predict the flight results. Reversal effects were studied in detail and it was shown that the simple criterion was affected only slightly by the addition of the short-period mode. (Also studied were the effects of drag variation (through use of landing gear and dive brakes) and c.g. shifts. The analyses indicated a spread of about 18 kt in the reversal speeds for extreme conditions of drag and c.g. configuration. Unfortunately, the flight tests were (later) conducted without either drag or c.g. changes (Ref. 67). However, the selected "comfortable" speed for a beam-guided approach was found to be limited by "loss of ability to control the flight path angle," as predicted. Also, the flight-determined "comfortable" approach speed range, between 130 and 140 kt, was satisfying close to the calculated reversal speed (corrected for weight differences) of 132 kt.

Example 2. Backside STOL Control as Influenced by Thrust Inclination

This example considers the conditions experimentally investigated in Ref. 55. A feature of this experiment was the use of an automatic inner, rate-command, attitude hold loop which eliminated attitude control problems from the path control picture. Also, the values of X_{δ_e} , Z_{δ_e} , and M_{δ_T} were

TABLE 29. TEST CONFIGURATIONS AND RANGE OF VARIABLES^a

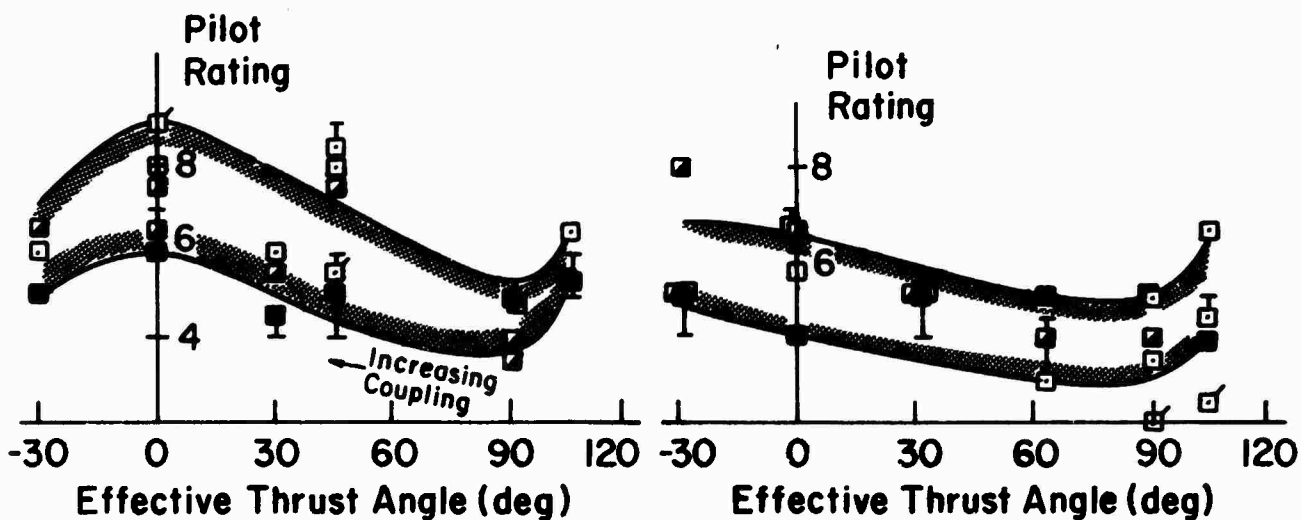
CONDITION NO.	DENOMINATOR		ATTITUDE RATE		SPEED		THROTTLE SENSITIVITY $Z_{\delta T}/X_{\delta T}$ g/in.	THRUST ANGLE ARC TAN $-Z_{\delta T}/X_{\delta T}$	X_W
	$1/T_{\theta 1}$ (ξ_3)	$1/T_{\theta 2}$ (ω_{θ})	ATTITUDE $1/T_{\theta i}$	THROTTLE $1/T_{\theta \theta}$	NUMERATOR ^b ATTITUDE $1/T_{u 1}$	THROTTLE $1/T_{u \theta}$			
1	.1	.5	-.09	0	.5	.5	-.146/-.0363	104	0
2				.1		NA	-.15/0	90	
3				.5		.5	-.106/.106	45	
4				.79			-.075/.13	30	
5				NA			0/.15	0	
6				-.59			.075/.13	-30	
7	.3	.3	-.03	0	.73	.9	-.146/-.0363	104	.1
8				.1		NA	-.15/0	90	
9				.3		.3	-.134/.067	63.5	
10				.79		.44	-.075/.130	30	
11				NA		.50	0/.150	0	
12				-.59		.56	.075/.13	-30	

^aDynamic characteristics valid for perturbation about 60 kt trim condition; $X_{u 1} = -0.10$; $Z_W = -0.50$; $Z_{u 1} = -0.40$.

^bNA in the limit when either X_{δ} or Z_{δ} are zero and the time constant is undefined, i.e., for

$$\theta_T = 90^\circ, N_{\delta T}^u = X_{\delta T}[s + (1/T_{u \theta})] = X_W Z_{\delta T}; \text{ for } 0^\circ, N_{\delta T}^u = -Z_{\delta T}[s + (1/T_{\theta \theta})] = -Z_{u 1} X_{\delta T}.$$

<u>Pilot</u>	<u>Code</u>
K	Solid
A	Open
J	Half Solid
F	Flagged



a) Extreme Backside, $1/T_{h1} = -.09$
Decoupled $N_{\delta_e}^{\theta} (1/T_{\theta_1} \neq 1/T_{\theta_2})$

b) Moderate Backside, $1/T_{h1} = -.03$
Coupled $N_{\delta_e}^{\theta} (1/T_{\theta_1} = 1/T_{\theta_2})$

Figure 36. Effect of Various Control and Configuration Characteristics on Manual STOL Mode Path Control (Ref. 55)

set to zero so that the Table 28 approximate factors were applicable. The configuration details are given in Table 29, and the pilot rating data obtained are shown in Fig. 36. The pilots were instructed specifically to use throttle as the primary h control for the data shown. Additional runs were also made using θ_c as the primary h control (Ref. 55), but for the backside conditions of interest here these all produced worse ratings than those shown. The purpose of the ensuing analysis and discussion is to illustrate how the problem area criteria already set forth explain the data trends.

Analysis

Considering θ_c as the effective stick input and recognizing the previously noted effects of high θ -loop gain, the applicable transfer functions for \dot{h} and u control are then those already given for the attitude constrained situation (Eqs. E-13 to E-17). Using these, the pertinent coupling numerators (see Table 28) and assuming $\theta_{CF} = \text{steady-state } \theta_{CF0}^*$:

$$\begin{aligned} \left. \frac{\dot{h}}{\delta T} \right|_{\theta_{CF}} &= \frac{-Z\delta T \left(s + \frac{1}{T_{h\theta}} \right) - \theta_{CF} Z\alpha \left(s + \frac{1}{T_{h1}} \right)}{\left(s + \frac{1}{T_{\theta 1}} \right) \left(s + \frac{1}{T_{\theta 2}} \right)} \equiv \Delta' \\ &= \frac{-Z\delta T \left(1 + \frac{\theta_{CF} Z\alpha}{Z\delta T} \right)}{\Delta'} \left[s + \frac{\frac{1}{T_{h\theta}} + \frac{\theta_{CF} Z\alpha}{Z\delta T} \left(\frac{1}{T_{h1}} \right)}{1 + \frac{\theta_{CF} Z\alpha}{Z\delta T}} \right] \\ &= \frac{A_h'}{\Delta'} \left(s + \frac{1}{T_{h\theta_{CF}}} \right) \end{aligned} \quad (E-25)$$

where

$$\theta_{CF} \equiv (\theta_{CF0})_{s=0} = - \left[\frac{(X_{\delta T} s + \frac{1}{T_{u\theta}})}{(X_{\alpha} - g) \left(s + \frac{1}{T_{u1}} \right)} \right]_{s=0} = - \frac{X_{\delta T} T_{u1}}{(X_{\alpha} - g) T_{u\theta}}$$

*For all the experimental conditions in Table 29, the ratio of the 3 sec to the steady-state value of $\theta_{CF}(t)$ lies between 0.89 and 1.16, i.e., roughly constant. Crossfeed is therefore considered to be reasonable in this sense, as discussed earlier.

$$\begin{aligned} \theta_{CF} \frac{Z_\alpha}{Z_{\delta T}} &= -\frac{X_{\delta T} Z_\alpha T_{u1}}{Z_{\delta T} (X_\alpha - g) T_{u0}} = -\frac{X_{\delta T} Z_\alpha \left(-Z_w + \frac{Z_{\delta T}}{X_{\delta T}} X_w \right)}{Z_{\delta T} (X_\alpha - g) \left(\frac{g Z_w}{X_\alpha - g} \right)} \\ &= \frac{X_{\delta T}}{Z_{\delta T}} \frac{Z_\alpha}{g} - \frac{X_\alpha}{g} \end{aligned} \quad (E-26)$$

$$\begin{aligned} \left. \frac{u}{\theta_c} \right|_{h \rightarrow \delta T} \theta_{CF} &= \frac{(X_\alpha - g) \left(s + \frac{1}{T_{u1}} \right) + \frac{Y_{Ph}}{s} \left[X_{\delta T} Z_\alpha - Z_{\delta T} (X_\alpha - g) \right]}{\Delta' + \frac{Y_{Ph}}{s} \dot{N}_{\delta T}^h \Big|_{\theta_{CF}} \equiv \Delta''} \\ &= \frac{(X_\alpha - g) \left\{ s^2 + \frac{s}{T_{u1}} - Y_{Ph} Z_{\delta T} \left[1 - \frac{X_{\delta T} Z_\alpha}{Z_{\delta T} (X_\alpha - g)} \right] \right\}}{s \Delta' + Y_{Ph} \dot{N}_{\delta T}^h \Big|_{\theta_{CF}} \equiv \Delta''} \quad (E-27) \\ &= \frac{A_u \left[s^2 + 2\zeta_1 \omega_1 s + \omega_1^2 \right]}{\left(s + \frac{1}{T_{u1}} \right) \left[s^2 + 2\zeta_2 \omega_2 s + \omega_2^2 \right]} \end{aligned}$$

Based on the foregoing relationships, the $\dot{h}/\delta T \Big|_{\theta_{CF}}$ transfer functions were computed for the conditions and parameters of Table 29. The resulting h loop was then closed with a pure gain pilot, $Y_{Ph} = K_h$, adjusted to give a high frequency asymptotic crossover of 0.5 rad/sec; i.e., $-K_h Z_{\delta T} (1 + \theta_{CF} Z_\alpha / Z_{\delta T}) = 0.5$. The resulting Δ'' characteristics were a low-frequency first-order pole almost equal to the first-order $\dot{h}/\delta T \Big|_{\theta_{CF}}$ zero, and a second-order oscillation with a (closed-loop) frequency, ω_2 , for all conditions, of about 0.72 ± 0.02 rad/sec, and a damping ratio of about 0.32 ± 0.06 . The same values of $Y_{Ph} = K_h$ used to obtain Δ'' yielded similar second-orders for the $u/\theta_c \Big|_{h \rightarrow \delta T} \theta_{CF}$ numerators (i.e., $\omega_1 = 0.71$ rad/sec, $\zeta = 0.35$ for Conditions 1-6 and $\omega_1 = 0.86$ rad/sec, $\zeta = 0.42$ for Conditions 7-12). Similar "tracking" of closed-loop poles and zeros is

also observed in Ref. 51 where it is shown to be true in general; such generic developments have not yet been attempted in the present instance. At any rate, the similar second orders cancel approximately, leaving only a low-frequency first-order pole for $u/\theta_c \big|_h \xrightarrow{\theta_{CF}} \delta_T$, shown in Table 30 together with other pertinent computational results now to be examined.

Discussion

Starting with zero thrust inclination (Conditions 5 and 11), the notion of crossfeed seems most appropriate, because pilots "naturally" pull the nose up when adding power (to reduce speed excursions and achieve a faster final climb rate). The magnitude of the crossfeed which appears quite high (0.15-0.16 rad/in. of throttle) is in fact reasonable in terms of the corresponding attitude/speed value. That is, one inch of throttle produces a steady-state u increment (see Eq. E-16) of $X_{\delta_T T \theta_1 T \theta_2} / T u_0 = 48.4 \text{ fps} \doteq 29 \text{ kt}$, so that a $\theta_{CF} = 0.15 \text{ rad/in.} = 8.6 \text{ deg/in.}$ converts to about 0.3 deg/kt. On this basis, the magnitudes of all other crossfeeds, except those which are negative, also appear reasonable.

The negative crossfeeds (Conditions 1, 7, and 8) go counter to the pilot's inherent training and are almost instinctively disliked. Also, even if used, they conflict with the primary task, as evidenced by the reduced net altitude gain, A_h' . On these two counts the conditions requiring negative crossfeed should be among the worst tested, which they are (Fig. 36a at 104 deg; Fig. 36b at 90 deg, 104 deg). On the other hand, those conditions requiring zero or small positive crossfeeds (i.e., Fig. 36a at 90 deg for the extreme, and Fig. 36b at 63.5 deg for the moderate, backside condition) are the best tested.

In connection with these last two conditions, 2 and 9 respectively, note that although the altitude bandwidths are about the same, the speed bandwidth* for Condition 9 is about twice that for Condition 2; but there is still

*These bandwidths, ω_h and ω_u , are, respectively, inversely proportional to the dominant response time constant for the h response to a step, crossfed δ_T input, and for the u response to a step θ_c with $h/\delta_T \big|_{\theta_{CF}}$ closed at the K_h gains shown.

TABLE 30. COMPUTED CLOSED-LOOP PARAMETERS AND PROPERTIES

	Cond.	Thrust Angle (deg)	θ_{CF} (rad/in.)	gK_h (in./ft)	$\frac{A'_h}{g} \left(\frac{1}{T_{h\theta_{CF}}} \right)^a$	ω_h^c	$\left(\frac{1}{T_{u1}} \right)^b$	ω_u^c	$\left(\frac{-u}{\theta} \right)_{h \rightarrow \delta_T}^{\text{steady-state}}$ (fps/rad)
Extreme Backside, $\frac{1}{T_{h1}} = -.09$ Decoupled $N_{\delta_e} \left(\frac{1}{T_{\theta_1}} \neq \frac{1}{T_{\theta_2}} \right)$	1	104	-.0363	5.69	.088(.06)	.60	.06	.06	52.2
	2	90	0	3.33	.15(.10)	.50	.10	.10	31.3
	3	45	.106	1.81	.276(.137)	.42	.14	.14	22.4
	4	30	.13	1.77	.283(.144)	.40	.15	.15	20.9
	5	0	.15	2.09	.239(.260)	.19	.28	.28	11.2
	6	-30	.13	3.77	.133(.192)	.33	.21	.21	14.9
Moderate Backside, $\frac{1}{T_{h1}} = -.03$ Coupled $N_{\delta_e} \left(\frac{1}{T_{\theta_1}} = \frac{1}{T_{\theta_2}} \right)$	7	104	-.0665	12.8	.039(.082)	.60	.073	.07	42.0
	8	90	-.0326	5.14	.098(.17)	.49	.163	.16	18.8
	9	63.9	.041	2.52	.199(.192)	.44	.19	.19	16.1
	10	30	.150	1.91	.262(.202)	.42	.20	.20	15.3
	11	0	.157	2.02	.247(.213)	.41	.21	.22	14.6
	12	-30	.117	3.03	.165(.229)	.38	.23	.23	13.3

a $\left. \frac{\delta_T}{\delta_T} \right|_{\theta_{CF}} = \frac{A'_h \left(s + \frac{1}{T_{h\theta_{CF}}} \right)}{\Delta'}$

Conds. 1-6: $\Delta' = (s + .1)(s + .5)$

Conds. 7-12: $\Delta' = (s + .3)(s + .3)$

b $\left. \frac{\delta_c}{\delta_c} \right|_{h \rightarrow \delta_T} = \frac{A'_u (s^2 + 2\zeta_1\omega_1 + \omega_1^2)}{\left(s + \frac{1}{T_{u1}} \right) (s^2 + 2\zeta_2\omega_2 + \omega_2^2)}$

$\omega_2 \doteq .72, \zeta_2 \doteq .32$

Conds. 1-6: $\omega_1 = .71, \zeta_1 = .35, A'_u/g = -1$

Conds. 7-12: $\omega_1 = .86, \zeta_1 = .42, A'_u/g = -.67$

c The ω_h, ω_u values are the 45 deg phase margin frequencies for the above two transfer functions, respectively.

reasonable separation (a factor of 2) between the secondary u and primary h responses for Condition 9. The faster u response and the increased stiffness in u (increasing $1/T_{u1}'$ is akin to increasing X_{u1}) for Condition 9 (63.5 deg, moderate) apparently is responsible for the somewhat improved ratings, over Condition 2 (90 deg, extreme) shown in Fig. 36.

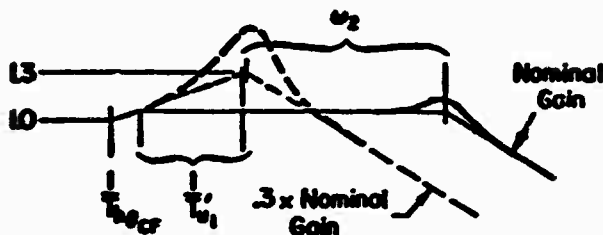
Notice that moderate Conditions 9-12, for thrust angles between 63.5 and -30 deg show a progressive reduction in ω_h and in the separation between ω_h and ω_{u1} . On both counts, the ratings should gradually degrade with decreasing thrust incidence, and this trend is evident in the Fig. 36b data.

An outstanding example of the reduced separation between ω_h and ω_{u1} is Condition 5 for extreme backside, 0 deg thrust inclination; in this instance, ω_{u1} is greater than ω_h , which is quite low. Thus, not only are the normally expected primary and secondary response characteristics reversed, but the primary altitude response, by itself, appears deficient. However, the closed h loop characteristic $\equiv \Delta'' = [s + (1/T_{u1}')] (s^2 + 2\zeta_2\omega_2s + \omega_2^2)$ shown in Table 30 as approximately constant for all conditions belies this apparent poor altitude control. This conflict in interpretation is resolved by considering the effects of K_h variations on the resulting closed h loop response characteristics. For instance, reducing K_h to three-tenths the value listed in Table 30 results in a decreased value of ω_2 as expected, but produces a disproportionate increase in the value of $1/T_{u1}'$ for Condition 5. (For other conditions the value of $1/T_{u1}'$ varies only slightly for similar gain changes.)

The nature of the specific changes for Condition 5 is illustrated in the tabulations and sketch shown below. It is apparent that a reduction in gain tends to produce an h overshoot in the frequency range of interest for control. The peak sketched corresponds to an effective (closed-loop) ζ of about 0.29, which produces about a 35% overshoot to a step input (in h_c). As noted earlier, Condition 5 is considerably more sensitive in this regard than the other conditions surrounding it. In the sense then that it is connected with such gain sensitivity, the originally noted poor ω_h shown in Table 30 can be taken as an indication of a piloting problem.

Finally, and still considering Condition 5, it is shown in Table 30 as having the lowest closed-loop u/θ steady-state response. It appears, for all

Gain	$\frac{1}{T_{\theta_{CF}}}$	$\frac{1}{T_{\theta_1}}$	ω_2	ζ_2	ω_1	ζ_1
Nominal (Table E-3)	.260	.26	.72	.32	.71	.35
0.3 x Nominal	.260	.34	.34	.39	.39	.64



Sketch Showing Bode Amplitude for

$$\frac{h}{h_c} = \frac{s + \frac{1}{T_{\theta_{CF}}}}{\left(s + \frac{1}{T_{\theta_1}}\right)(s^2 + 2\zeta_2\omega_2 s + \omega_2^2)}$$

these reasons, that Condition 5 is the worst of all those tested. Again, the data trends reflect this analytically-derived conclusion.

Example 3

We here examine a particular configuration (J4) taken from the Ref. 32 investigation to illustrate another facet of "backside" problems. In this instance, the backside, negative value of $1/T_{\theta_1}$ is also accompanied by a negative value of $1/T_{\theta_{CF}}$; the closed-loop implications of the latter are the specific purpose of the example analyses to be presented.

The objective of the referenced investigation was to examine flight path stability requirements as represented by boundary values (Ref. 16) of $(d\gamma/du)(\text{deg/kt}) = -3/T_{\theta_1}$. To obtain the desired large positive values of $d\gamma/du$ (negative values of $1/T_{\theta_1}$), a "basic" configuration was degraded by effectively varying X_w and X_u . In this process, the more negative values of $1/T_{\theta_1}$ also resulted in negative values of $1/T_{\theta_{CF}}$, in accordance with the approximate Eq. E718 relationship.

From the standpoint of open-loop characteristics, negative $1/T_{\theta_1}$ results in steady-state attitude-to-elevator responses which are reversed from the norm. That is, up elevator produces, eventually, a nose-down attitude,

although the initial response is correct (nose up). Hence, the aircraft is not easily trimmable, and the pilot starts with a net "burden" represented by poor unattended characteristics.

The negative value of $1/T_{\theta 1}$ therefore presents an immediate problem relative to the basic, inner, attitude loop integrity, as may be inferred in more detail from the system survey given in Fig. 37 for the example case. This figure displays, upper left, the basic block diagram and the pertinent open-loop airplane and pilot model transfer functions. The transfer functions are presented in an abbreviated notation where the leading number is the airplane gain, the single numbers in parentheses represent first-order factors, i.e., $(1/T)$ corresponds to $[s + (1/T)]$, and the double numbers represent second-order factors, i.e., (ζ, ω) corresponds to $s^2 + 2\zeta\omega s + \omega^2$. The lower left portion of the figure is a conventional root locus for increasing (pilot) gain. The right portion of the figure is a combined $s = j\omega$ and $s = -\sigma$ Bode root locus plot for the complete open-loop (upper left) transfer function. The $j\omega$ Bode is fairly standard with amplitude and phase shown by light solid lines and amplitude asymptotes and breakpoints shown dashed. The dotted lines show how the second-order poles are altered by increasing open-loop (pilot) gain, ω_p' decreasing and ω_{sp}' increasing; the corresponding changes in ζ_p' and ζ_{sp}' are "spotted" along the applicable dotted trajectories. The heavy solid σ Bode lines labeled $G(-\sigma)$ show how, as gain increases, the first-order poles in the closed-loop characteristic appear in the left and right planes, respectively, of the conventional root locus. For example, following the ω_p' migrations on both the Bode and conventional root loci, as gain increases, ω_p' decreases and ζ_p' increases, becoming unity when the dotted Bode trajectory intersects the $G(-\sigma)$ line. The gain at which this occurs corresponds to the horizontal slope of $G(-\sigma)$, about -12 dB. Continuing to increase gain decouples ω_p' into two first orders, labeled $1/T_{\theta 1}'$ and $1/T_{\theta 2}'$ which, for further gain increases, migrate toward $1/T_{\theta 1}$ and $1/T_{\theta 2}$, respectively. For $K_{p\theta} = 0.5$ the closed-loop poles shown as square symbols on the conventional root locus are also reflected as the intersections of the appropriate gain line with the dotted (second-order) and solid $G(-\sigma)$ Bode root locus lines. For $K_{p\theta} > 1$, the value of $1/T_{\theta 1}'$ is negative as reflected by a gain line intersection with $G(+\sigma)$. Thus, the Bode root locus format displays all the pertinent closed-loop information needed directly as a function of gain; whereas the

The figure consists of two vertically aligned plots sharing a common logarithmic frequency axis ω (rad/sec) ranging from 0.01 to 10.0.

The top plot shows Magnitude (dB) on the y-axis, ranging from -20 to 40. It features several curves:

- $G(j\omega)$: A solid curve with a peak at ω_p (approx. 33 dB).
- $G(-\sigma)$: A solid curve that rises from 0 dB at low frequencies.
- $G(\sigma)$: A solid curve that falls from 0 dB at low frequencies.
- $\text{OdB line for } K_p\theta = 0.5$: A dashed line with a slope of -20 dB/decade.
- Pilot Delay : A curve that starts at high magnitude and drops sharply.

 Key frequencies marked on the x-axis include ω_{sp} (approx. 0.72 rad/sec) and $1/\theta_1$, $1/\theta_2$, $1/L_\theta$ (approx. 1.0 rad/sec).

The bottom plot shows Phase (deg) on the y-axis, ranging from -200 to -600. The phase curve starts at -200 degrees at low frequencies, remains relatively flat until $\omega \approx 0.1$ rad/sec, then drops sharply to -600 degrees at $\omega \approx 1.0$ rad/sec.

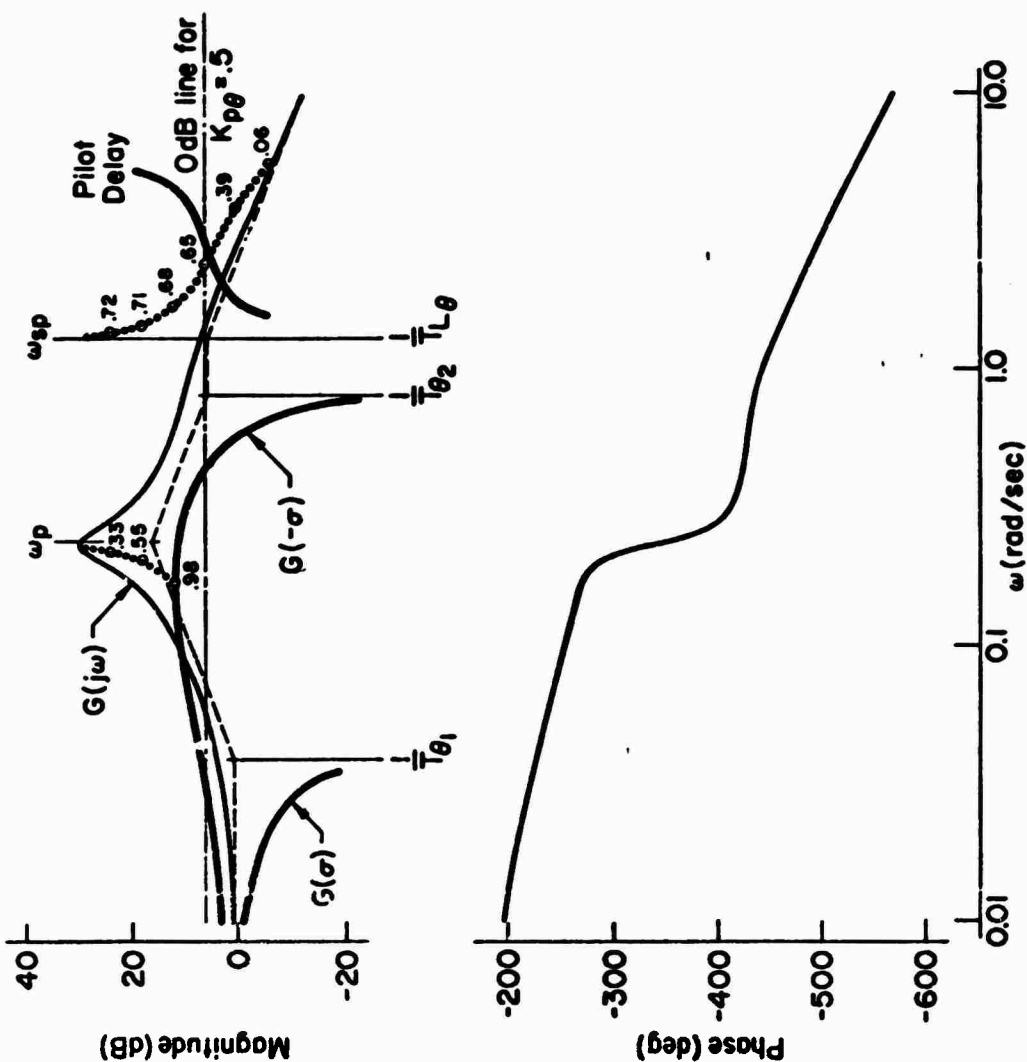


Figure 37. Attitude Loop System Survey

conventional root locus, although directly displaying the root trajectories, requires additional computations to locate the roots as a function of specific gains.

Examining Fig. 37 in detail, it may be seen first that the pilot model has been "adjusted" to include moderate lead ($TL_0 \doteq 0.77$ sec) and a corresponding time delay, $e^{-.33s}$, represented by its Padé approximant, $-(s-6)/(s+6)$. The lead is required to reduce the phase lag in the region of desirable cross-over frequencies ($\omega_{c_0} > 2$ rad/sec). For the assumed lead, and adequate gain and phase margin, crossovers up to about 3 rad/sec are possible for a corresponding $K_{p_0} \doteq 1.0$. At this gain, very low-frequency attitude "wandering" would still appear in θ/θ_c , because the closed-loop $1/T'_{\theta_1}$ pole would correspond essentially to a free s ; i.e., θ would ramp off at a low rate, as would the u response to θ_c , i.e., $u/\theta_c = (u/\theta)(\theta/\theta_c)$.

Increased gain requires increased TL_0 (to avoid short-period instability) which tends to increase the pilot's workload and degrade his opinion. However, even neglecting this aspect, the results are still unfavorable. That is, increased gain (over $K_{p_0} = 1$) pushes $1/T'_{\theta_1}$ into the right half root locus plane, so that the ramping responses now become divergent.

Reducing the gain (e.g., to $K_{p_0} = 0.5$), as shown in Fig. 37, sacrifices some of the desired bandwidth but eliminates the slow ramping or divergent tendencies. However, the steady-state θ response is now reversed, as for the bare (open-loop) airplane. Also, for ± 6 dB variation about this nominal gain, the closed-loop properties change over a range from those described above for $K_{p_0} = 1$, to a condition where the path modes ($1/T'_{\theta_1}$, $1/T'_{\theta_2}$) become coupled (at ω_p^1), undesirable (as noted earlier) from the standpoint of separating u and \dot{h} responses.

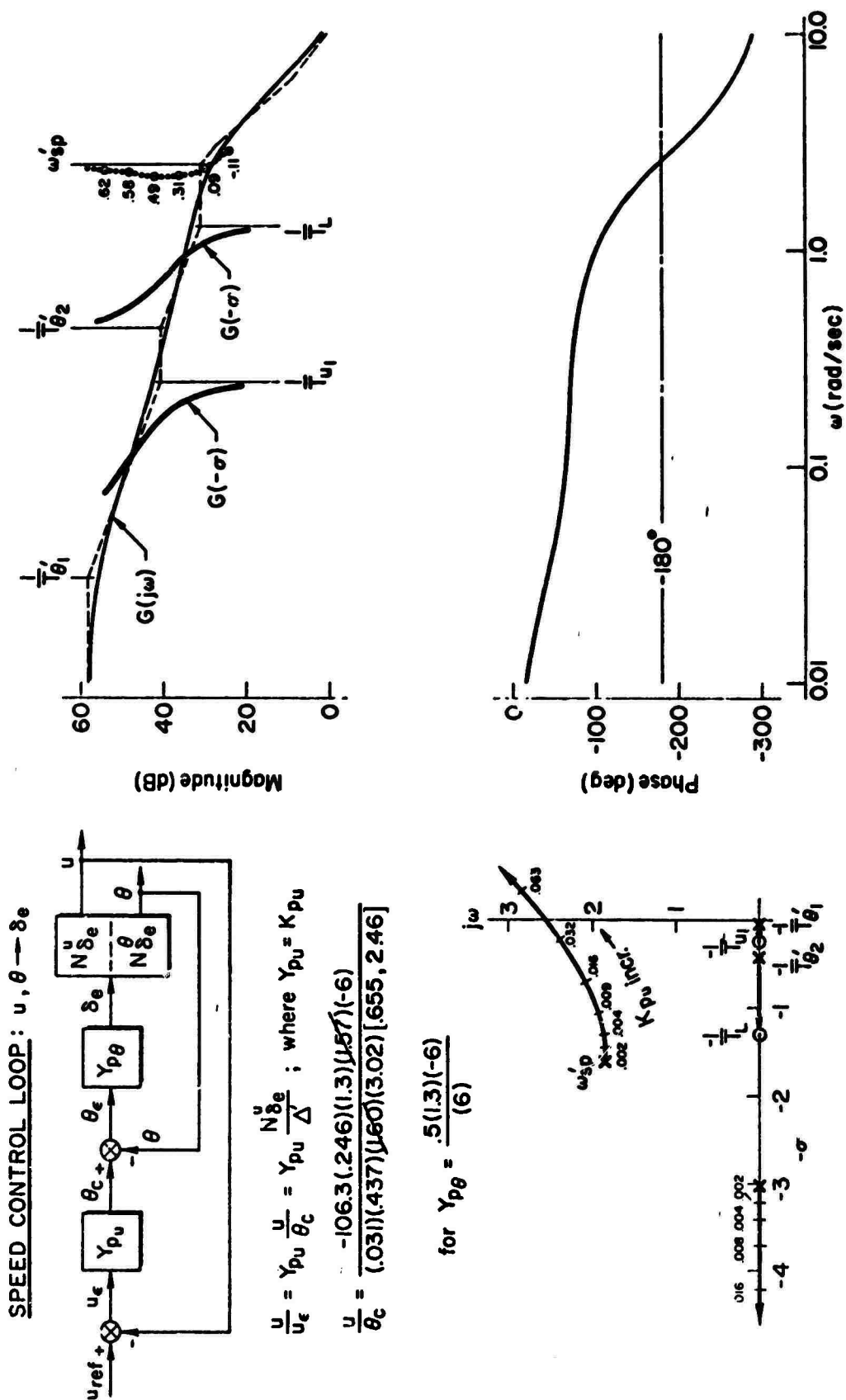
In effect, the pilot has no good adjustment possibilities for what is normally a simple and fundamental loop closure. If he sacrifices attitude bandwidth (low gain), he also incurs \dot{h} and u response coupling and poor low-frequency attitude regulation, all bad. If he increases bandwidth (high gain), he gets low-frequency attitude and speed divergence. He is "boxed in" by conflicting and/or compounding effects represented by extreme sensitivity to his exact "adjustments," and stemming basically from poor inherent speed stability

(i.e., $1/T_{\theta_1} = -X_u < 0$). In a sense, then, the pilot has little choice but to regulate also on speed, as illustrated in Fig. 38 for a "nominal" attitude gain, $K_{p\theta}$, of 0.5. This loop can be easily closed at frequencies up to a little more than 1 rad/sec. Such large crossovers and attendant high gain would, however, reduce the short-period damping ratio considerably (from 0.655 to about 0.3) and thereby further compound the attitude loop problem. For lower, more normal, crossovers, around 0.3 rad/sec, the reduction in ζ_{sp} to about 0.50 seems tenable. However, the attitude loop, normally regarded as fundamental, is now subservient to the relatively low bandwidth speed control loop. In fact, speed control governs the overall stability margin in this multiloop system; thus, the integrity of the attitude control is lost.

Also, the fact that u/θ_c must be closed for good regulation represents a violation of the control economy concept. Remember the first example, where it was noted that u excursions were ordinarily quite small for the STOL mode (nominally appropriate here because of the backside condition) even if u were not controlled at all. For the present example, not only must the u loop be closed, but it becomes just as important as the θ loop, thereby also violating desirable control hierarchy. That is, both attitude and u control actions are intertwined so that increased pilot attention and concentration is required.

The fact that the u loop must be closed is traceable to the quasi-divergent or ramping behavior of the u responses noted earlier. Such behavior represents poor speed "indexing" with attitude, which is always undesirable for both regulatory and trim management control. Good indexing means that a given discrete secondary input results in a predictable final value attained in a reasonable time (5-10 sec). In effect, good indexing is akin to constant gain over an adequate bandwidth (0.1 to 0.2 rad/sec). A glance at Fig. 38 shows that the u/θ_c indexing for this example is deficient in that the final value is slowly attained ($1/T_{\theta_1}'$) and is extremely sensitive to the θ_c input (high u/θ_c dc gain).

In conclusion, this example illustrates, without considering the additional problems directly associated with negative "static" flight path stability, $1/T_{h_1}$, many of the regulatory and response problems noted in Section II. The particular deficiencies observed, which stem specifically from poor control of attitude and speed undoubtedly contribute heavily to the recorded Cooper-Harper pilot rating of about 7-1/2 (Ref. 32).



Example 4

The final example considers "frontside" conditions which have inherently coupled path modes due to large positive X_α . As previously indicated, such conditions may result from airplane augmentation utilizing an angle-of-attack autothrottle. In fact, this example is based largely on the analysis of autothrottle-associated problems given in Ref. 51. Basically, the referenced study illustrated and confirmed how this "coupling" caused regulatory control problems during carrier approach flight operations.

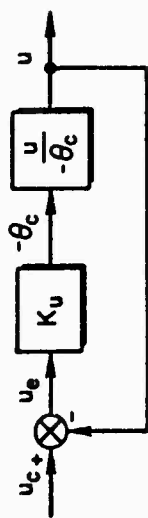
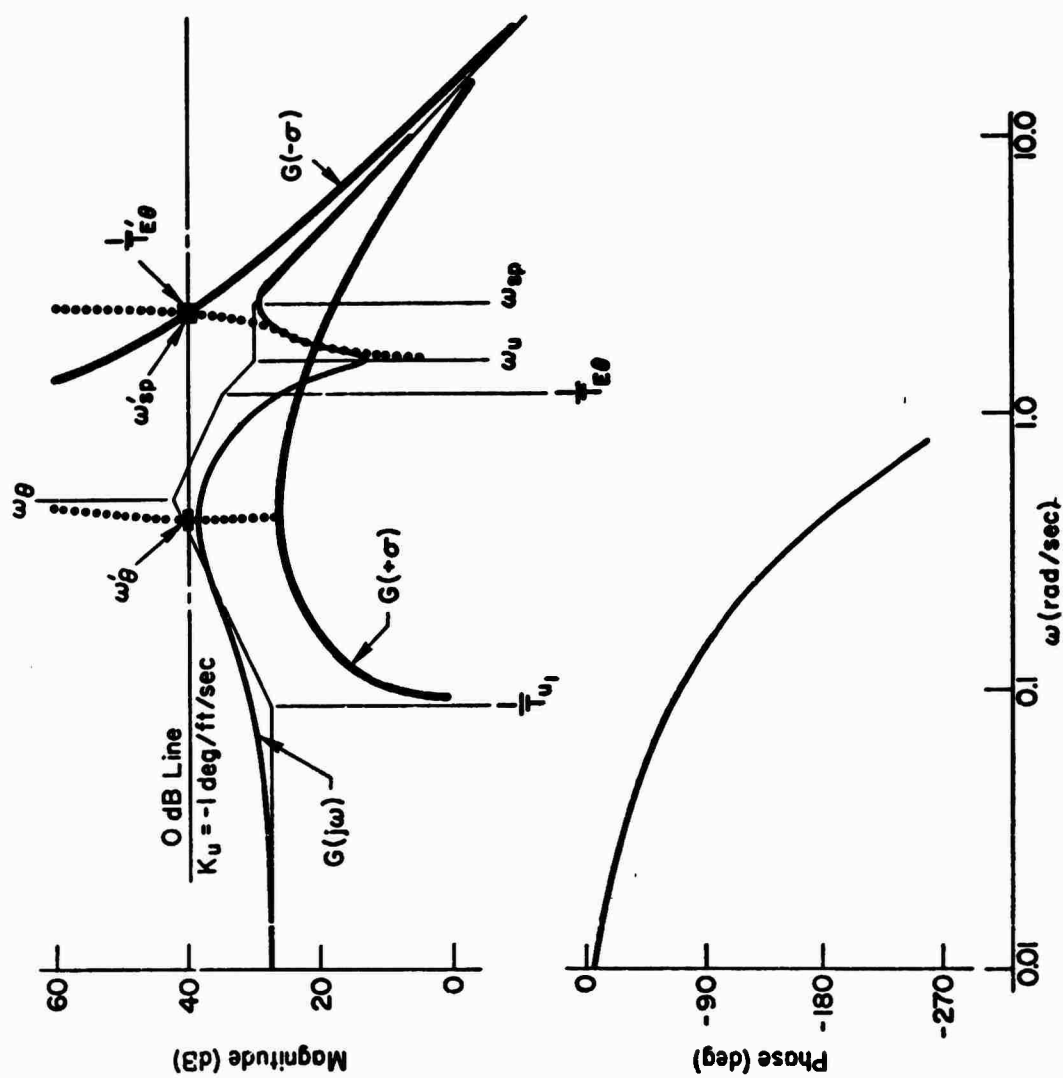
One of the specific primary control problems repeatedly encountered in the referenced study centered on loss of flexibility in the pilot's ability to trim airspeed when an off-nominal condition occurred (discussed in the preceding section, "Generic Longitudinal Path Control Considerations"). With the autothrottle engaged, no direct manual throttle input was possible for the U. S. Navy aircraft studied; in fact, all throttle or thrust activity was effectively keyed to elevator or attitude changes. This is consistent (as previously noted) with pilots' conventional use of attitude to exchange airspeed and altitude.

The generic aspects of the speed control problem with autothrottle engaged have already been discussed in the preceding section; specifically, it was noted there that the u/θ_c response given by:

$$\frac{A_u' \left(s + \frac{1}{T_{u1}} \right)}{[s^2 + 2\zeta_\theta \omega_\theta s + \omega_\theta^2]}$$

was oscillatory (due to ω_θ) and delayed (due to negative $1/T_{u1}$). These generic properties are also evident in the specific-aircraft system survey given in Fig. 39 (taken directly from Ref. 51); the transfer function shown reflects the full complement of poles and zeros obtained when simplifying assumptions are not used and thrust lag is included.

An examination of Fig. 39 shows that the closed-loop system is neutrally stable ($\zeta'_\theta = 0$) for moderate gain (i.e., 1 deg/fps) and that even for this gain level there is no effective regulation of airspeed. In fact, the effective



$$\frac{u}{-\theta_c} = \frac{-A_u \omega_{sp}^2 (1/T_{u1}) [\zeta_u, \omega_u]}{A_\theta [\zeta_\theta, \omega_\theta] (1/T_{E\theta}) [\zeta_{sp}, \omega_{sp}]}$$

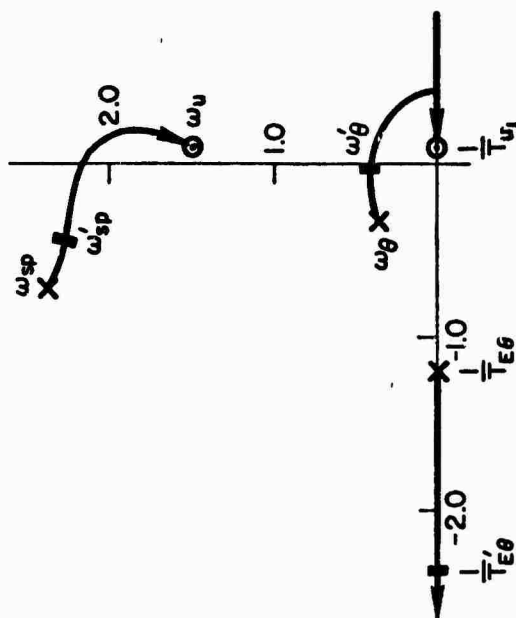


Figure 39. System Survey of Closed-Loop Airspeed Control With Attitude

closures are limited by potential instabilities, at ω'_θ and ω'_{sp} , to gains which are above those for a crossover condition. The nonexistent bandwidth, the poor closed-loop stability for reasonable gains, and the low-frequency droop infer low effective path damping and poor speed regulation with large attendant attitude excursions, all confirmed by the associated pilot comments as reported in Ref. 51. It appears that airspeed regulation with attitude is infeasible, and the pilot has therefore lost ability to regulate speed.

The foregoing conclusion is based on the use of only attitude (or associated elevator) inputs. It is logical to assume that given the use of the throttle the pilot could regain speed control. Unfortunately, this is not the case, because the coupling condition magnifies \dot{h} relative to u responses for θ_c inputs; and the resulting net u/θ_c gain with \dot{h} constrained is small (Eq. E-22).

Such specific situations, i.e., stick and throttle control for coupled, frontside conditions, were tested in the Ref. 55 investigation, previously exposed in Example 2. The results given in Fig. 40 show that only stick control of flight path through attitude commands (i.e., $\dot{h} \rightarrow \theta_c(\delta_s)$) is nearly satisfactory (i.e., $PR \dot{=} 4$); the pilots simply accepted the resulting (relatively small) airspeed excursions, while complaining about the loss of speed control. Attempts to use partitioned multiloop dual-control modes [i.e., $\dot{h} \rightarrow \theta_c(\delta_s)$, $u \rightarrow \delta_T$ or $\dot{h} \rightarrow \delta_T$, $u \rightarrow \theta_c(\delta_s)$] resulted in unacceptable to

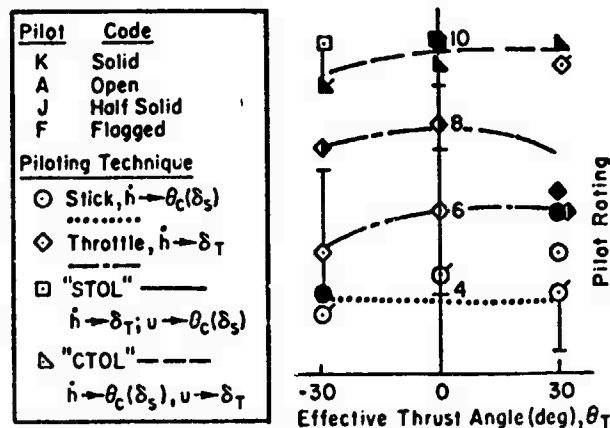


Figure 40. Effect of Control Techniques on Pilot Rating with Strong "Dynamic" Coupling ($\zeta_\theta = 0.6$, $\omega_\theta = 0.5$; $1/T_{h1} = +0.21$)

uncontrollable situations (i.e., $PR \approx 10$) because of the extreme coupling. Single-loop throttle control (i.e., $\dot{h} \rightarrow \delta_T$) was regarded as unacceptable in general. These results are consistent with the analytically derived expectations given in the preceding section, "Generic Longitudinal Path Control Considerations."

SUMMARY AND CONCLUSIONS

Approach path piloting techniques and experimentally-observed problem areas have been explored through application of pilot/vehicle analysis methods. Results have demonstrated that there are a large number of rules and/or aircraft parameters which must be considered in delineating "good" from "bad" handling qualities. The methodology and analytical considerations applied and described afford the basic framework for a systematic, logical, and effective design and specification procedure.